Chapter 6 — Formulae for Calculating the Velocity of Stars

First, the author studied the law of motion of stars in the air. The velocity of stars at distant points from the shell burst was then related to the initial velocity of each star. The conditions that produced these initial velocities were investigated, and from this information, equations useful in the designing of shells were developed.

6.1. Arrangement of Experimental Data

6.1.1. Photography with a Revolving Shutter Camera

The scale of the image taken on the dry plate of a cabinet was 1/757.6. This is based on the distance between the calibration poles. The images of the star flight lines were numbered from the lowest trajectory. For example, Shell No. 231 represents the lowest trajectory of the star from the Shell No. 23.

6.1.2. Photography with a 16-mm Movie Camera

The calibration poles were not clearly observed with the 16-mm movie camera, however, shells Nos. 22, 37, 49 and 51 barely indicated the position of the light of the calibration poles. The scale of the image was 1/142.9. Figure 22 shows the image from the 16-mm movie camera.

6.2. Trajectory of the Star in the Air

From the trajectories in the photographs, it became clear that the velocity of a star is 10–100 m/s, which is a fairly low velocity compared to the speed of sound. The simple approach to calculating air resistance outlined in

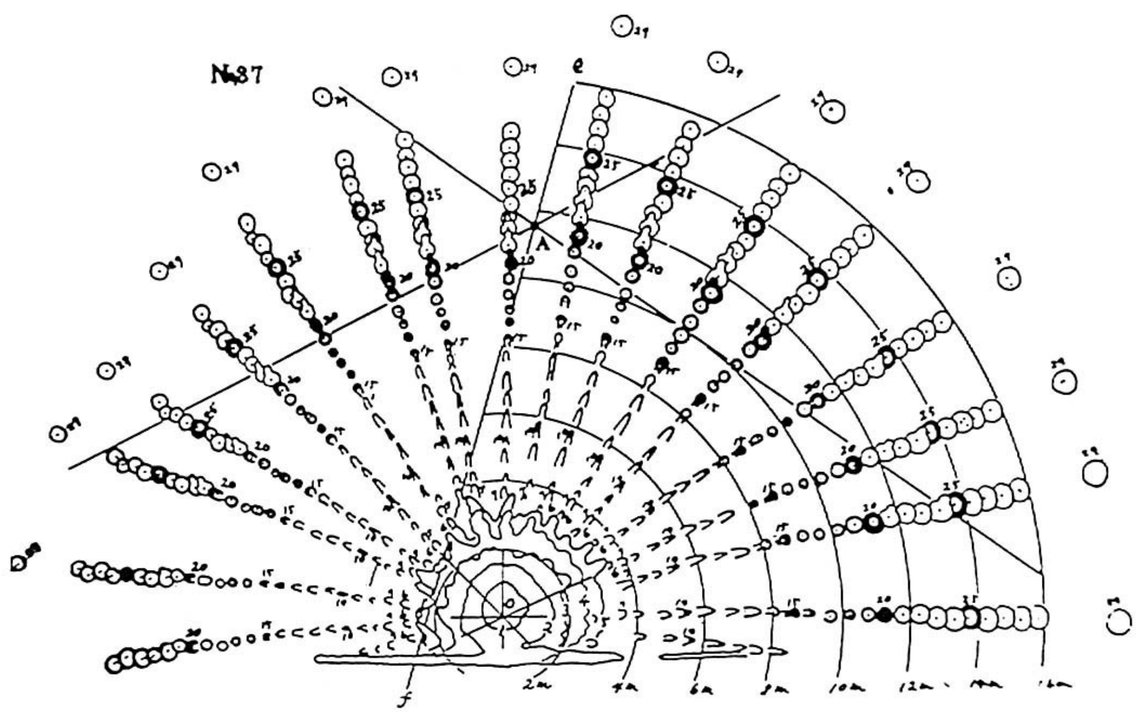

Figure 22. The trajectories photographed by the 16-mm movie camera.

Chapter 3 should therefore be adequate. In other words, it should be possible to use equation 38 for moving stars. To solve this equation for moving stars, it is sufficient to consider only the horizontal trajectories for various examples.

The above equation was modified to a more general formula:

$$\frac{d^2x}{dt^2} = -\frac{k}{p'(t)} v^n \tag{40}$$

From the results of the experiments, the values of n and k are obtained as follows. The sample stars used for these calculations should be selected so that the star's flight is as horizontal as possible and has a minimum deviation from the line of calibration poles. Flying stars are regarded as being free from the explosion gas.

6.2.1. The Reaction of Air upon the Star

The following calculation is for Star No. 481.

As described earlier, the trajectory of a star appeared on the photograph as a dotted line. Table 13 shows the order of calculation along the dotted line. The number on the left side shows each dot from the start on a trajectory that had the lowest horizontal flight. Number 1 means the dot nearest the burst point, 2, 3, 4, etc. are the order of the star's position as it traveled out from the center. The value of x is a coordinate on the x-axis associated with each dot numbered from the burst point. The value of Δx is the distance between 1 and 3, 2 and 4, 3 and 5, etc. (See Figure 23.)

Table 13. An Example of Calculations for a Star That Flew Horizontally.

Dot No.	x	Δx	v	$\bar{v}$	$\Delta \bar{v}$	$\frac{d\bar{v}}{dt}$
	m	m	m/s	m/s	m/s	m/s^2
1	15.96	—	—	—	—	—
2	18.92	5.88	73.5	73.5	—	—
3	21.84	5.40	67.5	67.5	–11.4	–143
4	24.32	4.92	61.5	62.1	–9.7	–121
5	26.76	4.68	58.5	57.8	–8.1	–101
6	29.00	4.34	54.3	54.0	–7.2	–90
7	31.10	3.92	49.0	50.6	–6.4	–80
8	32.92	3.64	45.5	47.6	–5.7	–71
9	34.74	3.62	45.3	44.9	–5.2	–65
10	36.54	3.50	43.8	42.4	–4.9	–61
11	38.24	3.20	40.0	40.0	–4.4	–55
12	39.74	3.00	37.5	38.0	–3.9	–49
13	41.24	2.86	35.8	36.1	–3.7	–46
14	42.60	2.74	34.5	34.3	–3.4	–43
15	43.98	2.60	32.5	32.7	–3.2	–40
16	45.20	2.40	30.0	31.1	–3.1	–39
17	46.38	2.36	29.5	29.6	—	—
18	47.56	—	—	—	—	—

Dots 1 2 3 4 5 6

|← Δx →|

|← Δx →|

|← Δx →|

Figure 23. Diagram of variables in Table 13.

For example from Table 13:
21.84 – 15.96 = 5.88
24.32 – 18.92 = 5.40
26.76 – 21.84 = 4.92

These were recorded at the heads of each intermediate dot (Figure 23). The time interval between each pair of dots is 2/25 seconds. Therefore the value of Δx divided by 2/25 s denotes the negative acceleration. The symbols v and dv/dt are used in place of $\bar{v}$ and $\frac{d\bar{v}}{dt}$ in the following paragraphs to avoid any confusion. Table 14 shows the values of such data obtained from the test shells.

Table 14a. Horizontal Velocities and Horizontal Negative Accelerations of Stars that Flew Almost Horizontally.

	x	v	$-\frac{dv}{dt}$	x	v	$-\frac{dv}{dt}$	x	v	$-\frac{dv}{dt}$
	m	m/s	m/s^2	m	m/s	m/s^2	m	m/s	m/s^2
Dot No.	Shell No. 31			Shell No. 41			Shell No. 51		
1	12.20	—	—	19.56	—	—	13.08	—	—
2	13.68	35.9	—	21.64	49.5	—	14.24	30.2	—
3	15.08	33.5	58	23.52	45.7	88	15.44	28.3	46
4	16.36	31.3	51	25.28	42.5	78	16.52	26.5	40
5	17.56	29.4	44	26.92	39.5	73	17.56	25.1	31
6	18.72	27.8	40	28.44	36.7	66	18.52	23.8	34
7	19.84	26.2	36	29.86	34.2	60	19.46	22.6	29
8	20.90	24.9	30	31.16	31.9	54	20.35	21.5	26
9	21.88	23.8	28	32.36	29.9	46	21.20	20.5	24
10	22.80	22.7	28	33.50	28.2	43	21.98	19.6	23
11	23.68	21.6	25	34.60	26.5	40	22.72	18.1	20
12	24.56	20.7	24	35.64	25.0	38	23.48	18.0	19
13	25.32	19.7	24	36.56	23.5	35	24.20	17.2	19
14	26.12	18.8	21	37.44	22.2	33	24.48	16.5	16
15	26.82	18.0	20	38.36	20.9	31	25.52	15.9	15
16	27.58	17.2	19	39.16	19.7	28	26.16	15.3	15
17	28.24	16.5	16	39.96	18.7	26	26.72	14.7	14
18	28.32	15.9	16	40.70	17.6	25	27.28	14.2	14
19	29.46	15.2	16	41.34	16.7	23	27.88	13.8	13
20	30.04	14.6	14	42.00	15.8	—	28.40	13.2	12
21	30.62	14.1	14	42.60	—	—	28.88	12.8	11
22	31.18	13.5	14	46.00			29.36	12.3	11
23	31.72	13.0	11				29.92	11.9	9
24	32.20	12.6	11				30.36	11.6	—
25	32.70	12.1	—				30.80	—	—
26	33.12	—	—				32.76		

Table 14b. Horizontal Velocities and Horizontal Negative Accelerations of Stars that Flew Almost Horizontally.

	x	v	$-\frac{dv}{dt}$	x	v	$-\frac{dv}{dt}$	x	v	$-\frac{dv}{dt}$
	m	m/s	m/s^2	m	m/s	m/s^2	m	m/s	m/s^2
Dot No.	Shell No. 62			Shell No. 72			Shell No. 82		
1	12.22	—	—	9.96	—	—	13.64	—	—
2	13.50	32.2	—	11.36	34.4	—	15.16	37.6	—
3	14.78	30.6	40	12.66	32.0	56	16.72	36.5	70
4	15.96	29.0	39	13.92	29.9	53	18.12	34.0	59
5	17.04	27.5	36	15.04	27.8	49	19.44	31.8	50
6	18.12	26.1	34	16.14	26.0	44	20.68	30.0	43
7	19.16	24.8	31	17.12	24.3	40	21.88	28.4	37
8	20.16	23.6	31	18.08	22.8	35	22.96	26.9	35
9	21.06	22.3	31	19.00	21.5	31	24.04	25.6	30
10	21.88	21.1	28	19.80	20.3	29	25.04	24.5	28
11	22.72	20.1	25	20.60	19.2	26	25.96	23.4	26
12	23.44	19.1	24	21.32	18.2	24	26.72	22.4	25
13	24.20	18.2	21	22.08	17.3	21	27.80	21.4	24
14	24.92	17.4	19	22.76	16.5	20	28.64	20.5	23
15	25.56	16.7	18	23.40	15.7	20	29.44	17.6	21
16	26.24	16.0	18	24.04	14.9	19	30.20	18.8	20
17	26.86	15.3	16	24.60	14.2	16	30.92	18.0	20
18	27.44	14.7	15	25.20	13.6	15	31.68	17.2	20
19	28.00	14.1	14	25.72	13.0	15	32.30	16.4	—
20	28.58	13.6	14	26.20	12.4	14	33.20	—	—
21	29.08	13.0	13	26.72	11.9	14	36.72		
22	29.58	12.6	—	27.20	11.3	—			
23	30.12	—	—	27.60	—	—			
24	32.48			29.80					

Table 14c. Horizontal Velocities and Horizontal Negative Accelerations of Stars that Flew Almost Horizontally.

	x	v	$-\frac{dv}{dt}$	x	v	$-\frac{dv}{dt}$	x	v	$-\frac{dv}{dt}$
	m	m/s	m/s^2	m	m/s	m/s^2	m	m/s	m/s^2
Dot No.	Shell No. 91			Shell No. 101			Shell No. 112		
1	13.16	—	—	15.92	—	—	13.84	—	—
2	14.78	37.9	—	17.66	41.5	—	15.06	29.5	—
3	16.20	34.8	71	19.24	38.4	70	16.20	28.0	38
4	17.52	32.2	59	20.72	35.7	56	17.24	26.5	35
5	18.79	30.1	49	22.08	33.9	49	18.32	25.2	31
6	19.98	28.3	44	23.44	32.0	44	19.34	24.0	30
7	21.13	26.6	40	24.68	30.4	39	20.26	22.8	28
8	22.16	25.1	35	25.88	28.9	38	21.12	21.8	26
9	23.12	23.8	31	27.00	27.4	36	21.98	20.7	25
10	24.00	22.6	29	28.04	26.0	34	22.72	19.8	23
11	24.88	21.5	28	29.04	24.7	31	23.50	18.9	21
12	25.72	20.4	26	29.76	23.5	26	24.22	18.1	20
13	26.50	19.4	24	30.88	22.6	25	24.92	17.3	19
14	27.26	18.5	23	31.80	21.5	24	25.56	16.6	18
15	27.94	17.6	23	32.60	20.7	23	26.18	15.9	18
16	28.60	16.7	21	33.36	19.5	23	26.78	15.2	15
17	29.24	15.9	20	34.12	18.6	21	27.50	14.7	—
18	39.86	15.1	20	34.88	17.8	19	28.00	—	—
19	30.48	14.3	19	35.56	17.1	18	31.20		
20	31.00	13.6	18	36.28	16.4	16			
21	31.56	12.9	18	36.88	15.8	—			
22	32.04	12.2	—	37.46	—	—			
23	32.50	—	—	40.56					
24	34.92								

Table 14d. Horizontal Velocities and Horizontal Negative Accelerations of Stars that Flew Almost Horizontally.

	x	v	$-\frac{dv}{dt}$	x	v	$-\frac{dv}{dt}$	x	v	$-\frac{dv}{dt}$
	m	m/s	m/s^2	m	m/s	m/s^2	m	m/s	m/s^2
Dot No.	Shell No. 132			Shell No. 142			Shell No. 153		
1	7.60	—	—	7.16	—	—	6.76	—	—
2	9.00	30.5	—	8.64	36.6	—	8.16	38.9	—
3	10.10	27.3	29	10.08	34.9	41	9.64	36.5	55
4	11.28	23.2	26	11.44	33.3	39	11.08	34.5	49
5	12.38	27.2	25	12.72	31.8	36	12.40	32.6	44
6	13.42	26.2	25	13.96	30.4	33	13.68	31.0	40
7	14.46	25.2	23	15.16	29.2	30	14.88	29.4	36
8	15.46	24.4	21	16.28	28.0	28	16.08	28.1	30
9	16.44	23.5	21	17.44	27.0	25	17.20	27.0	28
10	17.36	22.7	20	18.50	26.0	25	18.24	25.9	26
11	18.24	21.9	19	19.49	25.0	24	19.28	24.9	24
12	19.11	21.2	18	20.46	24.1	21	20.26	24.0	21
13	19.95	20.5	16	21.43	23.3	21	21.18	23.2	21
14	20.74	19.9	16	22.34	22.4	20	22.08	22.3	20
15	21.53	19.2	16	23.20	21.7	18	22.96	21.6	18
16	22.24	18.6	15	24.04	21.0	18	23.78	20.9	18
17	22.94	18.0	15	24.88	20.3	18	24.66	20.2	18
18	23.64	17.4	14	25.64	19.6	16	25.44	19.5	16
19	24.32	16.9	14	26.44	19.0	14	26.28	18.9	15
20	25.02	16.3	13	27.20	18.5	14	27.06	18.3	14
21	25.64	15.9	13	27.88	17.9	14	27.76	17.8	13
22	26.24	15.5	13	28.56	17.4	13	28.44	17.3	13
23	26.84	15.0	11	29.28	16.9	13	29.16	16.8	13
24	22.44	14.6	11	29.92	16.4	13	29.80	16.3	11
25	28.00	14.1	11	30.56	15.9	11	30.44	15.7	10
26	28.56	13.7	11	31.18	15.5	11	31.08	15.5	10
27	29.12	13.2	11	31.80	15.0	11	31.68	15.1	9
28	29.64	12.8	10	32.36	14.6	11	32.28	14.8	9
29	30.12	12.4	10	32.96	14.1	11	32.84	14.4	9
30	30.60	12.0	10	33.52	13.7	11	33.44	14.1	8
31	31.10	11.6	9	34.06	13.2	11	33.96	13.8	8
32	31.58	11.3	9	34.56	12.8	10	34.52	13.5	8
33	32.00	11.0	9	35.04	12.4	10	35.04	13.2	6
34	32.44	10.6	9	35.54	12.0	10	35.56	13.0	6
35	32.84	10.3	8	36.02	11.6	9	36.08	12.8	6
36	33.24	10.0	—	36.52	11.3	9	36.60	12.5	5

Table 14d. Horizontal Velocities and Horizontal Negative Accelerations of Stars that Flew Almost Horizontally. (Continued)

	x	v	$-\frac{dv}{dt}$	x	v	$-\frac{dv}{dt}$	x	v	$-\frac{dv}{dt}$
	m	m/s	m/s^2	m	m/s	m/s^2	m	m/s	m/s^2
Dot No.	No. 132			No. 142			No. 153		
37	33.64	—	—	36.96	10.9	9	37.04	12.3	4
38	33.88			37.40	10.5	9	37.54	12.2	4
39	35.88			37.78	10.2	9	38.00	12.0	—
40				38.20	9.8	9	38.44	—	—
41				38.56	9.5	—	41.12		
42				38.94	—	—			
43				40.56					

Table 14e. Horizontal Velocities and Horizontal Negative Accelerations of Stars that Flew Almost Horizontally.

	x	v	$-\frac{dv}{dt}$	x	v	$-\frac{dv}{dt}$	x	v	$-\frac{dv}{dt}$
	m	m/s	m/s^2	m	m/s	m/s^2	m	m/s	m/s^2
Dot No.	Shell No. 162			Shell No. 172			Shell No. 182		
1	4.92	—	—	5.96	—	—	4.96	—	—
2	6.80	47.8	—	6.78	29.8	—	6.12	28.3	—
3	8.40	45.3	59	7.92	28.9	23	7.20	27.5	21
4	10.16	43.1	51	9.04	28.0	21	8.32	26.6	20
5	11.86	41.2	48	10.20	27.2	20	9.36	25.9	20
6	13.48	39.3	44	11.28	26.4	20	10.40	25.1	20
7	15.00	37.7	41	12.32	25.6	19	11.40	24.3	19
8	16.48	36.0	39	13.30	24.9	18	12.36	23.6	19
9	17.91	34.6	35	14.32	24.2	18	13.24	22.9	16
10	19.28	33.2	34	15.28	23.5	16	14.12	22.3	16
11	20.55	31.9	31	16.20	22.9	16	15.00	21.6	16
12	21.76	30.7	29	17.08	22.3	16	15.88	21.0	15
13	22.92	29.6	28	17.99	21.6	16	16.70	20.4	14
14	24.12	28.5	28	18.82	21.0	16	17.48	19.9	14
15	25.20	27.4	26	19.68	20.5	13	18.24	19.3	14
16	26.32	26.4	24	20.46	20.0	13	19.00	18.8	13
17	27.32	25.5	23	21.27	19.5	13	19.72	18.3	11
18	28.30	24.6	21	22.12	19.0	13	20.44	17.9	10
19	29.24	23.8	20	22.80	18.5	13	21.16	17.5	10
20	30.16	23.0	20	23.52	18.0	11	21.84	16.1	10
21	31.08	22.2	19	24.20	17.6	10	22.46	16.7	10
22	31.96	21.5	18	24.92	17.2	10	23.12	16.3	10

Table 14e. Horizontal Velocities and Horizontal Negative Accelerations of Stars that Flew Almost Horizontally. (continued)

	x	v	$-\frac{dv}{dt}$	x	v	$-\frac{dv}{dt}$	x	v	$-\frac{dv}{dt}$
	m	m/s	m/s^2	m	m/s	m/s^2	m	m/s	m/s^2
Dot No.	Shell No. 162			Shell No. 172			Shell No. 182		
23	32.80	20.8	16	25.60	16.8	10	23.76	15.9	10
24	33.60	20.2	15	26.26	16.4	10	24.36	15.5	10
25	34.40	17.6	14	26.90	16.0	10	25.00	15.1	10
26	35.20	19.1	13	27.52	15.6	10	25.60	14.7	9
27	35.96	18.6	13	28.12	15.2	10	26.16	14.4	9
28	36.18	18.1	13	28.76	14.8	10	26.74	14.0	9
29	37.44	17.6	13	29.34	14.4	9	27.26	13.7	9
30	38.10	17.1	13	29.92	14.1	9	27.84	13.4	8
31	38.78	16.6	11	30.44	13.7	9	28.38	13.1	8
32	39.46	16.2	11	31.00	13.4	9	28.36	12.8	8
33	40.12	15.7	11	31.54	13.1	8	29.40	12.5	8
34	40.74	15.3	11	32.04	12.8	8	29.90	12.2	8
35	41.36	14.8	11	32.56	12.5	8	30.36	11.9	8
36	41.95	14.4	11	33.03	12.2	8	30.86	11.6	6
37	42.52	14.0	10	33.56	11.9	8	31.32	11.4	6
38	43.05	13.6	10	34.00	11.6	8	31.76	11.1	6
39	43.60	13.2	10	34.50	11.3	—	32.24	10.7	6
40	44.12	12.8	10	34.96	—	—	32.64	10.6	—
41	44.60	12.4	—	37.60			33.08	—	—
42	44.92	—	—			—	35.36		
43	48.00								

Table 14f. Horizontal Velocities and Horizontal Negative Accelerations of Stars that Flew Almost Horizontally.

	x	v	$-\frac{dv}{dt}$	x	v	$-\frac{dv}{dt}$	x	v	$-\frac{dv}{dt}$
	m	m/s	m/s^2	m	m/s	m/s^2	m	m/s	m/s^2
Dot No.	Shell No. 191			Shell No. 202			Shell No. 212		
1	5.40	—	—	8.46	—	—	8.08	—	—
2	6.62	29.8	—	10.34	48.5	—	9.32	37.0	—
3	7.78	28.9	24	12.20	45.6	69	10.92	35.4	40
4	8.92	27.9	24	14.00	43.0	61	12.32	33.8	39
5	9.96	27.0	23	15.68	40.8	51	13.64	32.3	36
6	11.08	26.1	21	17.26	38.9	45	14.88	30.9	34
7	12.16	25.3	20	18.78	37.2	41	16.08	29.6	31
8	13.12	24.5	20	20.24	35.6	40	17.24	28.4	30
9	14.08	23.7	19	21.68	34.0	38	18.32	27.2	28
10	15.00	23.0	18	23.24	32.6	34	19.42	26.2	25
11	15.88	22.3	18	24.32	31.3	31	20.44	25.2	24
12	16.80	21.6	18	25.52	30.1	29	21.44	24.3	23
13	17.63	20.7	18	26.64	29.0	28	22.40	23.4	21
14	18.46	20.2	16	27.80	27.9	26	23.30	22.6	19
15	19.22	19.5	16	28.90	26.9	25	24.16	21.9	19
16	19.97	18.9	15	29.94	25.9	24	25.04	21.1	19
17	20.94	18.3	15	30.92	25.0	23	25.88	20.4	16
18	21.46	17.7	15	31.92	24.1	21	26.70	19.8	16
19	22.14	17.1	15	32.80	23.3	20	27.42	19.1	15
20	22.82	16.5	14	33.72	22.5	20	28.16	18.6	14
21	23.46	16.0	13	34.64	21.7	19	28.96	18.0	14
22	24.10	15.5	13	35.46	21.0	18	29.60	17.5	13
23	24.72	15.0	11	36.28	20.3	18	30.36	16.5	13
24	25.34	14.6	11	37.08	19.6	16	31.04	16.0	13
25	25.90	14.1	11	37.44	19.0	15	31.68	15.5	13
26	26.48	13.7	10	38.66	18.4	15	32.32	15.1	11
27	27.04	13.3	10	39.37	17.8	15	32.88	14.7	11
28	27.56	12.9	9	40.08	17.2	15	33.52	14.2	11
29	28.06	12.6	9	40.77	16.6	14	34.08	13.8	11
30	28.56	12.2	9	41.40	16.1	14	34.64	13.4	10
31	29.08	11.9	8	42.10	15.5	14	35.18	13.1	9
32	29.52	11.6	8	42.65	15.0	13	35.74	12.7	9
33	30.00	11.3	8	43.24	14.5	11	36.26	12.4	9
34	30.46	11.6	—	43.84	14.1	11	36.76	12.0	9
35	30.88	—	—	44.40	13.6	11	37.24	11.7	9
36				44.50	13.2	11	37.72	11.4	8
37				45.44	12.8	11	38.18	11.1	—

Table 14f. Horizontal Velocities and Horizontal Negative Accelerations of Stars that Flew Almost Horizontally. (continued)

	x	v	$-\frac{dv}{dt}$	x	v	$-\frac{dv}{dt}$	x	v	$-\frac{dv}{dt}$
	m	m/s	m/s^2	m	m/s	m/s^2	m	m/s	m/s^2
Dot No.	Shell No. 191			Shell No. 202			Shell No. 212		
38				45.92	12.3	11	38.62	—	—
39				46.40	11.9	9	41.36		
40				46.88	11.6	9			
41				47.34	11.2	9			
42				47.76	10.9	—			
43				48.20	—	—			
44				50.44					

Table 14g. Horizontal Velocities and Horizontal Negative Accelerations of Stars that Flew Almost Horizontally.

	x	v	$-\frac{dv}{dt}$	x	v	$-\frac{dv}{dt}$	x	v	$-\frac{dv}{dt}$
	m	m/s	m/s^2	m	m/s	m/s^2	m	m/s	m/s^2
Dot No.	Shell No. 222			Shell No. 232			Shell No. 241		
1	8.66	—	—	6.80	—	—	9.44	—	—
2	10.54	48.7	—	8.46	41.1	—	11.56	51.0	—
3	12.56	46.4	58	10.08	39.0	51	13.52	47.4	83
4	14.30	44.1	55	11.60	37.0	46	15.32	44.4	68
5	16.00	42.0	51	13.00	35.3	43	17.08	42.0	58
6	17.68	40.0	46	14.36	33.6	40	18.68	39.8	51
7	19.33	38.3	43	15.68	32.1	36	20.26	37.9	46
8	20.36	36.6	40	16.92	30.7	34	21.72	36.1	44
9	22.22	35.1	36	18.22	29.4	31	23.14	34.4	41
10	23.68	33.7	35	19.32	28.2	30	24.44	32.8	40
11	25.02	32.3	34	20.40	27.0	27	25.70	31.2	38
12	26.28	31.0	33	21.46	25.9	26	26.92	29.8	35
13	27.48	29.7	30	22.46	24.9	25	28.08	28.5	34
14	28.62	28.6	29	23.44	23.9	24	29.20	27.4	33
15	29.72	27.4	29	24.42	23.0	23	30.28	26.2	31
16	30.34	26.3	26	25.32	22.1	21	31.30	25.1	29
17	31.34	25.3	24	26.12	21.3	21	32.22	24.1	28
18	32.88	24.4	23	26.94	20.4	20	33.20	23.2	25
19	33.80	23.5	23	27.30	19.7	18	34.08	22.2	23
20	34.76	22.6	21	28.52	19.0	18	34.94	21.4	23
21	35.60	21.8	20	29.24	18.3	16	35.84	20.6	23
22	36.48	21.0	18	29.96	17.7	15	36.64	19.9	23

Table 14g. Horizontal Velocities and Horizontal Negative Accelerations of Stars that Flew Almost Horizontally. (continued)

	x	v	$-\frac{dv}{dt}$	x	v	$-\frac{dv}{dt}$	x	v	$-\frac{dv}{dt}$
	m	m/s	m/s^2	m	m/s	m/s^2	m	m/s	m/s^2
Dot No.	Shell No. 222			Shell No. 232			Shell No. 241		
23	37.40	20.4	16	30.64	17.1	15	37.36	19.1	20
24	38.16	19.7	16	31.32	16.5	14	38.16	18.5	19
25	38.92	19.1	15	32.00	16.0	13	38.86	17.8	19
26	39.70	18.5	15	32.64	15.5	13	39.54	17.1	16
27	40.44	17.9	14	33.20	15.0	13	40.20	16.5	15
28	41.14	17.4	14	33.80	14.5	11	40.87	15.9	15
29	41.86	16.8	14	34.40	14.1	10	41.50	15.3	15
30	42.48	16.3	13	34.98	13.7	10	42.06	14.8	14
31	43.18	15.8	11	35.52	13.3	10	42.66	14.2	11
32	43.82	15.4	11	36.08	12.9	10	43.24	13.7	11
33	44.40	14.9	11	36.56	12.5	9	43.78	13.2	11
34	44.56	14.5	10	37.06	12.2	9	44.30	12.7	10
35	45.56	14.1	9	37.56	11.8	9	44.78	12.2	10
36	46.12	13.8	9	38.00	11.5	8	45.28	11.8	—
37	46.68	13.4	9	38.48	11.2	8	45.72	—	—
38	47.20	13.1	9	38.92	10.9	8	48.60		
39	47.68	12.7	9	39.32	10.6	8			
40	48.20	12.4	8	39.72	10.3	6			
41	48.72	12.1	8	40.12	10.1	—			
42	49.18	11.8	—	40.54	—	—			
43	49.60	—	—	42.00					
44	52.24								

Table 14h. Horizontal Velocities and Horizontal Negative Accelerations of Stars that Flew Almost Horizontally.

	x	v	$-\frac{dv}{dt}$	x	v	$-\frac{dv}{dt}$	x	v	$-\frac{dv}{dt}$
	m	m/s	m/s^2	m	m/s	m/s^2	m	m/s	m/s^2
Dot No.	Shell No. 281			Shell No. 291			Shell No. 302		
1	6.00	—	—	17.12	—	—	19.10	—	—
2	17.76	47.9	—	17.20	51.0	—	20.76	44.3	—
3	19.50	44.1	86	21.20	47.4	89	22.64	40.8	79
4	21.06	41.0	75	22.96	43.9	80	24.22	38.0	65
5	22.54	38.1	70	24.76	41.0	68	25.64	35.6	56
6	23.88	35.4	63	26.36	38.5	61	27.08	33.5	51
7	25.16	33.1	56	27.84	36.1	59	28.36	31.5	49
8	26.32	30.9	51	29.24	33.8	55	29.60	29.6	44
9	27.40	29.0	45	30.56	31.7	50	30.76	28.0	39
10	28.44	27.3	41	31.76	29.8	45	31.76	26.5	36
11	29.42	25.7	39	33.00	28.1	41	32.80	25.1	34
12	30.36	24.2	36	34.08	26.5	39	33.76	23.8	33
13	31.24	22.8	34	35.12	25.0	36	34.68	22.5	29
14	32.00	21.5	31	36.08	23.6	34	35.56	21.5	26
15	32.84	20.3	29	37.00	22.3	31	36.40	20.4	26
16	33.16	19.2	28	37.92	21.1	29	37.12	19.4	24
17	34.26	18.1	25	38.76	20.0	26	37.96	18.5	21
18	34.92	17.2	23	39.54	19.0	25	38.60	17.7	21
19	35.60	16.3	23	40.28	18.0	24	39.30	16.8	21
20	36.24	15.4	—	40.99	17.1	23	39.98	16.0	20
21	36.78	—	—	41.68	16.2	—	40.59	15.2	19
22	39.80			42.32	—	—	41.18	14.5	—
23				45.80			41.76	—	—
24							45.00		

Table 14i. Horizontal Velocities and Horizontal Negative Accelerations of Stars that Flew Almost Horizontally.

	x	v	$-\frac{dv}{dt}$	x	v	$-\frac{dv}{dt}$	x	v	$-\frac{dv}{dt}$
	m	m/s	m/s^2	m	m/s	m/s^2	m	m/s	m/s^2
Dot No.	Shell No. 312			Shell No. 343			Shell No. 352		
1	12.40	—	—	23.64	—	—	16.00	—	—
2	14.20	43.0	—	25.88	53.0	—	17.92	45.0	—
3	15.84	40.2	68	27.88	48.9	95	19.60	41.2	83
4	17.42	37.6	64	29.72	45.4	84	21.20	38.4	68
5	18.92	35.1	61	31.48	42.2	73	22.72	35.8	60
6	20.30	32.7	55	33.16	39.6	63	24.16	33.6	54
7	21.52	30.7	49	34.72	37.2	56	25.42	31.5	49
8	22.76	28.8	45	36.20	35.1	53	26.64	29.7	44
9	23.88	27.1	40	37.52	33.0	51	27.78	28.0	40
10	24.90	25.6	38	38.76	31.0	49	28.92	26.5	38
11	25.92	24.1	35	40.00	29.1	44	29.96	25.0	35
12	26.38	22.8	33	41.14	27.5	39	30.92	23.7	33
13	27.68	21.5	30	42.20	26.0	35	31.80	22.4	30
14	28.52	20.4	28	43.18	24.7	33	32.68	21.3	28
15	29.32	19.3	26	44.12	23.4	30	33.52	20.2	26
16	30.08	18.3	24	45.08	22.3	28	34.28	19.2	24
17	30.80	17.4	21	45.92	21.2	26	35.04	18.3	23
18	31.48	16.6	20	46.80	20.2	24	35.80	17.4	21
19	32.04	15.8	19	47.60	19.3	21	36.44	16.6	20
20	32.72	15.1	—	48.28	18.5	20	37.12	15.8	20
21	33.28	—	—	49.04	17.7	19	37.72	15.0	—
22	36.44			49.72	17.0	16	38.32	—	—
23				50.38	16.4	—	45.40		
24				51.08	—	—			
25				54.40					

Table 14j. Horizontal Velocities and Horizontal Negative Accelerations of Stars that Flew Almost Horizontally.

	x	v	$-\frac{dv}{dt}$	x	v	$-\frac{dv}{dt}$	x	v	$-\frac{dv}{dt}$
	m	m/s	m/s^2	m	m/s	m/s^2	m	m/s	m/s^2
Dot No.	Shell No. 362			Shell No. 371			Shell No. 382		
1	21.44	—	—	10.68	—	—	14.00	—	—
2	23.82	58.8	—	12.88	54.6	—	16.64	65.0	—
3	26.06	53.9	119	15.04	51.6	70	19.14	60.1	113
4	28.18	49.3	106	17.04	49.0	64	21.52	56.0	96
5	30.04	45.4	89	18.96	46.5	61	23.58	52.4	81
6	31.80	42.2	78	20.80	44.1	58	25.58	49.5	68
7	33.36	39.2	73	22.48	41.9	55	27.56	47.0	63
8	34.88	36.4	64	24.12	39.7	51	29.40	44.5	60
9	36.32	34.1	55	25.70	37.8	46	31.18	42.2	55
10	37.68	32.0	51	27.12	36.0	45	32.80	40.1	50
11	38.84	30.0	46	28.48	34.2	41	34.32	38.2	46
12	40.00	28.3	41	29.82	32.7	38	35.78	36.4	43
13	41.04	26.7	39	31.11	31.2	36	37.28	34.8	39
14	42.08	25.2	36	32.34	29.8	34	38.68	33.3	36
15	43.08	23.8	34	33.46	28.5	31	37.70	31.9	35
16	44.04	22.5	31	34.60	27.3	29	41.12	30.5	34
17	44.90	21.3	29	35.64	26.2	26	42.28	29.2	33
18	45.72	20.2	26	36.72	25.2	25	43.44	27.9	31
19	46.56	19.2	25	37.72	24.2	25	44.56	26.7	29
20	47.30	18.2	24	38.68	23.2	24	45.64	25.6	28
21	48.04	17.3	21	39.60	22.3	21	46.60	24.5	25
22	48.72	16.5	20	40.44	21.5	20	47.54	23.6	23
23	49.36	15.7	—	41.32	20.7	20	48.48	22.7	23
24	50.00	—	—	42.16	19.9	19	49.38	21.8	23
25	53.44			43.00	19.2	18	50.24	20.9	23
26				43.74	18.5	18	51.04	20.0	20
27				44.48	17.8	16	51.84	19.3	19
28				45.12	17.2	15	52.60	18.5	19
29				45.84	16.6	15	53.34	17.8	16
30				46.52	16.0	14	54.04	17.2	15
31				47.16	15.5	13	54.68	16.6	15
32				47.80	15.0	13	55.32	16.0	15
33				48.36	14.5	11	55.96	15.4	14
34				49.00	14.1	10	56.62	14.9	11
35				49.56	13.7	10	57.20	14.5	11
36				50.08	13.3	10	57.80	14.0	11
37				50.56	12.9	9	58.32	13.6	10

Table 14j. Horizontal Velocities and Horizontal Negative Accelerations of Stars that Flew Almost Horizontally. (continued)

	x	v	$-\frac{dv}{dt}$	x	v	$-\frac{dv}{dt}$	x	v	$-\frac{dv}{dt}$
	m	m/s	m/s^2	m	m/s	m/s^2	m	m/s	m/s^2
Dot No.	Shell No. 362			Shell No. 371			Shell No. 382		
38				51.04	12.6	9	58.84	13.2	10
39				51.60	12.2	—	59.34	12.8	—
40				52.08	—	—	59.64	—	—
41				54.60			60.20		

Table 14k. Horizontal Velocities and Horizontal Negative Accelerations of Stars that Flew Almost Horizontally.

	x	v	$-\frac{dv}{dt}$	x	v	$-\frac{dv}{dt}$	x	v	$-\frac{dv}{dt}$
	m	m/s	m/s^2	m	m/s	m/s^2	m	m/s	m/s^2
Dot No.	Shell No. 392			Shell No. 403			Shell No. 411		
1	8.68	—	—	12.40	—	—	7.44	—	—
2	11.00	53.5	—	15.28	67.3	—	11.40	46.0	—
3	12.96	48.5	106	17.80	62.9	108	13.12	44.0	50
4	14.72	45.0	78	20.18	58.7	99	14.86	42.0	50
5	16.40	42.3	55	22.56	55.0	85	16.48	40.0	46
6	18.12	40.6	53	24.44	51.9	70	18.04	38.3	43
7	19.66	38.1	53	26.48	49.4	63	19.52	36.6	41
8	21.16	36.4	41	28.44	46.9	59	21.00	35.0	38
9	22.56	34.8	39	30.28	44.7	53	22.44	33.6	34
10	23.96	33.3	36	32.02	42.7	60	23.80	32.3	31
11	25.28	31.9	33	33.64	40.8	46	25.00	31.1	30
12	26.60	30.7	30	35.24	39.0	44	26.14	29.9	30
13	27.72	29.5	29	36.80	37.3	40	27.28	28.7	28
14	28.92	28.4	26	38.31	35.8	36	28.40	27.7	26
15	30.08	27.4	25	39.67	34.4	34	29.50	26.6	25
16	31.16	26.4	24	41.00	33.1	33	30.56	25.7	24
17	32.20	25.5	23	42.32	31.8	30	31.56	24.7	23
18	33.16	24.6	21	43.56	30.7	29	32.52	23.9	21
19	34.12	23.8	20	44.76	29.5	28	33.48	23.0	21
20	35.08	23.0	17	45.88	28.5	25	34.36	22.2	19
21	36.00	22.3	18	47.04	27.5	24	35.24	21.5	19
22	36.92	21.6	16	48.08	26.6	21	36.04	20.7	19
23	37.80	21.0	16	49.16	25.8	21	36.88	20.0	18
24	38.60	20.3	16	50.20	24.9	21	37.68	19.3	18
25	39.40	19.7	14	51.16	24.1	20	38.44	18.6	18

Table 14k. Horizontal Velocities and Horizontal Negative Accelerations of Stars that Flew Almost Horizontally. (continued)

	x	v	$-\frac{dv}{dt}$	x	v	$-\frac{dv}{dt}$	x	v	$-\frac{dv}{dt}$
	m	m/s	m/s^2	m	m/s	m/s^2	m	m/s	m/s^2
Dot No.	Shell No. 392			Shell No. 403			Shell No. 411		
26	40.20	19.2	14	52.04	23.3	19	39.20	18.0	18
27	41.00	18.6	14	52.96	22.6	18	39.92	17.3	16
28	41.72	18.1	13	53.88	21.9	18	40.54	16.7	15
29	42.40	17.6	13	54.80	21.2	16	41.34	16.1	14
30	43.14	17.1	11	55.64	20.6	15	41.94	15.6	13
31	43.80	16.5	11	56.40	20.0	14	42.48	15.1	13
32	44.48	16.1	11	57.20	19.5	14	43.16	14.6	13
33	45.16	15.6	11	57.96	18.9	14	43.64	14.1	13
34	45.72	15.2	11	58.72	18.4	11	44.16	13.6	—
35	46.32	14.7	10	59.46	18.0	10	44.76	—	—
36	46.94	14.3	10	60.12	17.6	10	45.32		
37	47.46	13.9	10	60.80	17.2	10			
38	48.04	13.5	10	61.56	16.8	8			
39	48.56	13.1	10	62.20	16.5	8			
40	49.04	12.7	—	62.76	16.2	8			
41	49.60	—	—	63.40	15.9	—			
42	51.72			64.04	—	—			
43				67.12					

Table 14l. Horizontal Velocities and Horizontal Negative Accelerations of Stars that Flew Almost Horizontally.

	x	v	$-\frac{dv}{dt}$	x	v	$-\frac{dv}{dt}$	x	v	$-\frac{dv}{dt}$
	m	m/s	m/s^2	m	m/s	m/s^2	m	m/s	m/s^2
Dot No.	Shell No. 422			Shell No. 442			Shell No. 452		
1	8.72	—	—	6.64	—	—	8.40	—	—
2	10.72	45.8	—	8.20	40.2	—	10.44	47.4	—
3	12.40	43.6	53	9.72	38.7	36	12.18	44.7	64
4	14.04	41.6	47	11.28	37.3	35	14.00	42.3	56
5	15.68	39.4	45	12.76	35.9	35	15.62	40.2	49
6	17.24	38.0	40	14.16	34.5	33	17.20	38.4	44
7	18.72	36.5	38	15.48	33.3	30	18.70	36.7	40
8	20.16	35.0	35	16.80	32.1	29	20.12	35.2	35
9	21.52	33.7	34	18.04	31.0	28	21.58	33.9	33
10	22.88	32.3	34	19.36	29.9	25	22.84	32.6	33
11	24.10	31.0	31	20.48	29.0	24	24.06	31.3	31

Table 14l. Horizontal Velocities and Horizontal Negative Accelerations of Stars that Flew Almost Horizontally. (continued)

	x	v	$-\frac{dv}{dt}$	x	v	$-\frac{dv}{dt}$	x	v	$-\frac{dv}{dt}$
	m	m/s	m/s^2	m	m/s	m/s^2	m	m/s	m/s^2
Dot No.	Shell No. 422			Shell No. 442			Shell No. 452		
12	25.26	29.8	29	21.64	28.0	24	25.32	30.1	29
13	26.44	28.7	28	22.72	27.1	23	26.44	29.0	26
14	24.60	27.6	26	23.80	26.2	20	27.64	28.0	25
15	28.64	26.6	25	24.84	25.5	19	28.68	27.0	24
16	29.68	25.6	25	25.84	24.7	19	29.72	26.1	24
17	30.60	24.6	23	26.80	24.0	16	30.76	25.1	24
18	31.60	23.8	21	27.76	23.4	15	31.72	24.2	21
19	32.52	22.9	21	28.68	22.8	15	32.70	23.4	19
20	33.42	22.1	19	29.60	22.2	14	33.56	22.7	19
21	34.28	21.4	18	30.48	21.7	13	34.44	21.9	19
22	25.12	20.7	16	31.32	21.2	13	35.32	21.2	16
23	36.00	20.1	16	32.16	20.7	13	36.12	20.6	16
24	36.80	19.4	15	33.04	20.2	13	36.94	20.3	16
25	37.52	18.9	14	33.80	19.7	13	37.74	19.3	16
26	38.28	18.3	14	34.60	19.2	13	38.44	18.7	14
27	39.04	17.8	13	35.36	18.7	11	39.20	18.2	14
28	39.80	17.3	13	36.12	18.3	11	39.96	17.6	14
29	40.50	16.8	11	36.84	17.8	11	40.64	17.1	13
30	41.16	16.4	11	37.56	17.4	10	41.32	16.6	13
31	41.82	15.9	11	38.28	17.0	10	42.00	16.1	13
32	42.42	15.5	10	38.94	16.6	10	42.64	15.6	13
33	43.08	15.1	10	39.66	16.2	10	43.26	15.1	11
34	43.66	14.7	10	40.30	15.8	9	43.90	14.7	11
35	44.24	14.3	10	40.96	15.5	9	44.48	14.2	11
36	44.80	13.9	9	41.60	15.1	9	45.04	13.8	10
37	45.36	13.6	8	42.12	14.7	9	45.60	13.4	10
38	45.88	13.3	—	42.80	14.4	9	46.12	13.0	10
39	46.44	—	—	43.32	14.0	9	46.64	12.6	—
40	49.48			43.92	13.7	8	45.12	—	—
41				44.48	13.4	8	49.68		
42				45.00	13.1	—			
43				45.48	—	—			
44				48.88					

Table 14m. Horizontal Velocities and Horizontal Negative Accelerations of Stars that Flew Almost Horizontally.

	x	v	$-\frac{dv}{dt}$	x	v	$-\frac{dv}{dt}$	x	v	$-\frac{dv}{dt}$
	m	m/s	m/s^2	m	m/s	m/s^2	m	m/s	m/s^2
Dot No.	Shell No. 471			Shell No. 481			Shell No. 502		
1	11.44	—	—	15.96	—	—	6.20	—	—
2	13.64	56.5	—	18.92	73.5	—	7.96	42.3	—
3	15.88	53.3	83	21.84	67.5	143	9.58	40.4	45
4	17.98	50.0	75	24.32	62.1	121	11.16	38.7	41
5	20.00	47.3	63	26.76	57.8	101	12.68	37.1	39
6	21.80	45.0	58	29.00	54.0	90	14.08	35.6	35
7	23.52	42.7	55	31.10	50.6	80	15.48	34.3	35
8	25.12	40.6	50	32.92	47.6	71	16.84	32.8	35
9	26.76	38.7	46	34.74	44.9	65	18.08	31.5	33
10	28.24	36.9	44	36.54	42.4	61	19.32	30.3	29
11	29.70	35.2	41	38.24	40.0	55	20.56	29.2	28
12	31.04	33.6	40	39.74	38.0	49	21.66	28.1	26
13	32.36	32.0	38	41.24	36.1	46	22.76	27.1	24
14	33.64	30.6	35	42.60	34.3	43	23.84	26.2	23
15	34.86	29.2	34	43.98	32.7	40	24.84	25.3	21
16	35.96	27.9	30	45.20	31.1	39	25.82	24.5	20
17	37.04	26.8	29	46.38	29.6	35	26.74	23.7	20
18	38.04	25.7	26	47.56	28.3	33	27.68	22.9	19
19	39.14	24.7	24	58.68	27.0	30	28.64	22.2	18
20	40.16	23.8	23	49.72	25.9	29	29.50	21.5	16
21	41.08	22.9	23	50.76	24.7	28	30.32	20.9	15
22	41.96	22.0	21	51.72	23.7	25	31.08	20.3	15
23	42.80	21.2	19	52.60	22.7	24	31.92	19.7	15
24	43.64	20.5	19	53.48	21.8	23	32.72	19.1	14
25	44.52	19.7	19	54.36	20.9	23	33.44	18.6	13
26	45.28	19.0	18	55.20	20.0	20	34.16	18.1	13
27	46.08	18.3	16	55.96	19.3	19	34.92	17.6	13
28	46.80	17.7	15	56.68	18.5	19	35.60	17.1	11
29	47.48	17.1	15	57.48	17.8	18	36.22	16.7	10
30	48.16	16.5	14	58.20	17.1	18	36.88	16.3	10
31	48.84	16.0	13	58.90	16.4	16	37.52	15.9	10
32	49.52	15.5	13	59.52	15.8	15	38.10	15.5	10
33	49.76	15.0	11	60.16	15.2	15	38.76	15.1	9
34	50.76	14.6	10	60.76	14.6	15	39.38	14.8	9
35	51.30	14.2	10	61.40	14.0	15	39.96	14.4	9
36	51.92	13.8	—	61.96	13.4	14	40.50	14.1	9
37	52.40	—	—	62.40	12.9	13	41.08	13.7	9

Table 14m. Horizontal Velocities and Horizontal Negative Accelerations of Stars that Flew Almost Horizontally. (continued)

	x	v	$-\frac{dv}{dt}$	x	v	$-\frac{dv}{dt}$	x	v	$-\frac{dv}{dt}$
	m	m/s	m/s^2	m	m/s	m/s^2	m	m/s	m/s^2
Dot No.	Shell No. 471			Shell No. 481			Shell No. 502		
38	52.88			62.92	12.4	—	41.66	13.4	9
39				63.44	—	—	42.16	13.0	8
40				66.36			42.70	12.7	8
41							43.20	12.4	8
42							43.64	12.1	8
43							44.16	11.8	8
44							44.64	11.5	8
45							45.08	11.2	8
46							45.60	11.0	8
47							45.98	10.7	6
48							46.44	10.5	6
49							46.84	10.3	6
50							47.20	10.0	6
51							47.64	9.8	5
52							48.02	9.6	5
53							48.36	9.3	5
54							48.80	9.2	5
55							49.16	9.0	5
56							49.48	8.8	5
57							49.84	8.6	5
58							50.24	8.4	5
59							50.52	8.2	5
60							50.84	8.0	5
61							51.16	7.8	4
62							51.48	7.7	4
63							51.76	7.5	4
64							52.00	7.4	—
65							52.36	—	—
66									

Table 14n. Horizontal Velocities and Horizontal Negative Accelerations of Stars that Flew Almost Horizontally.

	x	v	$-\frac{dv}{dt}$	x	v	$-\frac{dv}{dt}$	x	v	$-\frac{dv}{dt}$
	m	m/s	m/s^2	m	m/s	m/s^2	m	m/s	m/s^2
Dot No.	Shell No. 503			Shell No. 505			Shell No. 542		
1	4.01	—	—	2.76	—	—	8.32	—	—
2	5.66	39.9	—	3.88	27.0	—	10.48	49.1	—
3	7.20	38.2	43	4.92	25.8	30	12.32	46.4	61
4	8.72	36.5	41	5.96	24.6	28	14.08	44.2	53
5	10.08	34.9	38	6.88	23.6	25	15.72	42.2	48
6	11.40	33.5	35	7.30	22.6	24	17.36	40.4	44
7	12.68	32.1	35	8.64	21.7	21	19.02	38.7	41
8	19.36	30.7	31	9.56	20.9	20	20.50	37.1	38
9	15.16	29.6	28	10.32	20.1	20	21.92	35.7	34
10	16.32	28.5	28	11.08	19.3	20	23.30	34.4	31
11	17.44	27.4	25	11.84	18.5	18	24.60	33.2	30
12	18.52	26.5	23	12.52	17.9	15	25.88	32.0	29
13	19.56	25.6	23	13.28	17.3	15	27.16	30.9	26
14	20.60	24.7	21	14.00	16.7	14	28.40	29.9	25
15	21.54	23.9	20	14.64	16.2	11	29.48	28.9	24
16	22.48	23.1	20	15.30	15.8	11	30.68	28.0	24
17	23.32	22.3	19	15.92	15.3	11	31.80	27.0	23
18	24.20	21.6	18	16.58	14.9	10	32.84	26.2	21
19	25.04	20.9	16	17.20	14.5	10	33.86	25.3	20
20	25.88	20.3	16	17.76	14.1	9	34.64	24.6	18
21	26.72	19.6	16	18.36	13.8	9	35.76	23.9	18
22	27.46	19.0	14	18.88	13.4	9	36.68	23.2	18
23	28.24	18.5	13	19.44	13.1	8	37.60	22.5	16
24	28.96	18.0	13	19.96	12.8	6	38.56	21.9	16
25	29.72	17.5	11	20.48	12.6	6	39.32	21.2	16
26	30.44	17.1	11	21.00	12.3	6	40.12	20.6	—
27	31.04	16.6	11	21.36	12.1	6	40.96	20.0	15
28	31.72	16.2	11	21.84	11.8	6	41.79	19.4	—
29	32.40	15.8	9	22.36	11.6	5	42.52	18.9	13
30	33.04	15.5	9	22.76	11.4	5	43.20	18.4	13
31	33.60	15.1	9	23.24	11.2	5	43.92	17.7	13
32	34.20	14.8	8	23.72	11.0	4	44.56	17.4	11
33	34.76	14.5	9	24.12	10.9	4	45.32	17.0	11
34	35.32	14.1	9	24.60	10.7	4	46.00	16.5	11
35	35.92	13.8	8	25.04	10.6	4	46.68	16.1	10
36	36.44	13.5	8	25.44	10.4	4	47.28	15.7	10
37	37.04	13.2	8	25.84	10.3	4	47.96	15.3	9

Table 14n. Horizontal Velocities and Horizontal Negative Accelerations of Stars that Flew Almost Horizontally. (continued)

	x	v	$-\frac{dv}{dt}$	x	v	$-\frac{dv}{dt}$	x	v	$-\frac{dv}{dt}$
	m	m/s	m/s^2	m	m/s	m/s^2	m	m/s	m/s^2
Dot No.	Shell No. 503			Shell No. 505			Shell No. 542		
38	37.54	12.9	8	26.24	10.1	4	48.48	15.0	9
39	38.00	12.6	8	26.72	10.0	4	49.12	14.6	9
40	38.48	12.3	8	27.12	9.9	4	49.72	14.3	9
41	39.00	12.0	8	27.48	9.7	4	50.28	13.9	9
42	39.40	11.7	8	27.88	9.6	3	50.84	13.6	8
43	39.94	11.4	6	28.24	9.5	3	51.36	13.3	8
44	40.36	11.2	6	28.64	9.4	3	51.96	13.0	8
45	40.80	10.9	6	29.04	9.3	3	52.44	12.7	6
46	41.28	10.8	6	29.44	9.2	3	52.92	12.5	6
47	41.68	10.4	5	29.78	9.1	3	53.44	12.2	6
48	42.12	10.2	5	30.16	9.0	3	53.92	12.0	6
49	42.52	10.0	5	30.52	8.9	2	54.44	11.7	6
50	42.92	9.8	5	30.88	8.85	1	54.88	11.4	6
51	43.28	9.6	5	31.24	8.80	1	55.36	11.2	6
52	43.68	9.4	5	31.56	8.75	1	55.80	10.9	6
53	44.00	9.2	5	31.92	8.70	1	56.20	10.7	6
54	44.32	9.0	5	32.28	8.65	1	56.66	10.5	6
55	44.72	8.8	4	32.64	8.60	1	57.06	10.2	6
56	45.08	8.7	4	32.96	8.60	1	57.44	10.0	6
57	45.36	8.5	4	33.28	8.55	0.9	57.86	9.8	6
58	45.76	8.4	4	33.60	8.53	0.6	58.24	9.5	6
59	46.08	8.2	—	33.92	8.50	0.4	58.64	9.3	5
60	46.36	—	—	34.24	8.50		59.00	9.1	5
61	48.88			34.52	8.50		59.24	8.9	5
62				—	8.50		59.40	8.7	5
63				—	8.50		59.92	8.5	5
64				35.56	—		60.28	8.3	4
65				37.56			60.56	8.2	4
66							60.92	8.0	4
67							61.20	7.9	4
68							61.55	7.7	4
69							61.80	7.6	3
70							62.12	7.5	3
71							62.44	7.4	3
72							62.80	7.3	—
73							63.08	—	—
74							65.36		

Table 14o. Horizontal Velocities and Horizontal Negative Accelerations of Stars that Flew Almost Horizontally.

	x	v	$-\frac{dv}{dt}$	x	v	$-\frac{dv}{dt}$
	m	m/s	m/s^2	m	m/s	m/s^2
Dot No.	Shell No. 543			Shell No. 544		
1	7.40	—	—	6.08	—	—
2	9.00	40.1	—	7.48	33.5	—
3	10.60	38.5	41	87.6	32.0	36
4	12.16	36.8	39	10.04	30.6	33
5	13.56	35.4	35	11.20	29.4	30
6	14.88	34.0	34	12.36	28.2	30
7	16.26	32.7	31	13.48	27.0	28
8	17.60	31.5	30	14.60	26.0	24
9	18.80	30.3	29	15.64	25.1	24
10	19.96	29.2	26	16.60	24.1	24
11	21.08	28.2	25	17.52	23.2	21
12	22.16	27.2	25	18.44	22.4	20
13	23.28	26.2	24	19.32	21.6	19
14	24.34	25.3	21	20.20	20.9	18
15	25.24	24.5	21	20.90	20.2	18
16	26.28	23.6	21	21.92	19.5	16
17	27.16	22.8	20	22.72	18.9	14
18	28.12	22.0	20	23.48	18.4	14
19	28.96	21.2	19	24.12	17.8	14
20	29.76	20.5	18	24.80	17.2	14
21	30.52	19.8	16	25.48	16.7	13
22	31.32	19.2	15	26.20	16.2	11
23	32.12	18.6	15	26.80	15.8	11
24	32.80	18.0	14	27.44	15.3	11
25	33.56	17.5	13	28.04	14.9	10
26	34.20	17.0	11	28.68	14.5	10
27	34.92	16.6	10	29.20	14.1	9
28	35.60	16.2	10	29.76	13.8	9
29	36.24	15.8	10	30.32	13.4	9
30	36.88	15.4	10	30.84	13.1	8
31	37.48	15.0	9	31.40	12.8	8
32	38.08	14.7	9	31.86	12.5	6
33	38.64	14.4	9	32.40	12.3	6
34	39.24	14.0	9	32.84	12.0	6
35	39.80	13.7	8	33.36	11.8	6
36	40.36	13.4	8	33.80	11.5	5
37	40.88	13.1	8	34.28	11.4	5

Table 14o. Horizontal Velocities and Horizontal Negative Accelerations of Stars that Flew Almost Horizontally. (continued)

	x	v	$-\frac{dv}{dt}$	x	v	$-\frac{dv}{dt}$
	m	m/s	m/s^2	m	m/s	m/s^2
Dot No.	Shell No. 543			Shell No. 544		
38	41.44	12.8	8	34.72	11.1	5
39	42.00	12.5	8	35.16	11.0	5
40	42.60	12.2	8	35.56	10.8	5
41	43.16	11.9	8	36.00	10.8	5
42	43.40	11.6	6	36.44	10.4	4
43	43.88	11.4	6	36.84	10.3	4
44	44.28	11.1	6	37.28	10.1	4
45	44.76	10.9	6	37.72	10.0	4
46	45.24	10.7	6	38.12	9.8	4
47	45.72	10.4	6	38.52	9.7	4
48	46.12	10.2	6	38.92	9.5	4
49	46.54	10.0	5	39.28	9.3	4
50	46.54	9.8	5	39.96	9.2	4
51	47.36	9.6	4	40.28	9.0	4
52	47.72	9.5	4	40.68	8.9	4
53	48.16	9.3	4	41.00	8.8	4
54	48.48	9.2	4	41.40	8.6	4
55	48.84	9.0	4	41.74	8.4	4
56	49.20	8.8	3	41.80	8.3	4
57	49.68	8.7	3	42.14	8.1	4
58	49.96	8.6	3	42.44	8.0	4
59	50.36	8.5	3	42.80	7.9	—
60	50.64	8.4	3	43.08	—	—
61	51.00	8.3	—	45.36		
62	51.24					

6.2.2 The Burn Time of Stars

The burn time of a star, not including the core, and initial ignition material is determined by counting the dots along the trajectory in the photograph. The number of dots is shown in Table 15.

I. The Stars of B_8.

Table 15a. Number of Dots in the Trajectory of the Stars.

No.*	n*	No.	n	No.	n
21	22	261	22	317	19
31	25	262	20	318	20
33	22	263	22	319	21
34	20	264	20	331	23
42	19	265	22	332	23
43	21	266	20	333	22
51	25	267	19	334	21
52	22	268	21	335	23
53	18	269	19	336	21
54	21	272	25	337	17
55	19	273	22	338	19
56	17	275	24	339	16
57	20	277	21	3310	18
62	23	278	20	3311	18
63	21	281	22	342	18
64	21	282	22	343	24
72	23	283	20	345	22
73	22	284	25	346	18
74	23	285	21	347	17
82	21	286	21	349	20
83	21	287	25	3410	20
84	22	288	20	3411	20
91	23	289	21	351	17
92	24	2810***	20	352	21
93	24	2811	21	353	21
94	22	2812	17	354	19
101	22	291	19	355	22
102	22	292	22	356	21
103	25	293	23	358	18
111	22	294	19	359	18
112	18	295	20	361	21
113	22	296	21	362	23
114	19	297	20	363	20
115	21	298	20	364	20
252	21	302	20	365	19
253	21	303	22	366	16
254	20	304	21	367	21
255	21	305	19	368	19
256	23	306	19	368	18
257	22	312	21	3610	19
258	21	313	23	3611	18
252'	21	314	22		
258'	25	315	18		
		316	19		

* No. denotes the number of the star.

** n denotes the number of dots counted along the trajectory in the photograph.

*** The first 1 or 2 digits (e.g., 28) denotes the shell number; the second 1 or 2 digits (e.g., 10) denotes which star this is from the horizontal position.

II. The Stars of B_{12}

Table 15b. Number of Dots in the Trajectory of the Stars.

No.*	n**	No.	n	No.	n
132	38	213	42	403	40
133	37	215	35	404	36
134	38	222	43	405	37
142	42	223	41	406	35
143	39	224	39	407	30
144	39	225	38	411	36
145	42	232	42	412	38
151	42	233	40	413	39
152	40	234	39	421	35
153	40	241	37	422	39
154	39	242	41	423	41
155	39	243	42	442	43
162	42	244	41	444	39
163	42	371	40	445	38
164	41	372	35	452	40
165	40	373	40	453	41
172	40	374	37	455	36
173	41	375	36	456	36
174	42	376	34	471	38
182	41	382	40	472	43
184	39	383	38	472	40
191	34	384	41	481	39
192	39	385	40	482	37
193	37	386	39	483	39
194	37	387	40	484	38
202	42	391	35	485	40
203	36	392	39	486	36
204	39	393	39	493	37
205	35	394	36	494	36
206	38	394	34	496	35

* No. denotes the number of the star.

** n denotes the number of dots counted along the trajectory in the photograph.

Table 16. The Burn Time, Burn Velocity and the Probability Deviation of the Burn Time (from the Image of the Trajectory of the Star).

	N	Σn	$\bar{n}$	T_1(s)	$R_1 - R_2$(mm)	w_1(mm/s)	R_T(s)	R_T/T_1
B_8	128	2658	20.77	0.53	1.35	1.63	0.055	0.066
B_{12}	90	3480	35.67	1.54	3.00	1.95	0.057	0.037
G_{12}	9	574	63.77	2.55	3.00	1.18	0.103	0.040

III. The Stars of G12

Table 15c. Number of Dots in the Trajectory of the Stars.

No.*	n**	No.	n
502	65	542	73
503	60	543	62
504	64	544	61
505	63	545	62
		546	64

* No. denotes the number of the star.

** n denotes the number of dots counted along the trajectory in the photograph.

The image of the trajectory of the stars in the photograph shows that at the start, the light output from the burning of the Black Powder type ignition composition was weak (Photo 8A). The revolving shutter did not capture the image of the trajectory at the start of the ignition. However, at the start of the color composition, the image was captured sharply. At the end, a core flash appeared. In this case, the light is too bright and could not be captured clearly. Consequently, the burn rate of the star can be calculated only during the color part of the composition.

Therefore, for the calculation of the burn time of the color part of the composition of a star, we can use the number of dots in Tables 15 a, b, and c. The burn time of the color part of the composition is therefore

$$T_1 = \frac{\Sigma n}{N} \times \frac{1}{25} = 0.04\bar{n}$$

where T_1 is the average burn time for N stars with the color composition, n is the number of dots, and $\bar{n}$ is the average number of dots per one star. The probability deviation of the burn time is

$$R_T = 0.6745 \times 0.04 \sqrt{\frac{\sum (n - \bar{n})^2}{N - 1}}$$

The burn velocity w_1 is as follows, when the burning proceeds from the surface towards the core

$$w_1 = \frac{R_1 - R_2}{T_1}$$

where R_1 is the radius after the ignition layer has burned off, and R_2 is the radius of the core. Table 16 shows the results of the above calculations.

From the above descriptions, the burn data of stars were obtained by means of three methods: stopwatch timing of stationary stars (4.3.1), from the 16-mm movie camera with stationary stars (4.3.1) and from the revolving shutter camera for moving stars. They are summarized in Table 17.

Table 17. Comparison of the Data for Burning Stars.

	Stationary		Moving
	Stopwatch (s)	16-mm Movie Camera (s)	Revolving Shutter Camera (s)
B_8	1.20 – 0.60 = 0.606	0.76	0.83
B_{12}	1.95 – 0.60 = 1.35	1.54	1.54
G_{12}	2.97 – 0.60 = 2.37	2.15	2.55

The data from the stopwatch shows the total burn time minus the burn time of the core. The data for the burn time of stars are not very different between stationary and moving stars.

6.2.3 The Sectional Density of Stars

Since stars are burning as they fly through the air, the sectional density changes with time. The sectional density of the star at the nth dot is calculated as:

$$p'_n = \frac{m_n}{\sigma_n}$$

where m_n is the mass of the star at the nth dot and σ_n is the sectional area at the dot. For convenience, the number of the dot is applied as $\nu = 0, 1, 2, 3, \ldots, 18, 19, 20$, etc. in the opposite order as the dot number $i = 20, 19, 18, 17, \ldots, 3, 2, 1, 0,$

etc. When the burn rate is kept constant, the sectional density p'_ν is denoted as

$$p'_\nu = \frac{m_\nu}{\sigma_\nu} = \frac{m_2 + \left\{\left(R_2 + \nu w_1/25\right)^3 - R_2^3\right\}\frac{4}{3}\pi\delta}{\left(R_2 + \nu w_1/25\right)^2 \pi}$$

where m_2 is the mass of the core.

For blue stars (B_8 and B_{12}) and green stars (G_{12}), the values of p'_ν were calculated as they are in Tables 18 and 19.

Table 18. Sectional Densities of Stars, g/cm^2.

I. Blue Stars (B_8 and B_{12}); $w_1/25 = 0.078$ cm/s, $\delta = 1.62$, $R_2 = 0.25$ cm

ν	p'_ν	ν	p'_ν	ν	p'_ν	ν	p'_ν
0	—	14	0.79	28	1.02	42	1.25
1	0.57	15	0.80	29	1.04	43	1.27
2	0.59	16	0.82	30	1.05	44	1.28
3	0.60	17	0.84	31	1.07	45	1.30
4	0.62	18	0.85	32	1.08	46	1.32
5	0.64	19	0.87	33	1.10	47	1.33
6	0.65	20	0.89	34	1.12	48	1.35
7	0.67	21	0.90	35	1.14	49	1.37
8	0.69	22	0.92	36	1.15	50	1.38
9	0.70	23	0.94	37	1.17	51	1.40
10	0.72	24	0.95	38	1.19	52	1.42
11	0.74	25	0.97	39	1.20		
12	0.75	26	0.99	40	1.22		
13	0.77	27	1.00	41	1.23		

II. Green Stars (G_{12}), $w_1/25 = 0.047$ cm/s, $\delta = 1.64$, $R_2 = 0.25$ cm

ν	p'_ν	ν	p'_ν	ν	p'_ν	ν	p'_ν
0	—	19	0.75	38	0.94	57	1.13
1	0.57	20	0.76	39	0.95	58	1.14
2	0.58	21	0.77	40	0.96	59	1.15
3	0.59	22	0.78	41	0.97	60	1.16
4	0.60	23	0.79	42	0.98	61	1.17
5	0.61	24	0.80	43	0.99	62	1.18
6	0.62	25	0.81	44	1.00	63	1.19
7	0.63	26	0.82	45	1.01	64	1.20
8	0.64	27	0.83	46	1.02	65	1.21
9	0.65	28	0.84	47	1.03	66	1.22
10	0.66	29	0.85	48	1.04	67	1.23
11	0.67	30	0.86	49	1.05	68	1.24
12	0.68	31	0.87	50	1.06	69	1.25
13	0.69	32	0.88	51	1.07	70	1.26
14	0.70	33	0.89	52	1.08		
15	0.71	34	0.90	53	1.09		
16	0.72	35	0.91	54	1.10		
17	0.73	36	0.92	55	1.11		
18	0.74	37	0.93	56	1.12		

6.2.4 Calculation of a Function, F(v) = kv^n.

In the equation of motion 40, the air resistance of kv^n is calculated by putting $(dv/dt)_\nu$ to $\frac{d^2x}{dt^2}$ and p'_ν to $p'(t)$.

$$-\left(\frac{dv}{dt}\right)p'_\nu = kv^n = F_\nu(v) \qquad (41)$$

The value of $-(dv/dt)_\nu$ the value $-dv/dt$ in Table 14 are usable. For the values, the number ν should be used. For example, Star No. 481 is used as the following example.

Dot No.	ν	$-\left(\frac{dv}{dt}\right)_\nu$ (m/s)	p'_ν (kg/m^2)	$\frac{F_\nu(v)}{100}$ (kg/m^2)	$\log\frac{F_\nu(v)}{100}$	v_ν (m/s)	log v_ν
39	0	—	—	—	—	—	—
38	1	—	5.7	—	—	12.4	—
37	2	13	5.9	0.77	$\bar{1}$.87	12.9	1.11
36	3	14	6.0	0.84	$\bar{1}$.92	13.4	1.13
35	4	15	6.2	0.93	$\bar{1}$.97	14.0	1.15
34	5	15	6.4	0.96	$\bar{1}$.98	14.6	1.16
33	6	15	6.5	0.98	$\bar{1}$.99	15.2	1.18
32	7	15	6.7	1.01	0.00	15.8	1.20
31	8	16	6.9	1.10	0.04	16.4	1.21
30	9	18	7.0	1.26	0.10	17.1	1.23
29	10	18	7.2	1.30	0.11	17.8	1.25
• • •	• • •	• • •	• • •	• • •	• • •	• • •	• • •
9	30	65	1.05	6.83	0.83	44.9	1.65
8	31	71	1.07	7.60	0.88	17.6	1.68
7	32	80	1.08	8.64	0.88	50.6	1.70
6	33	90	1.10	9.90	1.00	54.0	1.73
5	34	101	1.12	11.31	1.05	57.8	1.76
4	35	121	1.14	13.79	1.14	62.1	1.79
3	36	143	1.15	16.45	1.22	67.5	1.83
2	37	—	—	—	—	73.5	—
1	39	—	—	—	—	—	—

The notation $\bar{1}$ indicates that the characteristic of the logarithmic value is –1.

For example, if the number Z = X × 10^Y, where X is ⩾ 1 and <10, then the log (Z) is written as "Y.(logX)" where the dot is a decimal point. The characteristic (the number to the left of the decimal point) shows the power of 10 (i.e., Y), while the mantissa (the number to the right of the decimal point) shows the power to which ten must be raised to give X. If the number Z is less than one, the characteristic will be negative and is written with a bar over it. The mantissa is always positive.

The values v_ν were taken from Table 14. The relation of the stars concerning log v_ν and log F(v) are shown in Table 19.

Table 19a. The values of log v_ν and log $F_\nu(v)$.

ν	$\log v_\nu$	$\log \frac{F_\nu(v)}{100}$	$\log v_\nu$	$\log \frac{F_\nu(v)}{100}$
	Shell No. 31		Shell No. 41	
0	—	—	—	—
1	—	—	—	—
2	1.11	$\bar{1}.81$	1.22	0.13
3	1.13	$\bar{1}.92$	1.25	0.18
4	1.15	$\bar{1}.94$	1.27	0.21
5	1.16	$\bar{1}.95$	1.29	0.25
6	1.18	0.02	1.32	0.30
7	1.20	0.03	1.35	0.34
8	1.22	0.04	1.37	0.38
9	1.24	0.12	1.40	0.42
10	1.26	0.17	1.42	0.46
11	1.27	0.19	1.45	0.50
12	1.29	0.26	1.48	0.54
13	1.32	0.27	1.50	0.62
14	1.33	0.30	1.53	0.68
15	1.36	0.35	1.57	0.72
16	1.38	0.36	1.60	0.77
17	1.40	0.40	1.63	0.82
18	1.42	0.48	1.66	0.87
19	1.44	0.54	—	—
20	1.47	0.59	—	—
21	1.50	0.66		
22	1.53	0.73		
23	—	—		
24	—	—		

Table 19b. The values of log v_ν and log $F_\nu(v)$.

ν	$\log v_\nu$	$\log \frac{F_\nu(v)}{100}$	$\log v_\nu$	$\log \frac{F_\nu(v)}{100}$
	Shell No. 51		Shell No. 62	
0	—	—	—	—
1	—	—	—	—
2	1.08	$\bar{1}.73$	1.11	$\bar{1}.89$
3	1.09	$\bar{1}.82$	1.13	$\bar{1}.92$
4	1.11	$\bar{1}.83$	1.15	$\bar{1}.94$
5	1.12	$\bar{1}.89$	1.17	$\bar{1}.98$
6	1.14	$\bar{1}.93$	1.18	0.02
7	1.15	$\bar{1}.97$	1.20	0.08
8	1.17	$\bar{1}.98$	1.22	0.09
9	1.18	0.02	1.24	0.12
10	1.20	0.03	1.26	0.17
11	1.22	0.07	1.28	0.24
12	1.24	0.15	1.30	0.27
13	1.26	0.17	1.32	0.34
14	1.27	0.20	1.35	0.39
15	1.29	0.27	1.37	0.40
16	1.31	0.30	1.39	0.41
17	1.33	0.34	1.42	0.46
18	1.35	0.39	1.44	0.49
19	1.38	0.43	1.46	0.53
20	1.40	0.48	1.49	0.55
21	1.42	0.56	—	—
22	1.45	0.63	—	—
23	—	—		
24	—	—		

Table 19c. The values of log v_ν and log $F_\nu(v)$.

ν	$\log v_\nu$	$\log \frac{F_\nu(v)}{100}$	$\log v_\nu$	$\log \frac{F_\nu(v)}{100}$
	Shell No. 72		Shell No. 82	
0	—	—	—	—
1	—	—	—	—
2	1.08	$\bar{1}.92$	1.24	0.07
3	1.07	$\bar{1}.92$	1.26	0.08
4	1.11	$\bar{1}.97$	1.27	0.09
5	1.13	$\bar{1}.98$	1.29	0.13
6	1.15	0.02	1.31	0.18
7	1.17	0.10	1.33	0.21
8	1.20	0.14	1.35	0.24
9	1.22	0.15	1.37	0.26
10	1.24	0.18	1.39	0.31
11	1.26	0.25	1.41	0.35
12	1.28	0.29	1.43	0.42
13	1.31	0.33	1.45	0.48
14	1.33	0.37	1.48	0.53
15	1.36	0.45	1.50	0.60
16	1.39	0.52	1.53	0.68
17	1.41	0.57	1.56	0.77
18	1.44	0.62	—	—
19	1.48	0.66	—	—
20	1.51	0.70		
21	—	—		
22	—	—		

Table 19d. The values of log v_ν and log $F_\nu(v)$.

ν	logv_ν	log $\frac{F_\nu(v)}{100}$	logv_ν	log $\frac{F_\nu(v)}{100}$
	Shell No. 91		Shell No. 101	
0	—	—	—	—
1	—	—	—	—
2	1.11	0.03	1.22	$\bar{1}.97$
3	1.13	0.03	1.23	0.03
4	1.16	0.07	1.25	0.07
5	1.18	0.11	1.27	0.13
6	1.20	0.11	1.29	0.18
7	1.22	0.15	1.31	0.19
8	1.25	0.20	1.33	0.21
9	1.27	0.21	1.35	0.24
10	1.29	0.24	1.37	0.27
11	1.31	0.28	1.39	0.36
12	1.33	0.32	1.42	0.41
13	1.35	0.35	1.44	0.44
14	1.38	0.39	1.46	0.48
15	1.40	0.45	1.48	0.49
16	1.43	0.52	1.51	0.56
17	1.45	0.57	1.53	0.62
18	1.48	0.62	1.56	0.68
19	1.51	0.71	1.58	0.77
20	1.54	0.80	—	—
21	—	—	—	—
22	—	—		

Table 19e. The values of log v_ν and log $F_\nu(v)$.

ν	logv_ν	log $\frac{F_\nu(v)}{100}$	logv_ν	log $\frac{F_\nu(v)}{100}$
	Shell No 112		Shell No. 132	
0	—	—	—	—
1	—	—	—	—
2	1.18	$\bar{1}.95$	1.01	$\bar{1}.67$
3	1.20	0.03	1.03	$\bar{1}.73$
4	1.22	0.05	1.04	$\bar{1}.75$
5	1.24	0.09	1.05	$\bar{1}.76$
6	1.26	0.11	1.06	$\bar{1}.77$
7	1.28	0.15	1.08	$\bar{1}.83$
8	1.30	0.20	1.09	$\bar{1}.84$
9	1.32	0.24	1.11	$\bar{1}.85$
10	1.34	0.27	1.12	$\bar{1}.90$
11	1.36	0.32	1.14	$\bar{1}.91$
12	1.38	0.35	1.15	$\bar{1}.92$
13	1.40	0.38	1.16	$\bar{1}.93$
14	1.42	0.44	1.18	$\bar{1}.94$
15	1.45	0.48	1.19	0.02
16			1.20	0.03
17			1.22	0.04
18			1.23	0.08
19			1.24	0.09
20			1.26	0.13
21			1.27	0.13
22			1.28	0.17
23			1.30	0.18
24			1.31	0.18
25			1.33	0.24
26			1.34	0.27
27			1.36	0.30
28			1.37	0.33
29			1.39	0.34
30			1.34	0.38
31			1.42	0.43
32			1.44	0.43
33			1.45	0.46
34			1.47	0.51
35			—	—
36			—	—

Table 19f. The values of log v_ν and log $F_\nu(v)$.

ν	$\log v_\nu$	$\log \frac{F_\nu(v)}{100}$	$\log v_\nu$	$\log \frac{F_\nu(v)}{100}$
	Shell No. 142		Shell No. 153	
0	—	—	—	—
1	—	—	—	—
2	0.99	$\bar{1}.72$	1.09	$\bar{1}.38$
3	1.01	$\bar{1}.73$	1.09	$\bar{1}.38$
4	1.02	$\bar{1}.75$	1.10	$\bar{1}.49$
5	1.04	$\bar{1}.76$	1.11	$\bar{1}.58$
6	1.05	$\bar{1}.77$	1.11	$\bar{1}.59$
7	1.06	$\bar{1}.78$	1.12	$\bar{1}.60$
8	1.08	$\bar{1}.84$	1.13	$\bar{1}.74$
9	1.09	$\bar{1}.85$	1.14	$\bar{1}.75$
10	1.11	$\bar{1}.86$	1.15	$\bar{1}.76$
11	1.12	$\bar{1}.91$	1.16	$\bar{1}.83$
12	1.14	$\bar{1}.92$	1.17	$\bar{1}.83$
13	1.15	$\bar{1}.93$	1.18	$\bar{1}.84$
14	1.16	$\bar{1}.94$	1.19	$\bar{1}.90$
15	1.18	$\bar{1}.94$	1.20	$\bar{1}.90$
16	1.19	$\bar{1}.95$	1.21	$\bar{1}.95$
17	1.20	$\bar{1}.96$	1.23	0.04
18	1.22	0.04	1.24	0.05
19	1.23	0.05	1.25	0.05
20	1.24	0.06	1.26	0.10
21	1.25	0.10	1.28	0.13
22	1.27	0.11	1.29	0.17
23	1.28	0.12	1.31	0.23
24	1.29	0.18	1.32	0.23
25	1.31	0.24	1.33	0.24
26	1.32	0.25	1.35	0.30
27	1.34	0.26	1.37	0.32
28	1.35	0.31	1.38	0.33
29	1.37	0.34	1.40	0.40
30	1.38	0.34	1.41	0.44
31	1.40	0.41	1.43	0.48
32	1.42	0.43	1.45	0.51
33	1.43	0.44	1.47	0.60
34	1.45	0.50	1.49	0.65
35	1.47	0.53	1.51	0.70
36	1.48	0.58	1.54	0.75
37	1.50	0.62	1.56	0.81
38	1.52	0.67	—	—
39	1.54	0.69	—	—
40	—	—		
41	—	—		

Table 19g. The Values of log v_ν and log $F_\nu(v)$.

ν	$\log v_\nu$	$\log \frac{F_\nu(v)}{100}$	$\log v_\nu$	$\log \frac{F_\nu(v)}{100}$
	Shell No. 162		Shell No. 172	
0	—	—	—	—
1	—	—	—	—
2	1.11	$\bar{1}.77$	1.06	$\bar{1}.67$
3	1.12	$\bar{1}.78$	1.08	$\bar{1}.68$
3	1.13	$\bar{1}.79$	1.08	$\bar{1}.70$
4	1.15	$\bar{1}.81$	1.10	$\bar{1}.71$
5	1.16	$\bar{1}.86$	1.11	$\bar{1}.72$
6	1.17	$\bar{1}.87$	1.12	$\bar{1}.73$
8	1.19	$\bar{1}.88$	1.13	$\bar{1}.79$
9	1.20	$\bar{1}.89$	1.14	$\bar{1}.80$
10	1.21	$\bar{1}.90$	1.15	$\bar{1}.81$
11	1.22	$\bar{1}.98$	1.16	$\bar{1}.83$
12	1.23	$\bar{1}.99$	1.17	$\bar{1}.88$
13	1.25	0.00	1.18	$\bar{1}.89$
14	1.26	0.01	1.19	$\bar{1}.90$
15	1.27	0.02	1.20	$\bar{1}.90$
16	1.28	0.03	1.22	$\bar{1}.91$
17	1.29	0.07	1.23	$\bar{1}.92$
18	1.31	0.11	1.24	$\bar{1}.93$
19	1.32	0.14	1.25	$\bar{1}.94$
20	1.33	0.20	1.26	$\bar{1}.99$
21	1.35	0.23	1.27	0.07
22	1.36	0.27	1.28	0.08
23	1.38	0.27	1.29	0.09
24	1.39	0.30	1.30	0.09
25	1.41	0.35	1.31	0.10
26	1.42	0.38	1.32	0.20
27	1.44	0.42	1.34	0.20
28	1.46	0.46	1.35	0.21
29	1.47	0.46	1.36	0.22
30	1.49	0.48	1.37	0.23
31	1.50	0.52	1.38	0.29
32	1.52	0.57	1.40	0.29
33	1.54	0.59	1.41	0.32
34	1.56	0.64	1.42	0.35
35	1.58	0.67	1.44	0.36
36	1.59	0.70	1.45	0.38
37	1.62	0.75	1.46	0.43
38	1.63	0.78	—	—
39	1.66	0.85	—	—
40	—	—		
41	—	—		

Table 19h. The values of log v_ν and log $F_\nu(v)$.

ν	logv_ν	$\log\frac{F_\nu(v)}{100}$	logv_ν	$\log\frac{F_\nu(v)}{100}$
	Shell No. 182		Shell No. 191	
0	—	—	—	—
1	—	—	—	—
2	1.03	–1.54	1.05	–1.67
3	1.07	$\bar{1}.56$	1.06	$\bar{1}.68$
4	1.06	$\bar{1}.57$	1.08	$\bar{1}.70$
5	1.06	$\bar{1}.58$	1.09	$\bar{1}.76$
6	1.08	$\bar{1}.72$	1.10	$\bar{1}.77$
7	1.09	$\bar{1}.73$	1.11	$\bar{1}.78$
8	1.10	$\bar{1}.74$	1.12	$\bar{1}.84$
9	1.11	$\bar{1}.75$	1.14	$\bar{1}.85$
10	1.12	$\bar{1}.76$	1.15	$\bar{1}.90$
11	1.13	$\bar{1}.77$	1.16	$\bar{1}.91$
12	1.14	$\bar{1}.83$	1.18	$\bar{1}.92$
13	1.15	$\bar{1}.84$	1.19	0.00
14	1.16	$\bar{1}.85$	1.20	0.01
15	1.17	$\bar{1}.86$	1.22	0.05
16	1.18	$\bar{1}.91$	1.23	0.09
17	1.19	$\bar{1}.92$	1.25	0.10
18	1.20	$\bar{1}.93$	1.26	0.11
19	1.21	$\bar{1}.94$	1.28	0.12
20	1.22	$\bar{1}.95$	1.29	0.15
21	1.23	$\bar{1}.95$	1.31	0.16
22	1.24	$\bar{1}.96$	1.32	0.22
23	1.25	$\bar{1}.97$	1.33	0.23
24	1.26	0.02	1.35	0.23
25	1.27	0.10	1.36	0.24
26	1.29	0.14	1.38	0.27
27	1.30	0.15	1.39	0.30
28	1.31	0.16	1.40	0.31
29	1.32	0.19	1.42	0.34
30	1.33	0.23	1.43	0.38
31	1.35	0.23	1.45	0.41
32	1.36	0.24	1.46	0.41
33	1.37	0.32	—	—
34	1.39	0.33		
35	1.40	0.36		
36	1.41	0.36		
37	1.43	0.39		
38	1.44	0.38		
39	—	—		

Table 19i. The values of log v_ν and log $F_\nu(v)$.

ν	logv_ν	$\log\frac{F_\nu(v)}{100}$	logv_ν	$\log\frac{F_\nu(v)}{100}$
	Shell No. 202		Shell No. 212	
0	—	—	—	—
1	—	—	—	—
2	1.05	$\bar{1}.73$	1.07	$\bar{1}.67$
3	1.06	$\bar{1}.73$	1.08	$\bar{1}.73$
4	1.08	$\bar{1}.75$	1.09	$\bar{1}.75$
5	1.09	$\bar{1}.85$	1.10	$\bar{1}.76$
6	1.11	$\bar{1}.86$	1.12	$\bar{1}.77$
7	1.12	$\bar{1}.87$	1.13	$\bar{1}.78$
8	1.13	$\bar{1}.88$	1.14	$\bar{1}.84$
9	1.15	$\bar{1}.89$	1.15	$\bar{1}.89$
10	1.16	$\bar{1}.90$	1.17	$\bar{1}.90$
11	1.18	$\bar{1}.98$	1.18	$\bar{1}.91$
12	1.19	0.02	1.19	$\bar{1}.92$
13	1.21	0.03	1.20	0.00
14	1.22	0.05	1.22	0.01
15	1.24	0.08	1.23	0.02
16	1.25	0.09	1.24	0.03
17	1.27	0.10	1.26	0.07
18	1.28	0.11	1.27	0.08
19	1.29	0.14	1.28	0.12
20	1.31	0.20	1.30	0.15
21	1.32	0.21	1.31	0.16
22	1.34	0.24	1.32	0.24
23	1.35	0.27	1.34	0.25
24	1.37	0.28	1.35	0.26
25	1.38	0.31	1.37	0.31
26	1.40	0.36	1.39	0.36
27	1.41	0.38	1.40	0.38
28	1.43	0.41	1.42	0.41
29	1.45	0.43	1.44	0.46
30	1.46	0.47	1.45	0.50
31	1.48	0.49	1.47	0.52
32	1.50	0.53	1.49	0.57
33	1.51	0.57	1.51	0.60
34	1.53	0.63	1.53	0.64
35	1.55	0.66	1.55	0.66
36	1.57	0.67	—	—
37	1.59	0.72	—	—
38	1.61	0.78		
39	1.63	0.86		
40	1.66	0.93		
41	—	—		
42	—	—		

Table 19j. The Values of log v_ν and log $F_\nu(v)$.

ν	$\log v_\nu$	$\log \frac{F_\nu(v)}{100}$	$\log v_\nu$	$\log \frac{F_\nu(v)}{100}$
	Shell No. 222		Shell No. 232	
0	—	—	—	—
1	—	—	—	—
2	1.08	$\bar{1}.67$	1.01	$\bar{1}.54$
3	1.09	$\bar{1}.68$	1.03	$\bar{1}.68$
4	1.10	$\bar{1}.75$	1.04	$\bar{1}.70$
5	1.12	$\bar{1}.76$	1.05	$\bar{1}.71$
6	1.13	$\bar{1}.77$	1.06	$\bar{1}.72$
7	1.14	$\bar{1}.78$	1.07	$\bar{1}.78$
8	1.15	$\bar{1}.79$	1.09	$\bar{1}.79$
9	1.16	$\bar{1}.85$	1.10	$\bar{1}.80$
10	1.17	$\bar{1}.90$	1.11	$\bar{1}.86$
11	1.19	$\bar{1}.91$	1.12	$\bar{1}.87$
12	1.20	$\bar{1}.92$	1.14	$\bar{1}.88$
13	1.21	0.00	1.15	$\bar{1}.89$
14	1.23	0.05	1.16	$\bar{1}.94$
15	1.24	0.05	1.18	0.02
16	1.25	0.06	1.19	0.03
17	1.27	0.10	1.20	0.04
18	1.28	0.11	1.22	0.08
19	1.29	0.14	1.23	0.12
20	1.31	0.15	1.25	0.13
21	1.32	0.21	1.26	0.16
22	1.34	0.27	1.28	0.22
23	1.35	0.29	1.29	0.23
24	1.37	0.34	1.31	0.28
25	1.39	0.35	1.33	0.31
26	1.40	0.38	1.34	0.32
27	1.42	0.42	1.36	0.36
28	1.44	0.47	1.38	0.39
29	1.46	0.48	1.40	0.42
30	1.47	0.50	1.41	0.44
31	1.49	0.54	1.43	0.49
32	1.51	0.57	1.45	0.51
33	1.53	0.59	1.47	0.53
34	—	0.61	1.49	0.58
35	1.56	0.66	1.51	0.61
36	1.58	0.70	1.53	0.66
37	1.60	0.73	1.55	0.70
38	1.62	0.78	1.57	0.74
39	1.64	0.82	1.59	0.77
40	1.67	0.85	—	—
41	—	—	—	—

Table 19k. The values of log v_ν and log $F_\nu(v)$.

ν	$\log v_\nu$	$\log \frac{F_\nu(v)}{100}$	$\log v_\nu$	$\log \frac{F_\nu(v)}{100}$
	Shell No. 241		Shell No. 252	
0	—	—	—	—
1	—	—	—	—
2	1.09	$\bar{1}.77$	1.21	0.13
3	1.10	$\bar{1}.78$	1.24	0.14
4	1.12	$\bar{1}.83$	1.26	0.19
5	1.14	$\bar{1}.85$	1.28	0.25
6	1.15	$\bar{1}.85$	1.31	0.28
7	1.17	$\bar{1}.97$	1.33	0.32
8	1.19	0.01	1.36	0.37
9	1.20	0.02	1.38	0.40
10	1.22	0.03	1.41	0.45
11	1.25	0.07	1.44	0.48
12	1.25	0.15	1.46	0.53
13	1.27	0.17	1.49	0.59
14	1.28	0.20	1.52	0.65
15	1.30	0.26	1.55	0.70
16	1.31	0.28	1.58	0.76
17	1.33	0.29	1.61	0.80
18	1.35	0.29	1.64	0.86
19	1.37	0.34	—	—
20	1.38	0.40	—	—
21	1.40	0.42		
22	1.42	0.46		
23	1.44	0.48		
24	1.46	0.51		
25	1.47	0.52		
26	1.49	0.58		
27	1.52	0.60		
28	1.54	0.62		
29	1.56	0.66		
30	1.58	0.68		
31	1.60	0.74		
32	1.62	0.80		
33	1.65	0.87		
34	1.68	0.97		
35	—	—		
36	—	—		

Table 19l. The values of log v_ν and log $F_\nu(v)$.

ν	logv_ν	$\log\frac{F_\nu(v)}{100}$	logv_ν	$\log\frac{F_\nu(v)}{100}$
	Shell No. 261		Shell No. 272	
0	—	—	—	—
1	—	—	—	—
2	1.23	0.13	1.16	0.03
3	1.26	0.16	1.18	0.06
4	1.28	0.19	1.20	0.11
5	1.30	0.22	1.23	0.13
6	1.32	0.28	1.25	0.14
7	1.35	0.32	1.27	0.15
8	1.37	0.37	1.29	0.22
9	1.40	0.40	1.31	0.26
10	1.42	0.45	1.33	0.27
11	1.45	0.48	1.35	0.33
12	1.47	0.53	1.38	0.40
13	1.50	0.59	1.40	0.42
14	1.53	0.64	1.42	0.45
15	1.56	0.67	1.45	0.49
16	1.59	0.70	1.47	0.56
17	1.61	0.76	1.50	0.62
18	1.64	0.83	1.53	0.64
19	1.68	0.89	1.55	0.69
20	—	—	1.58	0.76
21	—	—	1.61	0.85
22			—	—
23			—	—

Table 19m. The values of log v_ν and log $F_\nu(v)$.

ν	logv_ν	$\log\frac{F_\nu(v)}{100}$	logv_ν	$\log\frac{F_\nu(v)}{100}$
	Shell No. 281		Shell No. 291	
0	—	—	—	—
1	—	—	—	—
2	1.21	0.17	1.16	0.07
3	1.24	0.19	1.18	0.10
4	1.27	0.24	1.21	0.16
5	1.29	0.27	1.23	0.20
6	1.32	0.31	1.26	0.26
7	1.34	0.36	1.28	0.29
8	1.37	0.38	1.31	0.32
9	1.39	0.43	1.33	0.38
10	1.42	0.46	1.36	0.40
11	1.45	0.48	1.37	0.43
12	1.47	0.53	1.41	0.48
13	1.45	0.59	1.44	0.52
14	1.53	0.62	1.47	0.55
15	1.55	0.67	1.49	0.57
16	1.58	0.75	1.52	0.62
17	1.62	0.86	—	—
18	1.66	0.94	—	—
19	—	—		
20	—	—		

Table 19n. The values of log v_ν and log $F_\nu(v)$.

ν	logv_ν	$\log\frac{F_\nu(v)}{100}$	logv_ν	$\log\frac{F_\nu(v)}{100}$
	Shell No. 302		Shell No. 312	
0	—	—	—	—
1	—	—	—	—
2	1.14	0.05	1.20	0.05
3	1.17	0.08	1.22	0.08
4	1.19	0.09	1.24	0.11
5	1.21	0.11	1.26	0.19
6	1.23	0.18	1.29	0.23
7	1.26	0.21	1.31	0.27
8	1.28	0.24	1.33	0.32
9	1.30	0.29	1.36	0.36
10	1.33	0.31	1.38	0.40
11	1.35	0.35	1.41	0.45
12	1.37	0.42	1.43	0.48
13	1.40	0.49	1.46	0.54
14	1.43	0.55	1.47	0.59
15	1.46	0.61	1.52	0.64
16	1.49	0.70	1.55	0.70
17	1.53	0.84	1.58	0.73
18	—	—	1.60	0.76
19	—	—	—	—
20			—	—

Table 19o. The values of log v_ν and log $F_\nu(v)$.

ν	logv_ν	log $\frac{F_\nu(v)}{100}$	logv_ν	log $\frac{F_\nu(v)}{100}$
	Shell No. 343		Shell No. 352	
0	—	—	—	—
1	—	—	—	—
2	1.23	$\bar{1}$.97	1.20	0.07
3	1.25	0.06	1.22	0.08
4	1.27	0.09	1.24	0.11
5	1.29	0.13	1.26	0.17
6	1.31	0.19	1.28	0.19
7	1.33	0.24	1.31	0.24
8	1.35	0.28	1.33	0.29
9	1.37	0.32	1.35	0.32
10	1.39	0.38	1.38	0.38
11	1.42	0.41	1.40	0.41
12	1.44	0.47	1.42	0.46
13	1.46	0.53	1.45	0.49
14	1.47	0.59	1.47	0.54
15	1.52	0.61	1.50	0.59
16	1.55	0.64	1.53	0.65
17	1.57	0.67	1.55	0.70
18	1.60	0.73	1.58	0.76
19	1.63	0.80	1.62	0.86
20	1.66	0.87	—	—
21	1.69	0.93	—	—
22	—	—		
23	—	—		

Table 19p. The values of log v_ν and log $F_\nu(v)$.

ν	logv_ν	log $\frac{F_\nu(v)}{100}$	logv_ν	log $\frac{F_\nu(v)}{100}$
	Shell No. 362		Shell No. 371	
0	—	—	—	—
1	—	—	—	—
2	1.22	0.07	1.10	$\bar{1}$.72
3	1.24	0.10	1.11	$\bar{1}$.73
4	1.26	0.17	1.12	$\bar{1}$.79
5	1.28	0.20	1.14	$\bar{1}$.81
6	1.31	0.23	1.15	$\bar{1}$.81
7	1.33	0.29	1.16	$\bar{1}$.87
8	1.35	0.33	1.18	$\bar{1}$.95
9	1.38	0.38	1.19	$\bar{1}$.96
10	1.40	0.41	1.20	0.00
11	1.43	0.46	1.22	0.05
12	1.45	0.49	1.24	0.05
13	1.48	0.55	1.25	0.09
14	1.51	0.61	1.27	0.15
15	1.53	0.64	1.28	0.16
16	1.56	0.72	1.30	0.19
17	1.59	0.79	1.32	0.23
18	1.63	0.82	1.33	0.23
19	1.66	0.89	1.35	0.26
20	1.69	0.98	1.37	0.33
21	1.73	1.03	1.38	0.35
22	—	—	1.40	0.36
23	—	—	1.42	0.39
24			1.44	0.44
25			1.46	0.48
26			1.47	0.53
27			1.49	0.56
28			1.52	0.59
29			1.53	0.63
30			1.56	0.68
31			1.58	0.69
32			1.60	0.74
33			1.62	0.78
34			1.64	0.81
35			1.67	0.84
36			1.69	0.87
37			1.71	0.91
38			—	—
39			—	—

Table 19q. The values of log v_ν and log $F_\nu(\nu)$.

ν	logv_ν	log $\frac{F_\nu(\nu)}{100}$	logv_ν	log $\frac{F_\nu(\nu)}{100}$
	Shell No. 382		Shell No. 392	
0	—	—	—	—
1	—	—	—	—
2	1.12	$\bar{1}.77$	1.12	$\bar{1}.77$
3	1.13	$\bar{1}.78$	1.13	$\bar{1}.78$
4	1.15	$\bar{1}.83$	1.14	$\bar{1}.79$
5	1.16	$\bar{1}.85$	1.16	$\bar{1}.81$
6	1.17	$\bar{1}.86$	1.17	$\bar{1}.81$
7	1.19	$\bar{1}.97$	1.18	$\bar{1}.87$
8	1.20	0.02	1.19	$\bar{1}.88$
9	1.22	0.02	1.21	$\bar{1}.89$
10	1.24	0.03	1.22	$\bar{1}.90$
11	1.25	0.07	1.23	$\bar{1}.91$
12	1.27	0.16	1.25	0.10
13	1.29	0.16	1.26	0.00
14	1.30	0.20	1.27	0.05
15	1.32	0.27	1.28	0.05
16	1.34	0.28	1.29	0.06
17	1.36	0.29	1.31	0.13
18	1.37	0.29	1.32	0.13
19	1.39	0.34	1.33	0.14
20	1.41	0.40	1.35	0.20
21	1.43	0.42	1.36	0.23
22	1.45	0.46	1.38	0.27
23	1.47	0.49	1.39	0.29
24	1.48	0.51	1.41	0.34
25	1.50	0.53	1.42	0.37
26	1.52	0.55	1.44	0.39
27	1.54	0.59	1.45	0.42
28	1.56	0.64	1.47	0.47
29	1.58	0.68	1.49	0.49
30	1.60	0.72	1.50	0.54
31	1.63	0.77	1.52	0.59
32	1.65	0.81	1.54	0.62
33	1.67	0.84	1.56	0.65
34	1.70	0.88	1.58	0.77
35	1.72	0.97	1.60	0.78
36	1.75	1.04	1.63	0.80
37	1.78	1.12	1.65	0.93
38	—	—	1.69	1.10
39	—	—	—	—
40			—	—

Table 19r. The values of log v_ν and log $F_\nu(\nu)$.

ν	logv_ν	log $\frac{F_\nu(\nu)}{100}$	logv_ν	log $\frac{F_\nu(\nu)}{100}$
	Shell No. 403		Shell No. 411	
0	—	—	—	—
1	—	—	—	—
2	1.21	$\bar{1}.67$	1.15	$\bar{1}.89$
3	1.22	$\bar{1}.68$	1.16	$\bar{1}.89$
4	1.23	$\bar{1}.70$	1.18	$\bar{1}.91$
5	1.23	$\bar{1}.81$	1.19	$\bar{1}.92$
6	1.25	$\bar{1}.81$	1.22	$\bar{1}.96$
7	1.26	$\bar{1}.83$	1.22	0.00
8	1.27	$\bar{1}.88$	1.24	0.04
9	1.28	$\bar{1}.99$	1.26	0.10
10	1.29	0.00	1.27	0.11
11	1.30	0.02	1.29	0.12
12	1.31	0.05	1.30	0.13
13	1.33	0.09	1.32	0.16
14	1.34	0.15	1.33	0.18
15	1.35	0.16	1.35	0.18
16	1.37	0.19	1.36	0.24
17	1.38	0.23	1.38	0.25
18	1.40	0.25	1.39	0.29
19	1.41	0.26	1.41	0.32
20	1.43	0.27	1.43	0.35
21	1.44	0.33	1.44	0.37
22	1.46	0.36	1.46	0.41
23	1.47	0.42	1.48	0.45
24	1.49	0.44	1.49	0.46
25	1.50	0.46	1.51	0.48
26	1.52	0.52	1.53	0.53
27	1.54	0.53	1.54	0.58
28	1.55	0.57	1.56	0.62
29	1.57	0.62	1.58	0.65
30	1.59	0.67	1.60	0.68
31	1.61	0.69	1.62	0.73
32	1.63	0.72	1.64	0.73
33	1.65	0.77	—	—
34	1.67	0.82	—	—
35	1.69	0.86		
36	1.72	0.91		
37	1.72	1.00		
38	1.77	1.07		
39	1.80	1.11		
40	—	—		
41	—	—		

Table 19s. The values of log v_ν and log $F_\nu(v)$.

ν	logv_ν	log$\frac{F_\nu(v)}{100}$	logv_ν	log$\frac{F_\nu(v)}{100}$
	Shell No. 422		Shell No. 442	
0	—	—	—	—
1	—	—	—	—
2	1.13	$\bar{1}.72$	1.13	$\bar{1}.67$
3	1.14	$\bar{1}.73$	1.14	$\bar{1}.68$
4	1.16	$\bar{1}.79$	1.15	$\bar{1}.75$
5	1.17	$\bar{1}.81$	1.16	$\bar{1}.76$
6	1.18	$\bar{1}.81$	1.17	$\bar{1}.77$
7	1.19	$\bar{1}.83$	1.18	$\bar{1}.83$
8	1.20	$\bar{1}.88$	1.19	$\bar{1}.79$
9	1.22	$\bar{1}.89$	1.20	$\bar{1}.80$
10	1.23	$\bar{1}.90$	1.21	$\bar{1}.86$
11	1.24	$\bar{1}.98$	1.22	$\bar{1}.87$
12	1.25	$\bar{1}.99$	1.23	$\bar{1}.88$
13	1.26	0.03	1.24	$\bar{1}.89$
14	1.28	0.05	1.25	$\bar{1}.94$
15	1.29	0.08	1.26	$\bar{1}.94$
16	1.30	0.12	1.27	$\bar{1}.65$
17	1.32	0.13	1.28	0.04
18	1.33	0.19	1.29	0.05
19	1.34	0.22	1.31	0.05
20	1.36	0.27	1.32	0.06
21	1.38	0.28	1.33	0.07
22	1.39	0.33	1.34	0.08
23	1.41	0.37	1.35	0.12
24	1.43	0.38	1.36	0.16
25	1.44	0.40	1.37	0.16
26	1.46	0.44	1.38	0.20
27	1.47	0.46	1.39	0.28
28	1.49	0.50	1.41	0.29
29	1.51	0.55	1.42	0.32
30	1.53	0.55	1.43	0.38
31	1.54	0.57	1.45	0.41
32	1.56	0.61	1.46	0.41
33	1.58	0.64	1.48	0.44
34	1.60	0.70	1.49	0.50
35	1.62	0.75	1.51	0.52
36	1.64	0.79	1.52	0.54
37	—	—	1.54	0.59
38	—	—	1.56	0.62
39			1.57	0.76
40			1.60	0.64
41			—	—
42			—	—

Table 19t. The values of log v_ν and log $F_\nu(v)$.

ν	logv_ν	log$\frac{F_\nu(v)}{100}$	logv_ν	log$\frac{F_\nu(v)}{100}$
	Shell No. 452		Shell No. 471	
0	—	—	—	—
1	—	—	—	—
2	1.11	$\bar{1}.77$	1.15	$\bar{1}.77$
3	1.13	$\bar{1}.78$	1.16	$\bar{1}.78$
4	1.14	$\bar{1}.79$	1.18	$\bar{1}.83$
5	1.15	$\bar{1}.85$	1.19	$\bar{1}.92$
6	1.17	$\bar{1}.86$	1.20	$\bar{1}.93$
7	1.18	$\bar{1}.94$	1.22	$\bar{1}.97$
8	1.19	$\bar{1}.95$	1.23	0.02
9	1.21	$\bar{1}.96$	1.25	0.02
10	1.22	$\bar{1}.97$	1.26	0.06
11	1.23	$\bar{1}.98$	1.28	0.12
12	1.25	0.02	1.29	0.16
13	1.26	0.03	1.31	0.16
14	1.27	0.10	1.33	0.18
15	1.29	0.11	1.34	0.23
16	1.30	0.12	1.36	0.28
17	1.31	0.10	1.38	0.29
18	1.33	0.13	1.39	0.31
19	1.34	0.22	1.41	0.35
20	1.36	0.23	1.43	0.40
21	1.37	0.23	1.45	0.43
22	1.38	0.29	1.47	0.50
23	1.40	0.35	1.49	0.52
24	1.42	0.36	1.51	0.56
25	1.43	0.37	1.53	0.59
26	1.45	0.39	1.55	0.61
27	1.46	0.42	1.57	0.64
28	1.48	0.47	1.59	0.67
29	1.50	0.51	1.61	0.72
30	1.51	0.54	1.63	0.76
31	1.53	0.55	1.65	0.79
32	1.55	0.58	1.68	0.83
33	1.57	0.64	1.70	0.92
34	1.58	0.69	1.73	0.97
35	1.60	0.75	—	—
36	1.63	0.81	—	—
37	1.65	0.87		
38	—	—		
39	—	—		

Table 19u. The values of log v_ν and log $F_\nu(v)$.

ν	logv_ν	log $\frac{F_\nu(v)}{100}$	logv_ν	log $\frac{F_\nu(v)}{100}$
	Shell No. 481		Shell No. 502	
0	—	—	—	—
1	—	—	—	—
2	1.11	$\overline{1}.89$	0.88	$\overline{1}.36$
3	1.13	$\overline{1}.92$	0.89	$\overline{1}.38$
4	1.15	$\overline{1}.97$	0.89	$\overline{1}.38$
5	1.16	$\overline{1}.98$	0.90	$\overline{1}.49$
6	1.18	$\overline{1}.99$	0.91	$\overline{1}.49$
7	1.20	0.00	0.92	$\overline{1}.51$
8	1.22	0.04	0.93	$\overline{1}.51$
9	1.23	0.10	0.94	$\overline{1}.52$
10	1.25	0.11	0.95	$\overline{1}.52$
11	1.27	0.15	0.96	$\overline{1}.53$
12	1.29	0.16	0.97	$\overline{1}.53$
13	1.30	0.19	0.98	$\overline{1}.54$
14	1.32	0.26	0.99	$\overline{1}.54$
15	1.34	0.27	1.00	$\overline{1}.63$
16	1.36	0.29	1.01	$\overline{1}.63$
17	1.38	0.32	1.02	$\overline{1}.64$
18	1.39	0.38	1.03	$\overline{1}.64$
19	1.41	0.40	1.04	$\overline{1}.78$
20	1.43	0.43	1.05	$\overline{1}.79$
21	1.45	0.47	1.06	
22	1.47	0.51	1.07	
23	1.49	0.57	1.08	$\overline{1}.80$
24	1.52	0.58	1.09	$\overline{1}.81$
25	1.54	0.62	1.10	$\overline{1}.81$
26	1.56	0.66	1.11	$\overline{1}.82$
27	1.58	0.69	1.12	
28	1.60	0.75	1.14	
29	1.63	0.80	1.15	$\overline{1}.89$
30	1.64	0.83	1.16	$\overline{1}.89$
31	1.68	0.88	1.17	$\overline{1}.89$
32	1.70	0.88	1.18	$\overline{1}.90$
33	1.93	1.00	1.19	$\overline{1}.95$
34	1.76	1.05	1.20	$\overline{1}.95$
35	1.79	1.14	1.21	$\overline{1}.96$
36	1.83	1.22	1.22	$\overline{1}.96$
37	—	—	1.23	0.01
38	—	—	1.25	0.09
39			1.26	0.09
40			1.27	0.10
41			1.28	0.13
42			1.29	0.17
43			1.31	0.17
44			1.32	0.18
45			1.33	0.21
46			1.35	0.27
47			1.36	0.29
48			1.38	0.32
49			1.39	0.32
50			1.40	0.35
51			1.42	0.39
52			1.43	0.41
53			1.45	0.45
54			1.47	0.49
55			1.48	0.51
56			1.50	0.57
57			1.52	0.59
58			1.54	0.59
59			1.55	0.61
60			1.57	0.66
61			1.59	0.68
62			1.61	0.73
63			—	—
64			—	—

Table 19v. The values of log v_ν and log $F_\nu(v)$.

ν	logv_ν	log $\frac{F_\nu(v)}{100}$	logv_ν	log $\frac{F_\nu(v)}{100}$
	Shell No. 503		Shell No. 505	
0	—	—	—	—
1	—	—	—	—
2	0.92	$\overline{1}.36$	0.93	$\overline{2}.76$
3	0.93	$\overline{1}.37$	0.93	$\overline{2}.78$
4	0.94	$\overline{1}.38$	0.93	$\overline{2}.78$
5	0.94	$\overline{1}.38$	0.93	$\overline{2}.78$
6	0.95	$\overline{1}.49$	0.93	$\overline{2}.78$
7	0.96	$\overline{1}.51$	0.94	$\overline{2}.78$
8	0.97	$\overline{1}.51$	0.94	$\overline{2}.78$
9	0.98	$\overline{1}.52$	0.94	$\overline{2}.85$
10	0.99	$\overline{1}.52$	0.94	$\overline{2}.85$
11	1.00	$\overline{1}.53$	0.95	$\overline{2}.85$
12	1.01	$\overline{1}.53$	0.95	$\overline{1}.15$

ν	logv_ν	log$\frac{F_\nu(v)}{100}$	logv_ν	log$\frac{F_\nu(v)}{100}$
	Shell No. 503		Shell No. 505	
13	1.02	$\bar{1}$.54	0.95	$\bar{1}$.32
14	1.03	$\bar{1}$.62	0.96	$\bar{1}$.32
15	1.04	$\bar{1}$.63	0.96	$\bar{1}$.32
16	1.05	$\bar{1}$.63	0.97	$\bar{1}$.34
17	1.06	$\bar{1}$.64	0.97	$\bar{1}$.34
18	1.07	$\bar{1}$.77	0.98	$\bar{1}$.34
19	1.08	$\bar{1}$.78	0.98	$\bar{1}$.36
20	1.09	$\bar{1}$.79	0.99	$\bar{1}$.48
21	1.10	$\bar{1}$.79	1.00	$\bar{1}$.49
22	1.11	$\bar{1}$.79	1.00	$\bar{1}$.49
23	1.12	$\bar{1}$.80	1.01	$\bar{1}$.51
24	1.13	$\bar{1}$.81	1.01	$\bar{1}$.51
25	1.14	$\bar{1}$.81	1.02	$\bar{1}$.52
26	1.15	$\bar{1}$.87	1.02	$\bar{1}$.52
27	1.16	$\bar{1}$.88	1.03	$\bar{1}$.52
28	1.17	$\bar{1}$.88	1.04	$\bar{1}$.62
29	1.18	$\bar{1}$.89	1.04	$\bar{1}$.63
30	1.19	$\bar{1}$.89	1.05	$\bar{1}$.63
31	1.20	$\bar{1}$.89	1.06	$\bar{1}$.64
32	1.21	$\bar{1}$.94	1.06	$\bar{1}$.64
33	1.22	$\bar{1}$.94	1.07	$\bar{1}$.72
34	1.23	$\bar{1}$.95	1.08	$\bar{1}$.73
35	1.24	0.00	1.09	$\bar{1}$.74
36	1.26	0.08	1.10	$\bar{1}$.74
37	1.27	0.08	1.11	$\bar{1}$.75
38	1.28	0.12	1.12	$\bar{1}$.88
39	1.29	0.18	1.13	$\bar{1}$.93
40	1.31	0.19	1.14	$\bar{1}$.93
41	1.32	0.19	1.15	$\bar{1}$.94
42	1.33	0.25	1.16	$\bar{1}$.99
43	1.35	0.27	1.17	0.00
44	1.36	0.30	1.19	0.04
45	1.38	0.31	1.20	0.05
46	1.39	0.33	1.21	0.05
47	1.41	0.38	1.22	0.16
48	1.42	0.38	1.24	0.19
49	1.44	0.42	1.25	0.20
50	1.46	0.47	1.27	0.28
51	1.47	0.48	1.29	0.33
52	1.49	0.53	1.30	0.33
53	1.51	0.58	1.32	0.34
54	1.53	0.59	1.34	0.36
55	1.54	0.63	1.35	0.43
56	1.56	0.66	1.37	0.45
57	1.58	0.69	1.39	0.50
58	—	—	1.41	0.53
59	—	—	—	—
60			—	—

Table 19w. The values of log v_ν and log $F_\nu(v)$.

ν	logv_ν	log$\frac{F_\nu(v)}{100}$	logv_ν	log$\frac{F_\nu(v)}{100}$
	Shell No. 542		Shell No. 543	
0	—	—	—	—
1	—	—	—	—
2	0.87	$\bar{1}$.23	0.92	$\bar{1}$.23
3	0.88	$\bar{1}$.26	0.93	$\bar{1}$.26
4	0.88	$\bar{1}$.26	0.93	$\bar{1}$.26
5	0.89	$\bar{1}$.38	0.94	$\bar{1}$.26
6	0.90	$\bar{1}$.40	0.94	$\bar{1}$.28
7	0.90	$\bar{1}$.40	0.95	$\bar{1}$.40
8	0.91	$\bar{1}$.42	0.96	$\bar{1}$.42
9	0.92	$\bar{1}$.42	0.97	$\bar{1}$.42
10	0.93	$\bar{1}$.52	0.98	$\bar{1}$.42
11	0.94	$\bar{1}$.53	0.98	$\bar{1}$.43
12	0.95	$\bar{1}$.53	0.99	$\bar{1}$.53
13	0.96	$\bar{1}$.54	1.00	$\bar{1}$.53
14	0.97	$\bar{1}$.54	1.01	$\bar{1}$.62
15	0.98	$\bar{1}$.63	1.02	$\bar{1}$.63
16	0.99	$\bar{1}$.63	1.03	$\bar{1}$.63
17	1.00	$\bar{1}$.64	1.04	$\bar{1}$.64
18	1.01	$\bar{1}$.64	1.05	$\bar{1}$.64
19	1.02	$\bar{1}$.64	1.06	$\bar{1}$.65
20	1.03	$\bar{1}$.66	1.06	$\bar{1}$.66
21	1.04	$\bar{1}$.66	1.08	$\bar{1}$.79
22	1.05	$\bar{1}$.66	1.09	$\bar{1}$.79
23	1.06	$\bar{1}$.67	1.10	$\bar{1}$.80
24	1.07	$\bar{1}$.68	1.11	$\bar{1}$.81
25	1.08	$\bar{1}$.69	1.12	$\bar{1}$.81
26	1.09	$\bar{1}$.69	1.13	$\bar{1}$.82
27	1.10	$\bar{1}$.70	1.14	$\bar{1}$.82
28	1.10	$\bar{1}$.70	1.15	$\bar{1}$.88

ν	$\log v_\nu$	$\log \frac{F_\nu(v)}{100}$	$\log v_\nu$	$\log \frac{F_\nu(v)}{100}$
	Shell No. 542		Shell No. 543	
29	1.11	$\bar{1}$.83	1.16	$\bar{1}$.89
30	1.12	$\bar{1}$.84	1.17	$\bar{1}$.84
31	1.13	$\bar{1}$.85	1.18	$\bar{1}$.89
32	1.14	$\bar{1}$.90	1.19	$\bar{1}$.94
33	1.16	$\bar{1}$.90	1.20	$\bar{1}$.95
34	1.16	$\bar{1}$.91	1.21	$\bar{1}$.95
35	1.18	$\bar{1}$.91	1.22	$\bar{1}$.96
36	1.19	$\bar{1}$.92	1.23	0.00
37	1.20	$\bar{1}$.97	1.24	0.08
38	1.21	$\bar{1}$.97	1.26	0.12
39	1.22	0.02	1.27	0.16
40	1.23	0.03	1.28	0.16
41	1.24	0.03	1.30	0.19
42	1.25	0.10	1.31	0.25
43	1.27	0.11	1.33	0.27
44	1.28	0.11	1.34	0.30
45	1.29	—	1.36	0.31
46	1.30	0.19	1.37	0.33
47	1.31	—	1.39	0.33
48	1.33	0.22	1.40	0.34
49	1.34	0.23	1.42	0.40
50	1.35	0.23	1.44	0.42
51	1.37	0.29	1.45	0.43
52	1.38	0.29	1.47	0.45
53	1.39	0.29	1.48	0.50
54	1.40	0.34	1.50	0.52
55	1.42	0.37	1.52	0.54
56	1.43	0.41	1.53	0.58
57	1.45	0.43	1.55	0.60
58	1.46	0.44	1.57	0.65
59	1.48	0.46	1.59	0.67
60	1.49	0.48	—	—
61	1.51	0.53	—	—
62	1.52	0.55		
63	1.54	0.57		
64	1.55	0.61		
65	1.57	0.66		
66	1.59	0.70		
67	1.61	0.73		
68	1.63	0.78		
69	1.65	0.82		
70	1.67	0.89		
71	—	—		
72	—	—		

6.2.5 Calculation of the Values *n* and *k* for the Motion Equation 40

A graph of the relationship of log *v* and log *F(v)* may be obtained as in Figure 24.

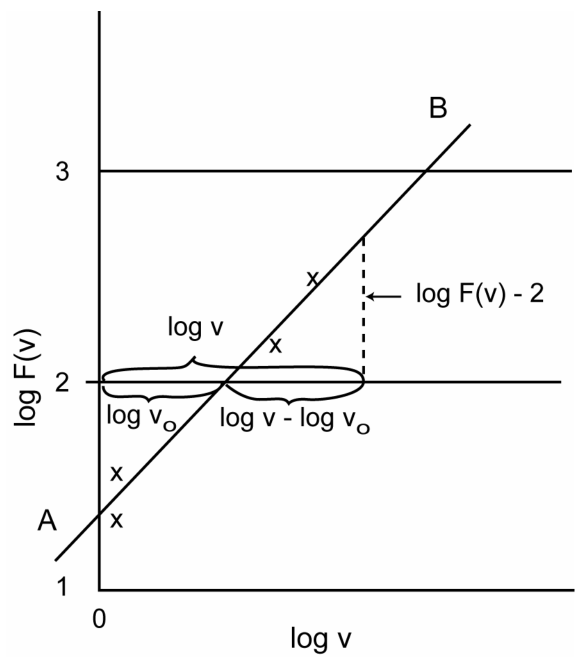

Figure 24. A graph for the relationship between v and F(v).

As a trial, a line AB is set as:

$$n' = \frac{\log F(v) - 2}{\log v - \log v_0}$$

where *n*' is the slope of AB and v_o is the value at log *F(v)*. From the above equation we have:

$$\log F(v) = n' \log v + (2 - n' \log v_0) \qquad (42)$$

On the other hand from equation 41

$$\log F_\mu(v) = n \log v_\mu + \log k \qquad (43)$$

Comparing equation 42 with 43, the next relations are obtained,

$$n' = n$$
$$2 - n' \log v_0 = \log k \qquad (44)$$

The values *n'* and log v_o can be obtained by the method shown in Figure 25, and the values of *n* and *k* can be calculated. Figure 25 shows the relations of log *v* and log *F(v)* = log($F_v(v)$/100) + 2 (Table 19).

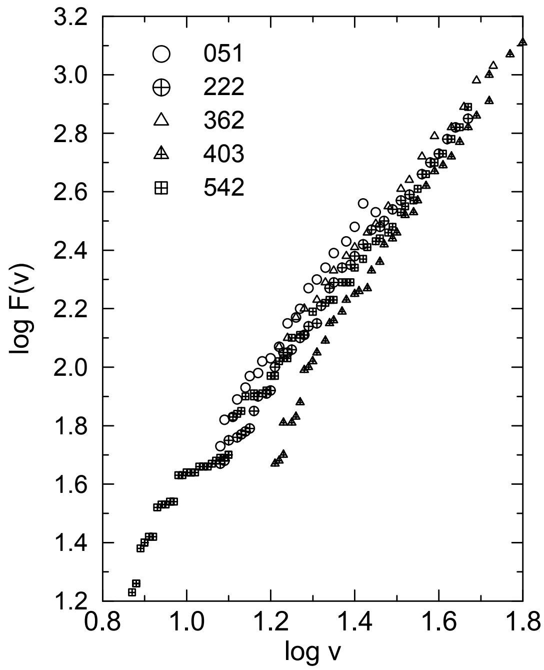

Figure 25. The relationship of log v and log $F_v(v)$ (See Table 19).

The values *n′* and log v_o and their average values and the probability deviations are shown in Table 20.

Table 20. The values *n′* and log v_o.

Star and Shell	No.	*n′*	log v_o
B_8D_4	31	2.08	1.18
	41	1.67	1.14
	51	2.27	1.18
	62	1.83	1.16
	72	1.90	1.13
	82	2.22	1.22
	91	1.83	1.13
	101	1.99	1.21
	112	2.20	1.18
$B_{12}D_4$	132	1.79	1.21
	141	2.05	1.20
	153	2.45	1.23
	262	2.02	1.24
	172	1.78	1.25
	182	2.02	1.23
	191	1.84	1.21
	202	1.83	1.20
	212	2.09	1.22
	222	1.89	1.22
	232	2.05	1.19
	241	1.85	1.19
B_8D_5	252	1.74	1.15
	261	1.72	1.16
	272	1.84	1.17
	281	1.75	1.14
	291	1.53	1.11
	302	1.85	1.14
	312	1.77	1.16
	343	1.97	1.22
	352	1.90	1.18
	362	1.89	1.18
$G_{12}D_5$	502	1.87	1.21
	503	1.93	1.22
	505	2.22	1.17
$B_{12}D_5$	371	1.84	1.20
	382	1.80	1.20
	392	2.17	1.26
	403	2.11	1.29
	411	1.30	1.23
	422	2.30	1.25
	442	2.24	1.27
	452	1.95	1.24
	471	1.92	1.23
	481	1.79	1.19
$G_{12}D_5$	542	1.85	1.22
	543	1.81	1.21
	544	1.91	1.21
Average:		1.93	1.20
Probability deviation:		0.140	0.027

In the Figure 26 the values of n for B_8 are biased toward lower values, and B_{12} is biased toward higher values. However, it could be assumed that they fall in line with each other.

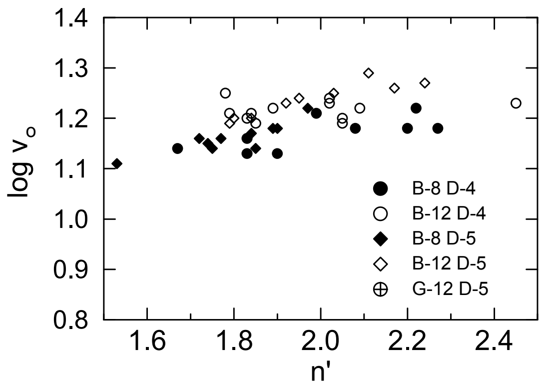

Figure 26. Ballistic constants log v_o and n'.

6.2.6 The Influence of Weather Conditions on the Ballistic Constants

On the first day of the test, it was calm with no wind. On the second day, it was windy (4–5 m/s) and a little rainy. If there were large influences on the values of n and log v_o, they would be divided into two groups. Figure 27 shows the values for n and log v_o obtained on the first and second days using different symbols. The values of n and log v_o of the first day appeared to be lower than those of the second day. However, for simplicity, these differences were ignored because such influences would probably not occur in practice. Therefore the average values of n and log v_o were used for the following calculations.

6.2.7. The Differential Equation Describing the Movement of Stars

From equation 44, the values of n and k are:

$n = n' = 1.93$

$\log k = 2 - n' \log v_o = 2 - 1.93 \times 1.20 = \bar{1}.684$

Publisher's note – there was no equation (45)

From above

$k = 0.483$

The differential equation for the horizontal motion of a star in the air should therefore be written as:

$$p'(t) = \frac{d^2 x}{dt^2} = -0.483 v^{1.93} \tag{46}$$

6.2.8 Formula for a Star Moving in a Horizontal Direction

From equation 46:

$$\frac{dv}{dt} = -k \frac{v^n}{p'(t)} \tag{47}$$

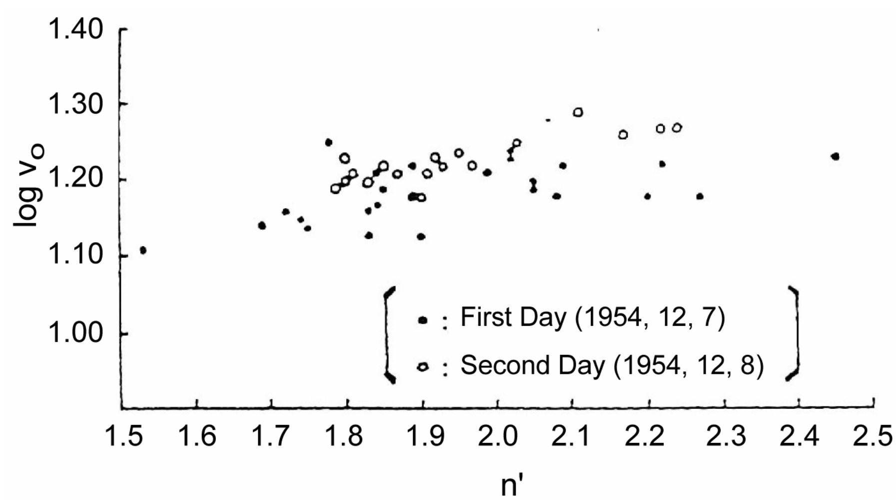

Figure 27. Influence of the weather on the ballistic constants.

where $k = 0.483$ and $n = 1.93$

Integrating equation 47 we have:

$$\int_{v_0}^{v} \frac{dv}{v^n} = -k\int_0^t \frac{dt}{p'(t)} \tag{48}$$

Here, v_o is the velocity at some start time ($t = 0$), and we can select any convenient value. Therefore, v_o is taken either as the initial velocity of the star or the velocity at the color change of the star. Solving equation 48 we have:

$$v = \left\{ v_0^{1-n} + (1-n)(-k)\int_0^t \frac{dt}{p'(t)} \right\}^{\frac{1}{1-n}} \tag{49}$$

Introducing

$$v = \frac{dx}{dt}$$

we have:

$$x = \int_0^t \left\{ v_0^{1-n} + (1-n)(-k)\int_0^t \frac{dt}{p(t)} \right\}^{\frac{1}{1-n}} dt \tag{50}$$

Equations 49 and 50 are the fundamental equations to express the relations t–v and t–x for horizontal movement.

(1) For Stars That Consist of a Single Composition

Using the symbols:

t	time
m	the mass at time t
r	the radius at time t
R	the initial radius at time $t = 0$
$p'(t)$	sectional density at time t

we have:

$$p'(t) = \frac{m}{\pi r^2} \tag{51}$$

On the other hand,

$$m = \frac{4}{3}\pi r^3 \delta$$

where δ is the density of the star.

Therefore,

$$p'(t) = \frac{4}{3} r\delta \tag{52}$$

Introducing the following formulas:

$$\left.\begin{aligned} r &= R - \omega t \\ \omega &= \frac{R}{T} \end{aligned}\right\} \tag{53}$$

where T is the total burning time of the star, we have:

$$v = R\left(1 - \frac{t}{T}\right) = R(1-\tau) \tag{54}$$

where

$$\tau = \frac{t}{T}\,. \tag{54'}$$

The symbol τ denotes the ratio of the burn time t to the total burn time T.

Next, the following calculation is carried out:

$$I = \int_0^t \frac{dt}{p'(t)} = \frac{3}{4}\frac{1}{R\delta}\int_0^t \frac{dt}{\left(1 - \frac{t}{T}\right)} \tag{55}$$

Introducing equation 54' and

$$d\tau = \frac{1}{T} dt \tag{55'}$$

into equation 55, we have:

$$\begin{aligned} I &= \frac{3}{4}\frac{T}{R\delta}\int_0^\tau \frac{d\tau}{(1-\tau)} \\ &= -\frac{3}{4} \cdot 2.303 \frac{T}{R\delta}\log(1-\tau) \end{aligned} \tag{56}$$

Introducing equation 56 into equation 49 we have:

$$\begin{aligned} v &= \left\{ \begin{aligned} & v_0^{1-n} + (1-n)(-k) \times \left(-\frac{3}{4} \times 2.303\right) \\ & \frac{T}{R\delta}\log(1-\tau) \end{aligned} \right\}^{\frac{1}{1-n}} \\ &= v_0 \left\{ \begin{aligned} & 1 + \frac{(1-n)(-k)\times(-3\times 2.303)}{4v_0^{1-n}} \cdot \\ & \frac{T}{R\delta}\log(1-\tau) \end{aligned} \right\}^{\frac{1}{1-n}} \end{aligned} \tag{57}$$

Introducing a new symbol into equation 57

$$A_s = \frac{-(1-n)(-k)\times(-3\times 2.303)}{4v_0^{1-n}} \cdot \frac{T}{R\delta} \quad (58)$$

and calculating it with n = 1.93 and k = 0.483, we obtain:

$$\begin{aligned} A_s &= 0.774 \frac{v_o^{0.93} T}{R\delta} \\ &= 0.774 v_o^{0.93} \frac{1}{R/T} \cdot \frac{1}{\delta} \end{aligned} \quad (58')$$

The value of A_s is almost proportional to the value of v_o and inversely proportional to the burn rate R/T and the density δ of the star.

From equation 57:

$$v = v_0 \int_0^\tau \left\{1 - A_s \log(1-\tau)\right\}^{-1.075} d\tau$$

For comparison with the results of the following section, it is convenient to write this as:

$$v = v_0 \int_0^\tau \left\{1 - \left(\frac{A_S}{3}\right) \log(1-\tau)^3\right\}^{-1.075} \mathrm{d}\tau \quad (59)$$

Considering equations 56 and 59 we have from equation 50:

$$x = v_0 T \int_0^\tau \left\{1 - \left(\frac{A_S}{3}\right) \log(1-\tau)^3\right\}^{-1.075} \mathrm{d}\tau \quad (60)$$

Equations 59 and 60 are practical equations to calculate the motion of a star that consists of a single composition.

(2) For Stars That Consist of More Than One Type of Composition (Color Changing Stars)

In this case the layer of each color has an individual burn time (T_i), outside radius (R_i), and density (δ_i). (See Figure 28.)

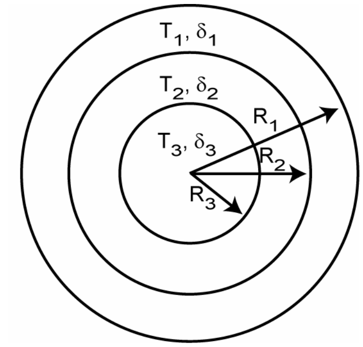

Figure 28. A color changing star.

First, the value of the sectional density is denoted as:

$$p'(t) = \frac{m}{\pi r^2} \quad (61)$$

The value of m is denoted as:

$$m = \frac{4}{3}\pi \left\{ \begin{aligned} &\left(r^3 - R_2^3\right)\delta_1 + \left(R_2^3 - R_3^3\right)\delta_2 \\ &+ \left(R_3^3 - R_4^3\right)\delta_3 + \ \dots \end{aligned} \right\} \quad (62)$$

$$\begin{aligned} r &= R_1 - \omega_1 t = R_1 - \frac{R_1 - R_2}{T_1} t \\ &= R_1 \left\{ 1 - \frac{t}{\left(\dfrac{T_1}{1-(R_2/R_1)}\right)} \right\} \end{aligned} \quad (63)$$

Setting an equation as:

$$T_1' = \frac{T_1}{1-(R_2/R_1)} \quad (64)$$

Equation 63 becomes

$$r = R_1 \left(1 - \frac{t}{T_1'}\right) = R_1\left(1 - \tau_1'\right) \quad (65)$$

here $\tau_1' = t/T_1'$. When R_2 = 0, equation 65 coincides with equation 54, and it becomes the case of the single colored star, where $T_1' = T_1$. In the same manner as shown in the previous section, the following integration was carried out.

$$I = \int_0^t \frac{dt}{p'(t)} = \int_0^t \frac{\pi r^2}{m(t)} dt$$

When the value m (see equation 62) is introduced into the above formula, we have

$$I = \int_0^t \frac{\pi r^2 dt}{\frac{4}{3}\pi \left\{ \begin{array}{l} \left(r^3 - R_2^3\right)\delta_1 + \left(R_2^3 - R_3^3\right)\delta_2 + \\ \left(R_3^3 - R_4^3\right)\delta_3 + \ldots \end{array} \right\}}$$

When the next symbol c is introduced into the above equation:

$$c = -\left\{ \begin{array}{l} \left(\delta_1 - \delta_2\right) R_2^3 + \left(\delta_2 - \delta_3\right) R_3^3 + \\ \left(\delta_3 - \delta_4\right) R_4^3 + \ldots \end{array} \right\} \quad (66)$$

we have

$$I = \frac{3}{4}\int_0^t \frac{r^2 dt}{r^3 \delta_1 + c}$$

Equation 65 is introduced into the above equation

$$I = \frac{3}{4}\int_0^{\tau'} \frac{T_1' R_1^2 \left(1-\tau'\right)^2 d\tau}{R_1^3 \left(1-\tau'\right)^3 \delta_1 + c}$$

This integral is evaluated by making the substitution

$$y = (1-\tau)^3$$

$$d\tau = -\frac{1}{3}(1-\tau)^{-2} dy$$

which leads to

$$\int \frac{T_1' R_1^2 \left(1-\tau'\right)^2 d\tau}{R_1^3 \left(1-\tau'\right)^3 \delta_1 + c}$$

$$= \int -\frac{1}{3}\frac{T_1' R_1^2 dy}{R_1^3 \delta_1 y + c}$$

$$= -\frac{1}{3} T_1' R_1^2 \int \frac{dy}{R_1^3 \delta_1 y + c}$$

$$= -\frac{1}{3}\frac{T_1' R_1^2}{R_1^3 \delta_1} \ln(R_1^3 \delta_1 y + c) + C$$

$$= -\frac{1}{3}\frac{T_1'}{R_1 \delta_1} 2.303 \log((1-\tau)^3 + b) + C'$$

where C and C' are constants of integration, and b is given by

$$b = \frac{c}{R_1^3 \delta_1}$$

$$= -\left\{ \begin{array}{l} \left(1 - \frac{\delta_2}{\delta_1}\right)\left(\frac{R_2}{R_1}\right)^3 + \left(\frac{\delta_2}{\delta_1} - \frac{\delta_3}{\delta_1}\right)\left(\frac{R_3}{R_1}\right)^3 + \\ \left(\frac{\delta_3}{\delta_1} - \frac{\delta_4}{\delta_1}\right)\left(\frac{R_4}{R_1}\right)^3 + \ldots \end{array} \right\} \quad (67)$$

The definite integral from $\tau = 0$ to $\tau = \tau$ is then

$$I = -\frac{2.303}{4}\frac{T_1'}{R_1 \delta_1} \log \frac{(1-\tau)^3 + b}{1+b} \quad (68)$$

If the density is the same for all layers,

$$\delta_1 = \delta_2 = \delta_3 = \ldots$$

then the value of b becomes 0 ($b = 0$). When the density of the star increases toward the center:

$$\delta_1 < \delta_2 < \delta_3 < \ldots$$

then we have $b > 0$.

On the contrary, when the density decreases towards the center:

$$\delta_1 > \delta_2 > \delta_3 > \ldots$$

then we have $b < 0$.

When the density does not change through all the layers, the value of $b = 0$, and we have the same equation as equation 65. When equation 68 is introduced into equation 49, we have:

$$v = \left\{ \begin{array}{l} v_0^{1-n} + (1-n)(-k) \times \left(-\frac{2.303}{4}\right) \times \\ \frac{T_1'}{R_1 \delta_1} \log \frac{\left(1-\tau\right)^3 + b}{1+b} \end{array} \right\}^{\frac{1}{1-n}}$$

$$= v_0 \left\{ \begin{array}{l} 1 + \frac{(1-n)(-k) \times (-2.303)}{4 v_0^{1-n}} \times \\ \frac{T_1'}{R_1 \delta_1} \log \frac{\left(1-\tau\right)^3 + b}{1+b} \end{array} \right\}^{\frac{1}{1-n}} \quad (69)$$

In equation 58, a symbol A_s was set as:

$$A_s = \frac{-(1-n)(-k)\times(3\times -2.303)}{4v_0^{1-n}} \cdot \frac{T_1'}{R_1\delta_1} \quad (70)$$

Introducing $n = 1.93$ and $k = 0.483$:

$$A_s = 0.774\ v_0^{0.93}\frac{1}{R_1/T_1'}\cdot\frac{1}{\delta_1} \quad (70')$$

Then from equation 69:

$$v = v_0\left\{1-\left(\frac{A_S}{3}\right)\log\frac{(1-\tau')^3+b}{1+b}\right\}^{-1.075} \quad (71)$$

When $b = 0$, this equation coincides with equation 59. And from equation 50, considering equations 68 and 70, we have:

$$x = v_0T_1'\int_0^{\tau_1'}\left\{1-\left(\frac{A_S}{3}\right)\log\frac{(1-\tau_1')^3+b}{1+b}\right\}^{-1.075} d\tau_1' \quad (72)$$

This equation perfectly coincides with equation 60 when $b = 0$.

Equations 71 and 72 are practical equations to obtain the relationship of $v - t$ and $x - t$ when the first layer of the star is burning. To obtain the relationship of $v - t$ and $x - t$, when the second and subsequent layers are burning, first calculate the final velocity of the first layer. This velocity is then regarded as the initial velocity of the second layer v_o and in place of R_1, T_1', and δ_1, use R_2, T_2', δ_2 and equations 71 and 72 to calculate the values of v and x. This repeats for the next layer, etc.

6.2.9 The Curvature of the Trajectory of the Star

The curvature of the trajectory of a star should be reasonable for our purpose. Therefore, when we design a chrysanthemum, we should obtain a proper value of the radius of curvature.

Symbols:

- ρ radius of curvature
- *m* mass of star
- g acceleration due to gravity
- *v* velocity of star
- θ inclination of trajectory

The centrifugal force must be equal to the centripetal force. Therefore,

$$\frac{mv^2}{\rho} = -mg\cos\theta$$

From this relation:

$$\rho\cos\theta = -\frac{v^2}{g} \quad (72')$$

This equation gives the radius of curvature at any point of the trajectory. (See Figure 29.)

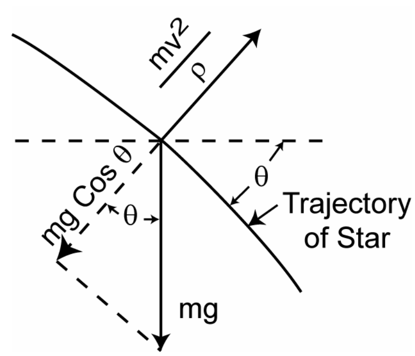

Figure 29. The curvature of the trajectory of a star.

6.3 Initial Velocity of Stars

The cutting of the image of a flying star by the revolving shutter is not good at the start because of interference from the sparks of the prime, which covered the surface of the star. Therefore, the initial velocity of stars should be calculated from where the image of the stars first becomes clear, near the bursting point. (See Figure 30.)

6.3.1 The Formula of Initial Velocity Deduced from a Dot near the Bursting Point

The equation of the motion of a star can be written as:

$$\frac{dv}{dt} = -g\sin\theta - \frac{kv^2}{p'} \tag{73}$$

where $\frac{dv}{dt}$ is the acceleration in the direction of the movement, g is the acceleration due to gravity, k is a constant, and p' is the sectional density of the star. To solve equation 73, the following assumptions could be made because the initial calculation points are so near the bursting point:

1) the acceleration due to gravity only affects the trajectory in the vertical direction, not in the horizontal direction.
2) the constant k does not change during the motion.
3) the sectional density does not change during the motion.

With these assumptions, the equation of motion can approximately be divided into two parts:

the horizontal direction:

$$\frac{dv_x}{dt} = -\frac{k}{p'}v_x^2 \tag{74-1}$$

and the vertical direction:

$$\frac{dv_y}{dt} = -g - \frac{k}{p'}v_y^2 \tag{74-2}$$

Author's note:

In this case the author could not find a good dynamic calculation for the motion of the stars because the trajectories of the stars near the bursting point are invisible, as they are in Figure 30. Therefore, the following is based on an approximate calculation.

From equation 74-1 we have:

$$\frac{dx}{dt}\cdot\frac{dv}{dx} = -\frac{k}{p'}v^2 \quad \text{or}$$

$$v\frac{dv}{dx} = -\frac{kv^2}{p'}$$

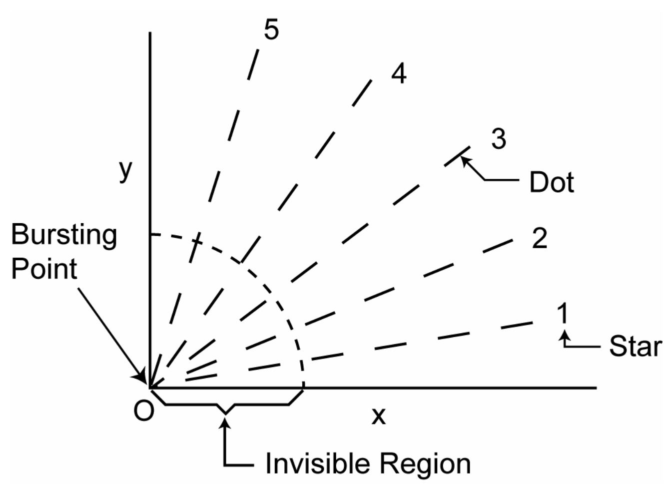

Figure 30. The image of stars near the blasting point on the photograph.

From this equation:

$$\frac{dv}{v_x} = -\frac{k}{p'}dx$$

Integrating this equation:

$$[\ln v_x]_{V_x}^{v_x} = -\frac{k}{p'}[x]_0^x$$

$$V_x = ve^{\frac{k}{p'}x} \qquad (75)$$

From equation 74-2:

$$V_y \frac{dv_y}{dy} = -\frac{k}{p'}v_y^2 - g$$

Integrating equation 75 we have:

$$V_y^2 = v_y^2 e^{2\frac{k}{p'}y} + \frac{g}{\frac{k}{p'}}\left(e^{2-\frac{k}{p'}y} - 1\right) \qquad (76)$$

The initial velocity of the star can be written approximately as:

$$V^2 = V_x^2 + V_y^2$$

Therefore, the combination of equations 75 and 76, gives us:

$$V^2 = v_x^2 e^{2\frac{k}{p'}x} + v_y^2 e^{2\frac{k}{p'}y} + \frac{gp'}{k}\left(e^{2\frac{k}{p'}y} - 1\right) \qquad (77)$$

This equation is not exact, but the author used it to calculate the approximate initial velocity of a star.

6.3.2 Calculation of the Velocities of Stars near the Bursting Point from the Dots on Photographs

The first dots in the photograph were not captured clearly by the revolving shutter. Therefore, the first dot of every trajectory was omitted. The difference between the coordinates of $x_4 - x_2$ and that between $y_4 - y_2$ were calculated and multiplied by the shutter constant of 12.5. From this we obtained the velocity of the third dot head x_3, y_3. Table 21 shows the data obtained by this method.

Table 21. Velocities of Stars near the Bursting Point.

Star No.	x_3 (m)	v (m/s)	y_3 (m)	u (m/s)
21	21.78	44.0	4.59	7.5
22	20.00	40.8	9.40	17.3
23	19.58	35.5	12.94	20.0
24	16.62	29.3	15.44	25.5
25	12.96	22.5	17.86	30.0
26	7.24	21.0	18.40	38.5
27	4.52	12.0	18.16	41.5
28	2.32	4.5	18.68	40.0
31	15.08	33.5	2.32	3.3
32	14.68	31.8	4.89	9.5
33	13.76	29.8	7.70	14.5
34	12.88	27.5	10.76	20.5
35	17.08	22.0	13.63	20.5
36	8.20	20.5	13.16	30.5
37	5.72	10.8	16.92	27.3
38	2.80	6.3	16.88	33.3
39	0.00	0.0	17.84	28.8
41	23.52	45.5	4.32	6.8
42	25.52	37.5	8.16	10.5
43	20.88	42.0	10.96	20.5
44	19.84	34.5	15.80	25.0
45	16.56	29.3	18.68	30.5
46	11.80	26.5	18.08	40.0
51	15.44	23.5	4.16	5.0
52	11.92	23.5	6.03	10.5
53	12.80	18.3	8.68	11.5
54	8.72	13.0	9.72	18.0
55	5.60	12.5	10.68	23.0
56	3.66	8.3	10.64	24.0
57	1.30	3.0	9.20	24.0
61	14.88	33.5	1.78	2.0
62	14.78	30.8	4.63	7.5
63	12.70	29.8	6.64	14.0
64	9.96	24.0	8.70	20.0
65	8.96	21.8	10.60	24.8
66	5.94	14.0	12.44	29.0
67	4.24	10.0	12.56	28.5
68	1.12	2.0	12.00	32.5
69	–0.32	2.8	12.76	30.0
71	15.00	31.8	1.54	1.0
72	12.66	32.0	4.40	9.8

Star No.	x_3 (m)	v (m/s)	y_3 (m)	u (m/s)
73	11.52	25.0	7.28	14.5
74	9.40	23.5	9.48	18.0
75	7.86	18.5	10.84	25.5
76	4.88	15.0	9.52	27.0
77	6.36	6.3	11.24	27.0
78	–1.48	4.0	12.80	26.5
81	15.96	36.0	0.72	0.0
82	16.72	37.5	3.90	6.5
83	15.02	38.0	5.56	11.0
84	10.34	27.3	8.88	22.0
85	6.36	19.3	9.28	27.0
86	4.76	14.5	9.84	34.0
87	2.88	7.8	11.32	29.5
88	–0.14	–0.3	11.12	30.5
91	16.20	34.3	3.48	6.3
92	12.72	33.5	5.96	13.8
93	10.40	31.5	6.96	17.8
94	10.28	26.8	10.00	23.8
95	9.88	16.5	16.60	25.0
96	4.20	7.3	17.48	30.5
101	19.20	38.5	4.32	6.0
102	16.28	38.0	6.34	14.3
103	16.12	32.0	11.56	22.0
104	Image not clear			
105	8.88	20.5	16.84	36.5
106	7.36	15.8	18.52	34.0
107	2.60	5.5	17.62	38.0
108	0.44	2.0	17.78	33.5
111	12.20	33.0	1.50	2.0
112	16.20	29.3	4.90	2.3
113	13.56	27.5	6.36	12.0
114	12.00	23.0	9.04	15.0
115	8.00	22.0	8.96	23.0
116	2.08	5.0	13.20	28.5
117	–1.24	–2.0	14.36	27.5
131	11.48	33.8	1.84	3.8
132	10.11	28.5	4.90	12.8
133	9.80	28.0	6.20	20.0
134	7.56	20.3	7.44	24.8
135	2.76	10.3	8.84	30.0
141	10.84	38.0	0.90	1.5
142	10.08	35.0	3.92	11.5
143	8.32	28.0	6.60	21.5

Star No.	x_3 (m)	v (m/s)	y_3 (m)	u (m/s)
144	7.04	20.3	9.56	25.5
145	3.64	12.5	9.88	33.0
146	–1.44	3.5	12.56	27.5
151	11.52	44.5	2.92	11. 8
152	10.76	41.8	5.60	19.5
153	9.64	36.5	8.64	31.0
154	7.00	26.8	10.44	38.5
155	1.18	4.0	11.40	42.0
161	9.32	52.0	1.42	7.5
162	8.40	42.0	3.44	17.0
163	6.90	36.0	4.94	25.0
164	6.04	26.8	7.84	33.8
165	3.10	13.5	9.08	39.0
166	–0.08	0.0	12.52	42.5
171	8.52	30.5	2.06	6.8
172	7.92	28.5	3.94	13.3
173	6.28	23.0	5.36	19.0
174	4.22	15.5	7.20	21.3
175	1.84	7.5	10.32	27.5
181	9.96	31.5	3.04	8.5
182	7.20	27.5	5.30	19.3
183	5.04	18.5	6.88	25.0
184	3.08	11.8	8.20	30.5
185	0.72	17.5	9.84	35.5
191	7.78	28.8	1.96	11.5
192	6.20	23.0	3.62	14.8
193	4.04	17.8	4.78	20.5
194	2.92	11.0	6.40	23.0
195	–0.24	–1.5	7.48	27.0
201	13.16	49.5	1.54	4.5
202	12.20	45.8	4.37	10.0
203	10.96	40.0	7.74	27.5
204	9.80	30.8	11.40	34.0
205	6.12	22.8	11.76	42.0
206	2.60	9.8	12.32	44.5
207	–1.08	–3.5	12.00	43.5
211	11.76	36.5	1.10	2.5
212	10.92	37.5	3.88	11.5
213	9.56	31.0	6.18	18.8
214	7.68	23.8	8.00	23.8
215	4.78	15.3	9.48	29.5
216	2.68	8.8	10.43	32.5

Star No.	x_3 (m)	v (m/s)	y_3 (m)	u (m/s)
217	–0.34	–0.8	11.52	30.0
221	15.68	48.0	1.70	4.3
222	12.56	47.0	5.12	12.8
223	12.58	40.0	9.00	27.5
224	9.72	29.8	12.00	35.0
225	6.04	22.5	11.80	41.8
226	3.06	11.3	13.16	46.5
227	–0.72	–2.0	15.80	45.0
231	12.18	39.0	1.02	1.5
232	11.60	36.5	4.26	15.5
233	9.70	31.3	7.10	21.0
234	7.40	23.5	9.28	27.5
235	4.04	13.0	11.76	35.5
236	0.12	1.8	11.24	32.3
241	13.52	47.0	3.48	10.5
242	11.88	41.8	6.76	21.5
243	9.50	34.0	9.80	33.3
244	6.02	21.8	12.08	41.0
245	–0.52	–0.8	15.60	45.0
251	21.30	42.5	1.86	12.5
252	17.76	43.5	4.36	7.3
253	18.13	39.0	6.60	12.0
254	16.40	39.5	8.30	17.5
255	18.36	31.8	11.92	23.0
256	13.16	28.0	14.00	27.0
257	11.12	19.5	16.83	29.0
258	8.38	18.5	16.96	33.3
259	6.06	12.3	18.76	37.0
2510	–1.82	–3.3	16.92	41.5
261	19.28	51.5	2.76	6.5
262	26.00	42.0	4.64	4.3
263	20.76	33.5	9.88	18.5
264	13.76	36.0	12.36	21.5
265	17.42	32.0	14.06	24.5
266	15.52	26.0	18.34	29.5
267	12.80	19.8	19.24	31.5
268	9.28	18.5	18.92	35.8
269	–0.76	11.5	17.80	44.5
271	20.64	46.0	0.44	–1.3
272	22.64	41.3	5.00	7.5
273	21.76	39.5	7.00	11.0
274	19.84	36.8	10.22	17.5
275	18.20	33.5	12.24	20.0

Star No.	x_3 (m)	v (m/s)	y_3 (m)	u (m/s)
276	17.48	29.3	14.36	21.3
277	12.60	24.0	17.28	31.5
278	6.68	14.3	18.20	38.5
279	–1.32	–2.3	18.44	34.0
281	23.88	45.5	2.00	1.8
282	21.36	46.5	5.36	10.0
283	19.92	43.0	7.76	14.5
284	18.76	42.5	9.92	21.0
285	19.72	32.5	14.64	22.0
286	17.24	31.5	17.24	30.3
287	13.84	31.0	18.48	36.3
288	10.96	23.8	18.84	37.5
289	11.04	18.0	23.40	35.5
2910	5.28	9.8	23.20	39.8
2911	1.84	3.5	22.96	39.0
2912	–0.58	–0.5	23.32	40.5
291	13.88	33.3	2.76	5.0
292	11.44	33.0	3.94	9.8
293	10.36	30.5	5.98	16.3
294	9.20	26.5	7.04	18.0
295	8.86	21.5	8.72	19.5
296	8.20	21.0	10.24	24.0
297	6.20	13.5	11.92	23.0
298	3.44	8.0	12.52	28.0
299	2.32	5.0	13.32	26.0
2910	0.52	1.3	11.96	32.5
301	13.00	35.0	6.60	0.0
302	17.64	33.5	2.68	3.0
303	16.22	30.0	5.56	3.0
304	14.84	32.5	7.64	15.0
305	13.22	29.0	9.14	16.8
306	11.00	23.5	11.88	24.5
307	8.54	22.0	12.00	28.8
308	7.96	18.0	14.10	28.0
309	4.20	10.3	15.20	37.5
3010	3.56	7.5	16.16	33.5
3011	1.56	4.0	17.20	38.0
311	15.80	41.0	0.78	0.5
312	15.84	40.3	2.96	5.5
313	15.60	41.0	4.58	10.0
314	17.72	34.3	8.40	14.3
315	15.74	25.0	10.74	18.0
316	12.72	30.5	11.64	27.5
317	12.96	25.0	13.64	24.0
318	9.96	25.5	13.00	31.8

Star No.	x_3 (m)	v (m/s)	y_3 (m)	u (m/s)
319	7.16	16.8	14.76	35.0
3110	5.20	14.0	14.04	35.0
3111	3.00	9.5	13.16	38.8
3112	–0.70	1.8	16.74	35.8
331	17.60	42.8	2.52	4.3
332	18.08	41.0	5.14	10.3
333	11.32	36.8	7.32	12.5
334	17.50	32.0	10.84	16.8
335	13.08	31.0	11.20	24.8
336	11.60	26.5	13.04	28.5
337	9.20	19.5	15.76	30.0
338	6.80	14.3	16.64	31.5
339	5.42	11.0	17.28	33.3
3310	2.28	5.0	18.64	36.0
3311	–1.36	–3.0	18.04	34.0
341	26.04	52.0	1.12	0.8
342	23.14	55.3	6.72	15.3
343	27.88	48.0	5.10	7.5
344	26.24	43.5	12.20	19.0
345	27.00	47.0	14.30	21.5
346	17.76	30.0	24.52	34.5
347	17.56	27.5	24.56	43.5
348	Image not clear			
349	7.80	16.3	24.48	49.0
3410	2.92	6.5	27.32	45.0
3411	–0.96	–.03	28.20	41.5
351	25.52	37.5	4.34	4.3
352	19.60	41.5	5.96	10.8
353	19.16	38.0	8.76	16.0
354	18.44	34.0	13.32	23.0
355	16.96	31.3	10.50	24.8
356	12.92	27.5	16.30	33.5
357	Image not clear			
358	3.56	7.0	18.50	35.5
359	0.64	2.5	17.28	43.3
361	29.08	45.0	5.56	8.5
362	26.06	54.8	6.64	11.3
363	27.52	47.5	10.46	14.8
364	25.08	43.5	14.30	22.0
365	25.28	28.5	21.28	22.0
366	21.36	27.5	20.76	28.0
367	15.52	33.0	20.84	37.5
368	14.16	29.0	27.68	43.5
369	11.54	15.8	28.56	40.5
3610	2.50	3.5	30.22	41.8

Star No.	x_3 (m)	v (m/s)	y_3 (m)	u (m/s)
3611	–0.66	–1.8	31.56	44.0
371	15.04	52.0	3.12	9.8
372	14.32	49.8	5.36	17.0
373	12.94	46.0	7.84	26.0
374	10.68	36.8	10.36	34.5
375	8.54	29.5	12.16	39.8
376	5.60	20.5	13.56	46.0
377	3.04	10.8	14.48	49.0
378	0.06	0.5	13.60	40.5
381	17.44	71.5	0.50	1.5
382	19.16	61.5	4.64	13.3
383	19.02	50.0	9.84	24.0
384	15.76	49.8	11.80	36.0
385	11.76	45.0	12.80	48.5
386	9.36	29.5	16.68	51.0
387	5.72	18.3	17.68	54.0
388	1.78	7.3	16.16	61.5
389	1.44	5.0	16.56	50.0
391	16.36	47.8	2.40	5.8
392	12.96	46.5	4.80	16.3
393	13.18	38.0	8.44	23.5
394	12.12	31.3	11.16	27.0
395	7.44	22.5	13.44	40.0
396	6.66	16.8	15.84	38.3
397	–2.12	–6.5	15.08	45.0
398	–1.20	–3.8	14.66	49.0
401	18.58	65.0	1.92	5.3
402	15.82	73.8	5.22	23.8
403	17.80	61.3	10.36	34.3
404	17.04	47.5	15.96	43.5
405	14.24	40.0	18.24	50.0
406	11.36	27.0	22.88	52.0
407	5.84	17.5	21.36	56.5
408	2.26	6.0	23.36	54.5
411	13.12	43.3	2.22	5.5
412	12.32	40.0	4.98	14.8
413	11.20	37.0	6.08	13.8
414	9.32	32.0	8.60	26.3
415	8.52	29.0	10.44	33.5
416	6.08	20.8	11.44	35.0
417	3.66	11.0	13.52	35.5
418	0.73	3.5	11.98	38.3
419	1.82	5.3	11.76	37.0

Star No.	x_3 (m)	v (m/s)	y_3 (m)	u (m/s)
421	12.84	45.8	2.06	6.0
422	12.40	41.5	4.72	14.3
423	11.24	39.8	7.20	23.5
424	10.44	36.0	9.28	30.0
425	8.28	28.5	12.04	39.0
426	5.96	21.5	13.44	44.0
427	3.04	10.5	14.36	46.3
431	12.16	43.8	2.96	16.3
432	11.36	39.5	5.24	18.0
433	10.40	35.8	9.08	24.3
434	9.34	31.8	9.68	32.5
435	7.24	25.5	11.36	39.0
436	4.58	17.0	11.88	41.5
437	2.30	7.5	14.64	41.8
438	–1.20	–2.5	14.28	41.5
451	14.98	47.0	1.34	2.8
452	12.18	44.5	4.56	15.5
453	10.36	37.0	7.20	26.3
454	10.12	31.5	10.24	30.3
455	7.64	23.0	12.04	35.8
456	4.28	16.0	11.28	41.0
457	3.16	6.5	14.36	42.8
458	–1.16	–3.0	14.68	44.3
461	10.36	42.5	1.96	5.8
462	9.72	38.5	4.40	16.0
463	9.12	35.8	6.64	24.0
464	7.44	29.5	9.00	33.8
465	5.30	21.0	10.16	38.0
466	3.76	12.5	12.52	39.5
467	0.84	3.5	12.96	41.0
468	–1.36	–5.0	11.56	42.0
471	15.88	54.3	2.64	9.8
472	14.94	50.5	5.12	16.5
473	13.66	46.5	8.34	27.0
474	13.50	38.5	11.80	32.0
475	9.42	33.0	12.60	42.0
481	21.84	67.5	4.36	11.8
482	22.24	54.5	9.96	23.5
483	18.32	54.0	9.68	28.0
484	14.64	43.0	10.76	30.5
485	16.54	49.5	13.04	38.5
486	8.36	31.5	15.76	57.0
487	6.64	16.3	23.64	51.0
488	2.40	6.0	21.83	54.0

Star No.	x_3 (m)	v (m/s)	y_3 (m)	u (m/s)
489	–1.40	–2.0	22.20	54.0
491	10.64	41.5	1.46	5.3
492	—	—	—	—
493	9.16	37.0	5.24	19.5
494	6.40	31.8	5.78	17.8
495	—	—	—	—
496	4.94	16.8	10.96	36.0
497	2.20	10.0	8.96	41.0
498	–1.56	–5.5	9.48	36.5
501	15.00	36.0	2.38	4.5
502	9.58	40.0	4.12	16.5
503	7.20	38.3	4.88	25.5
504	7.84	32.0	7.64	30.0
505	4.92	26.0	7.60	39.5
506	4.80	19.8	10.80	43.0
507	2.14	8.0	11.32	45.0
508	–0.56	2.5	10.40	41.0
511?	Image not clear			
521?	Image not clear			
531	Image not clear			
532	15.70	40.5	7.0	16.5
533	17.08	36.5	10.90	21.3
534	—	—	—	—
535	1.92	54.5	12.94	39.0
536	5.16	16.3	14.16	44.0
537	–0.92	–2.5	14.36	41.0
538	–3.58	–11.5	13.16	39.0
539	Image not clear			
5310	9.80	22.5	9.88	21.5
5311	13.04	25.5	8.60	15.0
541	11.96	52.0	2.92	12.5
542	12.32	45.0	6.12	21.0
543	10.60	39.5	9.04	32.5
544	8.76	32.0	10.24	35.5
545	6.40	23.3	11.56	41.0
546	3.52	13.0	13.00	46.0
547	1.04	3.0	13.04	47.0
548	–0.96	–3.3	13.12	46.5

6.3.3 Calculation of Initial Velocities at the Bursting Point from the nearest Dots of the Trajectories

The velocities v_x and v_y and the points x_3 and y_3 are obtained from Table 21. When these data are introduced into equation 77 using the value for k/p', which is known, we can obtain the approximate initial velocity of each star.

When deriving equation 77, we assumed $n = 2$ (see equations 74-1 and 74-2). Therefore, the value of k will not be the same as it was previously when $n = 1.93$. Figure 26 shows $\log v_o = 1.218$ when n = 2.

$$\log k = 2 - n \log v_0 = 2 - 2.0 \times 1.218 = \bar{1}.564$$

From this value we obtain

$$k = 0.366$$

Therefore, the values of the stars B_8, B_{12} and G_{12} are calculated as

$$B_8 : \frac{k}{p'} = \frac{0.366}{10.0} = 0.0366$$

$$B_{12} : \frac{k}{p'} = \frac{0.366}{14.2} = 0.0259$$

$$G_{12} : \frac{k}{p'} = \frac{0.366}{14.5} = 0.0253$$

The units for the above values of the sectional density p' are kg/m^2. In this calculation the value σ was an average value of the initial and those at the point (x_3, y_3). The mass m was assumet to be contant during the initial period from the bursting to the dotted position of each trajectory of a star.

The results of the calculations are shown in Table 22, where the symbols are as follows:

$V =$ initial velocity (m/s) for each star

$\bar{V} =$ average initial velocity for one star

$\Delta v / \bar{V} =$ ratio of the deviations of the initial velocity and the average velocity for one star

$r / \bar{V} =$ ratio of the probability deviations of the initial velocities to the average for a star

$$r = 0.6745 \sqrt{\frac{\Sigma \Delta v}{n-1}}$$

where n means the number of stars calculated for the initial velocity for one star.

$\theta =$ angle of elevation of the star

Table 22. Velocities of Stars and the Deviations of Velocity from the Mean Value and the Angle of Elevation of Each Star.

Star No.	$\bar{V}$ (m/s)	$\Delta v / \bar{V}$ (%)	θ
21	98.5	+17.0	11°55'
22	89.7	+6.6	25°11’
23	82.0	–2.5	33°28’
24	73.9	–12.2	42°54’
25	73.1	–13.1	54°02’
26	35.6	+1.7	63°20'
27	86.3	+2.6	76°01’
28	84.0	–0.2	82°53’
31	58.7	-0.1	8°46’
32	58.1	-1.1	18°26’
33	53.9	-8.3	29°15’
34	56.4	-4.0	39°52’
35	53.5	-9.0	46°18’
36	60.3	+2.6	58°05’
37	59.4	+1.1	71°19’
38	67.2	+14.3	80°35’
39	61.5	+4.6	90°00
41	103.0	+14.3	10°26’
42	97.5	+3.2	17°45’
43	96.9	+2.5	27°42’
44	87.4	–7.5	38°31’
45	85.5	–9.5	48°27’
46	91.7	–3.0	56°52’
51	42.9	+7.7	15°05’

Star No.	$\bar{V}$ (m/s)	$\Delta v / \bar{V}$ (%)	θ
52	40.5	+1.7	27°02’
53	36.6	+8.1	34°09’
54	39.4	–1.1	48°07’
55	41.3	+3.7	62°20’
56	40.7	+2.2	71°01’
57	37.4	+6.1	81°58’
61	57.1	+8.8	6°51’
62	55.6	+5.9	17°36’
63	52.3	–0.3	27°37’
64	47.0	–10.4	41°47’
65	50.6	–3.6	49°48’
66	52.8	+0.6	63°39’
67	50.7	–3.4	71°21’
68	54.1	+3.1	84°40’
69	52.1	–0.7	93°41’
71	55.3	+15.2	5°53’
72	53.1	+10.6	19°12’
73	44.7	–6.9	32°18’
74	44.9	–6.4	45°16’
75	48.7	+1.5	54°03’
76	45.3	–5.6	62°52’
77	44.7	–6.9	88°10’
78	47.2	–1.6	96°36’
81	64.6	+12.5	2°35’
82	70.1	+22.1	13°07’
83	68.2	+18.8	20°20’
83'	59.8	+4.2	27°02’
84	52.5	–8.6	40°40’
85	47.8	–16.7	55°35’
86	54.3	–5.4	64°11’
87	49.1	–14.5	75°44’
88	50.3	–12.4	90°41’
91	63.1	+12.2	12°09’
92	56.3	+0.1	25°08’
93	53.1	–5.6	33°47’
94	52.5	–6.7	44°13’
95	52.9	–6.0	58°59’
96	59.6	+6.0	76°30’
101	78.1	+4.7	12°41’
102	71.6	–4.0	22°47’
103	67.3	–9.8	35°39’
104	71.0	–4.8	48°42’
105	77.6	+4.0	62°12’
106	75.3	+1.0	68°20’

Star No.	$\bar{V}$ (m/s)	$\Delta v / \bar{V}$ (%)	θ
107	77.3	+3.6	81°36’
108	75.5	+5.2	88°25’
111	51.7	+9.3	7°01’
112	50.4	+6.6	16°50’
113	48.0	+1.5	25°08’
114	41.9	–11.4	38°00’
115	44.0	–7.0	48°15’
116	47.4	+0.2	81°03’
117	47.6	+0.7	94°04’
131	46.1	+8.3	9°06’
132	41.1	–3.4	25°53’
133	43.2	+1.5	38°29’
134	40.4	–5.1	53°15’
135	42.0	–1.3	72°40’
141	50.5	+7.9	4°45’
142	48.1	+2.6	21°16’
143	44.8	–4.5	38°25’
144	43.6	–7.0	53°38’
145	47.5	+1.3	67°51’
151	61.8	+1.3	14°12’
152	60.7	–0.5	27°30’
153	62.5	+2.4	41°51’
154	61.0	–0.0	56°11’
154’	60.9	–0.2	69°49’
155	59.2	–3.0	84°16’
181	42.6	–1.7	16°58’
182	41.3	–4.7	36°22’
183	38.7	–10.7	53°47’
184	42.3	–2.4	69°25’
185	51.7	+19.3	85°49’
191	36.3	+6.4	14°09'
192	32.8	–2.6	30°17’
193	32.2	–4.2	49°18'
194	32.1	–4.5	65°29’
195	35.7	+4.9	41°10’
201	70.0	+1.1	6°41’
202	65.8	+7.6	19°42’
203	64.3	–1.2	35°14'
204	63.0	–3.2	49°19’
205	65.4	+0.5	62°23’
206	64.8	–0.4	78°05’
207	62.1	–4.5	95°52’

Star No.	$\bar{V}$ (m/s)	$\Delta v/\bar{V}$ (%)	θ
211	49.8	+4.7	5°23’
212	52.2	+9.7	19°33’
213	47.0	+1.2	32°52’
214	48.9	+2.8	46°11’
215	44.3	–6.9	62°02’
216	46.7	–1.8	75°40’
217	44.1	–7.3	91°18’
221	72.4	+16.4	6°10’
222	67.6	–0.7	22°12’
223	67.1	–1.4	35°34’
224	63.8	–6.3	51°00’
226	65.1	–4.3	62°54’
226	69.2	+1.7	76°55’
227	71.2	+4.6	92°39’
231	53.7	+6.2	4°49’
232	53.1	+5.0	20°10’
233	49.2	–2.7	26°13’
234	47.6	–5.9	51°26’
235	53.3	+5.4	71°03’
236	46.6	–7.9	96°06’
241	68.2	+2.4	14°25’
242	63.6	–4.5	29°39’
243	63.1	–5.3	45°54’
244	64.2	–3.6	63°30’
244'	69.9	+4.9	77°02’
245	70.8	+6.3	91°52’
251	92.8	+18.9	4°59’
252	84.6	+8.4	13°50’
252’	79.8	+3.0	19°27’
253	77.2	–1.1	26°51’
254	68.9	–11.8	37°49’
255	67.5	–13.6	46°47’
256	66.3	–15.1	56°38’
257	71.5	–8.4	63°35’
258	80.1	+2.6	72°06’
258’	88.9	+13.9	77°56’
259	81.3	+1.1	76°08’
261	104.8	+19.9	8°09’
262	109.3	+25.0	10°06’
263	85.1	+0.8	25°29’
264	81.5	–6.8	33°25’
265	76.3	–12.7	38°54’
266	78.7	–10.0	49°46’

Star No.	$\bar{V}$ (m/s)	$\Delta v/\bar{V}$ (%)	θ
267	76.7	–12.3	56°22’
268	51.2	–7.1	63°53’
268'	88.2	+0.9	80°25’
269	89.7	+2.3	92°33’
271	97.9	+20.3	1°13’
272	95.5	+17.4	13°14’
273	89.7	+10.2	17°51’
274	82.0	+0.8	27°15’
275	74.9	+8.0	33°57’
276	69.5	–14.2	39°26’
277	75.1	–7.7	53°55’
277'	77.7	–4.5	62°52’
278	81.7	–0.4	69°51’
278'	78.5	–3.5	77°22’
279	72.3	–11.1	94°06’
281	109.1	+15.8	4°49’
282	102.9	+9.2	14°06’
283	92.3	–2.0	21°19’
284	91.2	–3.2	27°53’
285	80.0	–15.1	36°35’
286	86.1	–8.6	45°00’
287	89.7	–4.6	51°38’
288	87.4	–7.2	59°47’
289	94.4	+0.2	64°45’
2810	99.9	+6.0	77°11’
2811	96.6	+2.5	85°25’
2812	101.0	+7.2	91°25’
291	56.1	+14.4	11°16’
292	52.3	+6.6	18°59’
293	50.4	+2.8	29°59’
294	45.8	–6.6	37°25’
295	42.9	–12.5	44°33’
296	48.2	–1.7	51°19’
297	43.9	–10.5	62°17’
298	49.4	+0.7	74°39’
299	47.6	–3.0	80°07’
2910	53.9	+9.9	87°31’
301	57.8	–4.9	2°56’
302	64.4	+6.0	8°39’
303	55.6	–8.5	18°56’
304	61.0	+0.4	27°16’
305	54.9	–7.6	34°39’
306	52.6	–13.4	47°13’
307	54.8	–9.8	54.34
308	54.7	–10.0	60°33’

Star No.	$\bar{V}$ (m/s)	$\Delta v/\bar{V}$ (%)	θ
309	70.5	+16.0	74°33’
3010	65.9	+8.5	77°34’
3011	76.0	+25.1	84°49’
311	73.2	+7.7	2°50’
312	74.5	+9.6	10°36’
313	76.0	+11.8	16°24’
314	71.9	+5.8	25°22’
315	61.5	–9.5	34°18’
316	69.0	+1.5	42°28’
317	67.8	–0.3	46°27’
318	66.2	–2.6	52°32’
319	67.5	–0.3	64°08’
3110	64.7	–4.8	69°41’
3111	67.0	–1.4	77°10’
3112	56.0	–17.6	93°44’
331	81.9	+14.8	8°09’
332	81.1	+13.7	15°52’
333	75.9	+6.4	22°56’
334	68.0	–4.6	31°46’
335	65.1	–8.7	40°34’
336	64.6	–9.4	48°21’
337	65.0	–8.8	60°03’
338	65.7	–7.9	67°47’
339	69.2	–3.0	72°35’
3210	76.7	+7.6	83°01’
3311	71.2	–0.2	44°19’
341	134.9	+5.1	2°28’
342	131.0	+4.4	10°23’
343	134.0	+2.0	16°11’
344	119.0	–7.3	24°57’
345	133.1	+3.7	27°56’
346	111.0	–13.5	51°09’
347	124.4	–3.1	54°27’
349	127.3	–0.8	72°20’
3410	129.2	+0.6	83°54’
3411	139.9	+9.0	91°57’
351	96.0	+16.2	9°39’
352	86.9	+5.2	16°55’
353	82.5	–0.2	24°03’
354	80.0	–3.2	35°50’
355	75.3	–8.9	40°32’
356	79.0	–4.3	51°35’
358	75.6	–8.5	77°07’
359	85.6	+3.6	87°48’

Star No.	$\bar{V}$ (m/s)	$\Delta v/\bar{V}$ (%)	θ
361	131.3	+7.2	10°49’
362	143.5	+17.2	14°19’
363	132.9	+8.5	19°58’
364	128.8	+5.2	29°41’
365	92.0	–24.9	40°06’
366	91.0	–25.7	43°32’
367	103.9	–15.2	53°20’
368	115.9	–5.4	58°02’
369	125.4	+2.4	68°00’
3610	134.7	+10.0	85°16’
3611	148.0	+20.8	91°12’
371	79.9	+9.1	11°42’
372	75.5	+5.7	20°25’
373	73.1	+2.4	31°11’
374	68.3	–4.4	44°08’
375	68.3	–4.4	54°57’
376	72.2	+1.1	67°34’
377	75.1	+5.2	78°09’
378	60.9	–14.7	89°45’
381	112.4	+19.6	1°40’
382	102.6	+9.2	13°37’
383	88.9	–5.4	27°21’
384	91.2	–3.0	36°50’
385	93.0	–1.0	47°25’
386	90.0	–4.2	60°42’
387	91.1	–3.1	72°04’
388	96.4	+2.6	83°43’
389	80.2	–14.7	94°58’
391	73.6	+9.2	8°21’
392	68.8	+2.1	20°19’
393	62.6	–7.1	32°38’
394	58.6	–13.0	42°40’
395	65.8	–2.4	61°02’
396	64.9	–3.7	67°02’
397	70.1	+4.0	82°00’
398	74.7	+10.8	94°41’
401	105.5	+0.2	6°24’
402	115.0	+9.2	18°16’
403	108.3	+2.8	30°12’
404	101.3	–3.8	43°09’
405	98.6	–6.4	52°02’
406	104.9	–0.4	63°36’
407	103.8	–1.4	74°42’
408	105.2	–0.1	84°29’

Star No.	$\bar{V}$ (m/s)	$\Delta v / \bar{V}$ (%)	θ
411	61.5	+8.4	9°36’
412	58.5	+3.1	22°00’
413	55.8	–1.6	28°31’
414	54.5	–3.9	42°05’
415	59.2	+4.4	50°48’
416	55.8	–1.6	62°01’
417	56.5	–0.4	74°51’
418	55.4	–2.3	86°13’
419	53.4	–5.9	98°48’
421	64.5	–2.1	7°05’
422	65.6	–0.4	20°52’
423	61.7	–6.3	32°40’
424	62.6	–5.0	41°39’
425	66.4	+0.8	55°29’
426	69.2	+5.1	66°05’
427	71.1	+7.9	78°03’
431	61.5	+0.4	13°40’
432	57.9	–5.5	24°45’
433	56.7	–7.5	34°16’
434	60.2	–1.8	46°03’
435	63.2	+3.1	57°29’
436	62.2	+1.5	68°55’
437	65.0	+6.1	81°04’
438	63.5	+3.6	94°48’
441	56.3	–2.0	10°43’
442	53.6	–6.7	24°22’
443	55.0	–4.3	36°03’
444	57.7	+0.4	50°26’
445	57.4	–0.1	62°27’
446	59.4	+3.4	73°18’
447	60.6	+5.5	86°17’
448	59.6	+3.7	96°43’
451	69.2	+9.0	5°12’
452	64.2	+1.2	20°31’
453	61.5	–3.1	34°47’
454	57.2	–6.7	45°21’
455	59.2	–6.7	53°36’
456	60.4	–4.8	69°13’
457	65.8	+3.7	81°37’
458	68.2	+7.5	94°31’
46-n	All images were not clear		
471	32.6	+6.9	9°26’
472	77.4	+0.2	18°56’
473	75.8	–2.1	31°26’

Star No.	$\bar{V}$ (m/s)	$\Delta v / \bar{V}$ (%)	θ
474	72.1	–0.7	41°10’
475	74.3	–3.8	53°14’
476	77.4	+0.2	64°35’
477	78.0	+1.0	78°27’
478	80.6	+4.3	38°24’
481	120.0	+21.7	11°19’
482	102.9	+4.4	24°08’
483	95.3	–3.3	27°51’
484	76.6	–22.3	36°19’
485	95.2	–3.4	38°15’
486	96.7	–1.7	60°45’
487	100.7	+2.1	74°19’
488	97.5	+0.9	83°45’
489	100.1	+1.5	93°36’
491 (G12)	54.8	+5.3	7°49’
492 (C12)	—	—	—
493 (B12)	53.1	+2.0	29°47’
494 (G12)	44.2	–15.1	42°05’
495 (C12)	—	—	—
496 (B12)	54.2	+4.1	65°44’
497 (G12)	56.5	+8.5	78°22’
498 (B12)	49.5	–4.9	99°21’
501	53.3	–6.9	9°03’
502	54.9	–4.1	23°17’
503	55.2	–3.6	34°09’
504	55.0	–3.9	44°17’
505	57.8	+1.0	57°06’
506	63.0	+10.1	66°03’
507	62.9	+9.9	79°18’
508	55.8	–2.6	93°05’
532 (B_{12})	65.2	–2.2	24°02’
533 (G_{12})	67.9	+1.8	32°32’
534 (C_{12})	—	—	—
535 (B_{12})	69.1	+3.6	58°23’
536 (G_{12})	68.6	+2.8	70°00’
536’ (C_{12})	—	—	—
537 (B_{12})	62.0	+7.0	93°40’
538 (G_{12})	67.4	+1.0	105°14’
541	72.0	+7.3	13°43’
542	67.2	+0.1	26°26’

Star No.	$\bar{V}$ (m/s)	$\Delta v/\bar{V}$ (%)	θ
543	67.4	+0.4	40°28'
544	62.9	–6.3	49°28'
545	63.8	–4.9	61°03'
546	68.1	+1.5	74°51'
547	68.0	+1.3	85°27'
548	67.5	+0.6	94°11'

Table 23. The Average Initial Velocity $\bar{V}$, the Ratio of the Probable Deviation of the Initial Velocity $R/\bar{V}$ and the Angle Deviations from Vertical Plane of the Trajectories of the Stars.

Shell No.	Shell Symbol	$\bar{V}$ (m/s)	$R/\bar{V}$ (%)	θ_{xz} (°)	θ_{yz} (°)
1	D_4B_8**HW**$_8$	—	—	—	—
2	D_4B_8**HW**$_{16}$	84.14	6.6	+6	+14
3	D_4B_8**HM**$_4$	58.78	4.8	–5.5	+6
4	D_4B_8**HM**$_8$	94.50	5.9	–2.5	+7
5	D_4B_8**SW**$_8$	39.83	3.7	±0	+5
6	D_4B_8**SW**$_{16}$	52.48	3.8	±0	–12
7	D_4B_8**SM**$_4$	47.99	5.8	±0	+9
8	D_4B_8**SM**$_8$	57.41	10.0	–12	–10
9	D_4B_8**PW**$_8$	56.25	5.2	±0	±0
10	D_4B_8**PW**$_{16}$	74.59	3.7	–7	–10
11	D_4B_8**PM**$_4$	47.29	4.9	±0	+5
12	D_4B_8**PM**$_8$	—	—	—	—
13	D_4B_{12}**HW**$_8$	42.56	3.5	±0	±0
14	D_4B_{12}**HW**$_{16}$	46.90	3.9	±0	±0
15	D_4B_{12}**HM**$_4$	61.02	1.2	–7	±0
16	D_4B_{12}**HM**$_8$	60.33	9.1	±0	–16
17	D_4B_{12}**SW**$_8$	36.84	4.2	—	—
18	D_4B_{12}**SW**$_{16}$	43.32	7.6	±0	–12
19	D_4B_{12}**SM**$_4$	33.82	4.0	—	—
20	D_4B_{12}**SM**$_8$	65.06	2.6	–10	±0
21	D_4B_{12}**PW**$_8$	47.57	4.2	±0	+6
22	D_4B_{12}**PW**$_{16}$	68.06	3.1	—	—
23	D_4B_{12}**PM**$_4$	50.58	4.2	±0	±0
24	D_4B_{12}**PM**$_8$	66.63	3.3	±0	–7
25	D_5B_8**HW**$_8$	78.08	7.6	±0	±0
26	D_5B_8**HW**$_{16}$	87.42	8.8	–2	+4
27	D_5B_8**HM**$_4$	81.37	7.7	±0	+3
28	D_5B_8**HM**$_8$	94.23	5.8	—	—
29	D_5B_8**SW**$_8$	49.05	5.9	±0	+9
30	D_5B_8**SW**$_{16}$	60.75	8.4	±0	+7
31	D_5B_8**SM**$_4$	67.97	5.6	±0	±0

Shell No.	Shell Symbol	$\bar{V}$ (m/s)	$R/\bar{V}$ (%)	θ_{xz} (°)	θ_{yz} (°)
32	$D_5B_8\mathbf{SM}_8$	—	—	—	—
33	$D_5B_8\mathbf{PW}_8$	71.31	6.2	—	—
34	$D_5B_8\mathbf{PW}_{16}$	128.38	4.4	±0	–3
35	$D_5B_8\mathbf{PM}_4$	82.63	5.6	±0	+10
36	$D_5B_8\mathbf{PM}_8$	122.49	10.7	±0	±0
37	$D_5B_{12}\mathbf{HW}_8$	71.41	5.1	–2	+7
38	$D_5B_{12}\mathbf{HW}_{16}$	93.98	6.6	–8	±0
39	$D_5B_{12}\mathbf{HM}_4$	67.39	5.5	–5	+1
40	$D_5B_{12}\mathbf{HM}_8$	105.32	4.9	–16	±0
41	$D_5B_{12}\mathbf{SW}_8$	56.73	3.0	±0	+4
42	$D_5B_{12}\mathbf{SW}_{16}$	65.87	3.5	±0	+3
43	$D_5B_{12}\mathbf{SM}_4$	61.28	3.1	+7	±0
44	$D_5B_{12}\mathbf{SM}_8$	57.45	2.8	±0	–10
45	$D_5B_{12}\mathbf{PW}_8$	63.46	4.2	±0	±0
46	$D_5B_{12}\mathbf{PW}_{16}$	—	—	—	—
47	$D_5B_{12}\mathbf{PM}_4$	77.25	2.9	±0	±0
48	$D_5B_{12}\mathbf{PM}_8$	98.58	7.6	—	—
49	$D_5C_{12}G_{12}B_{12}\mathbf{SW}_8$	52.06		–3	±0
50	$D_5G_{12}\mathbf{SW}_8$	57.24	4.4	±0	±0
51	$D_5C_8\mathbf{SW}_8$	*	—	—	—
52	$D_5C_{12}\mathbf{SW}_8$	*	—	—	—
53	$D_5C_{12}G_{12}B_{12}\mathbf{PW}_8$	66.70	—	–7	±0
54	$D_5G_{12}\mathbf{PW}_8$	67.11	2.8	–8	+5
55	$D_5C_8\mathbf{PW}_8$	*	—	—	—
56	$D_5C_{12}\mathbf{PW}_8$	*	—	—	—

* In the case of star **C** the image on the photograph did not show any dots because of the weak light intensity and the production of trailing sparks. Therefore, with the **C** stars, the author could not use this method to obtain data for the velocity of these stars.

6.4 Calculation of the Initial Velocity of Stars using a 16-mm Movie Camera and Comparison of those Results with Those Previously Calculated

The images from the 16-mm movie camera appear more clearly at the bursting point than images captured by the revolving shutter, especially for **C** stars. However, the problems with images from the 16-mm camera are: the scale was different throughout the picture and the number of frames per second was not constant. Therefore the 16-mm movie camera was not useful to determine the exact initial velocity of stars; only the data from the revolving shutter were useful. However, the 16-mm camera gave clear images of the burning of the burst charge, which was very useful in studying the action of the bursting charge. (See section 6.5.3.)

6.4.1 The Scale of the Photograph Using the 16-mm Movie Camera

On the graph of trajectories (Sect. 6.2.1), the scale of the images was investigated. The arrangement of the star positions is shown in Figure 31. The deviation of the flight surface of the photograph is ignored, and the surface of the flight paths of the stars is denoted by XYX'. The stars that flew from the bursting point flew along this surface. From the position of camera Z, the flight paths are photographed not on the real surface, but as they are on an imagined surface that would be perpendicular to the axis of the camera. The camera was set so that its optical axis came perpendicular to the ground, and the flight surface of the stars also came to the ground in the same way (i.e., perpendicular to the ground). Therefore, the scale of the image along a vertical line does not change with changes in position. However, the scale along a horizontal line changes according to its position (Figure 32).

Table 24. The Difference in Distance from the Bursting Point Due to the Scale Effect.

$-X_o$ (m)	$-X$ (m)
–40.00	–35.68
–35.00	–31.47
–30.00	–27.25
–25.00	–22.92
–20.00	–18.51
–15.00	–14.01
–10.00	–9.41
–5.00	–4.74
±0.00	±0.00

X_o (m)	X (m)	X/X_o
5.00	4.87	0.97
10.00	9.83	0.98
15.00	14.85	0.99
20.00	20.01	1.00
25.00	25.24	1.01
30.00	30.61	1.02
35.00	36.09	1.03
40.00	41.67	1.04

The quadrant of the image of the flight surface *Oec*' (Figure 31) is the object of analysis. The distance ratio X/X_o at the point X_o = 40 m (40 m signal light) was calculated as 1.04 (Table 24). This means that in the image of the photograph, the scale is almost uniform everywhere in the quadrant.

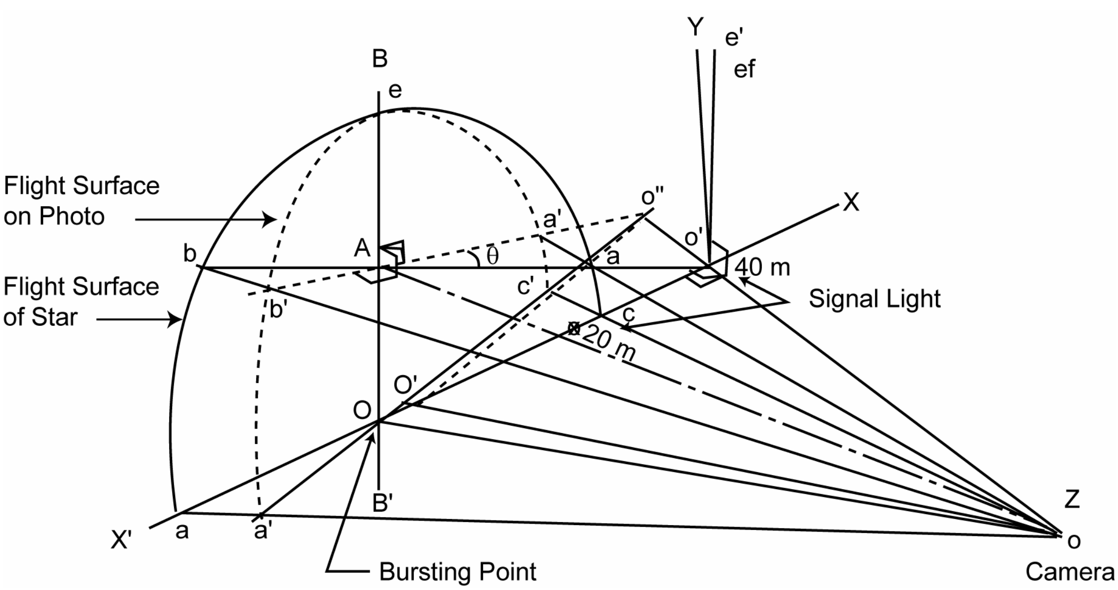

Figure 31. Arrangement of testing devices when using the 16-mm camera.

The symbols in Figure 32 show:

Z	Position of camera
X-X'-X'	Flying star surface perpendicular to the ground
A	Point opposite the camera axis (center of photograph)
AZ	Light axis of camera
X'-o-o'-X	Horizontal base line, including bursting point to 20 m signal light, 40 m signal light (the camera is aimed at the 40 m signal light so that the camera axis o'-X crossed X-X' at the point o' of X-X' making a right angle with it.
Ao	Difference between the altitude of the camera and the bursting point
a-b-e-c	Direction of flight surface. The stars fly along this surface.
a'-b'-e-c'	Area of the image of stars photographed
o"	The position of the 20 m standard light on the photograph

6.4.2 Number of Frames for Each Star Image

The number of frames per second of the movie camera was not constant for every star. Therefore, it is necessary to obtain the number star by star. For this purpose, the number of frames was determined based on the time progression of the image from the revolving shutter. This was possible because each star was photographed by both the movie camera and the revolving shutter camera at the same time.

For the standard, two or three stars were selected so that they appeared in the image, if possible, parallel to the vertical line *BAB*' (Figure 31).

The method used to obtain the relationship of the number of frames and time is as follows. First, from the data of the revolving shutter camera, the relationship of the flight distance from the bursting point and the time is obtained. Second, from the data of the movie camera, the relationship of the flight distance and number of frames is obtained. With the combination of the

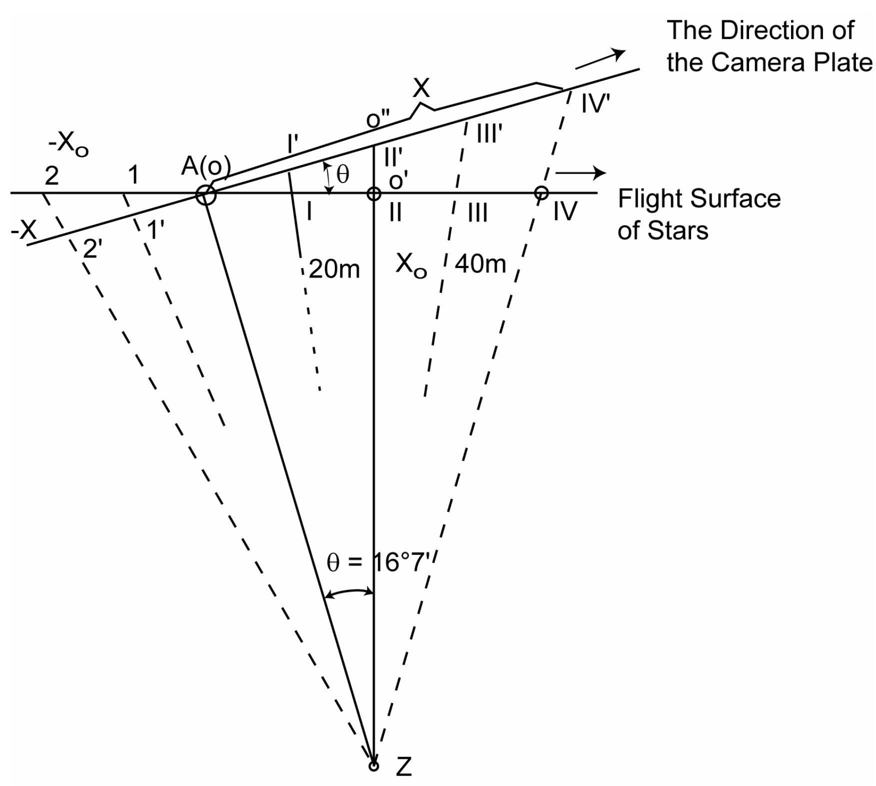

Figure 32. The relation of the flight surface of stars with relationship to the ground and that of the image on the photograph.

two we have the relationship of the number of frames to the distance.

The graph in Figure 33 shows the procedure for this method. From the image of the revolving shutter camera, the star images (dots) with their relationship to time and distance are plotted in curve B against the distance scale (A). Then from the image of the movie camera, the closed points in the star light line are plotted as (C) against the distance scale (A). The relationship between (B) and (C) is obtained through the medium of (A). The number of frames per second was calculated as 80.6 as indicated in Figure 33.

6.4.3 Comparison of the Data of Initial Velocities of Star from the Revolving Shutter Camera and the Movie Camera

Using the above method, the initial velocity within the ¼ circle of each image from the movie camera can be obtained. The process is as follows: The relationship of the number of the frame (n) and the flight distance of the star (D_m) is plotted in a graph. The curve is extrapolated to the bursting point to obtain the relationship D_m:n. This then is converted to the initial velocity (dm/s).

The data for 8 mm stars were obtained by averaging the flight paths. The data for 12 mm stars were obtained from each flight path then averaged.

The 8 mm stars did not produce good images because of the weak light from the prime composition, so the data were not very accurate. Table 25 shows the results.

Table 25. Comparison of Initial Velocity Data of from the Revolving Shutter and the Movie Camera.

Shell No.	Star	Frames per Sec.	$\bar{V}'$ (m/s)	$\bar{V}$ (m/s)	$\Delta\bar{V}$ (m/s)
28	B_8	126	139	94	45
34	B_8	123	128	128	0
36	B_8	113	147	122	25
37	B_{12}	111	78.8	71.4	7.4
40	B_{12}	116	114.0	105.3	8.7
42	B_{12}	105	72.4	65.9	6.5
43	B_{12}	108	67.4	61.3	6.1
44	B_{12}	96	57.6	57.5	0.1
45	B_{12}	107	63.4	63.5	–0.1
47	B_{12}	106	74.1	77.3	–0.2

Note: $\bar{V}'$ = data from 16-mm movie camera.

$\bar{V}$ = data from revolving shutter camera.

$\Delta\bar{V} = \bar{V}' - \bar{V}$

Shell 28 showed a very large difference between $\bar{V}'$ (the movie camera) and $\bar{V}$ (the high speed camera). This may be due to the difference in placement of the movie camera, which was set on the second day. The data from Shells

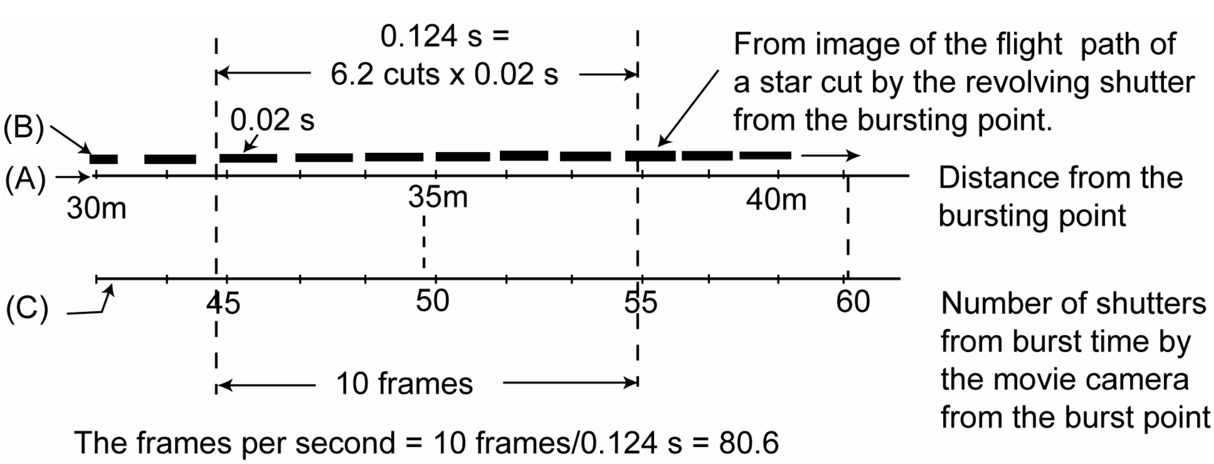

Figure 33. Calculation of the number of frames per second from sample shell star 491.

34, 44, 45, and 47 coincide very well for both cameras. The data for Shells 34, 42, and 43 are quite close for both cameras.

6.5 Initial Velocity of Star Due To the Explosion (Bursting)

Using the data for the initial velocity at the bursting (explosion) of the shell, a formula for calculating the initial velocity of the stars was developed based upon the type of shell construction.

Generally, there were fairly large variations in the manufacturing processes, especially with different pasting operations. Therefore, when building the empirical formula, we must include theoretical considerations to avoid misleading results.

6.5.1 The Influence of Various Manufacturing Processes on the Value of Initial Velocity of the Star

Before this work, we must first examine how the initial velocities vary even when we use shells of the same construction. The sample shells were of different types. In this study, the author did not use shells of the same construction; none the less, the analysis could still be made provided that appropriate theoretical considerations were taken into account.

Shells that could be compared:

	No.	Description
(1)	49	$D_5S_{12}G_{12}B_{12}\mathbf{SW}_8$
	50	$D_5G_{12}\mathbf{SW}_8$
	41	$D_5B_{12}\mathbf{SW}_8$
(2)	53	$D_5S_{12}G_{12}B_{12}\mathbf{PW}_8$
	54	$D_5G_{12}\mathbf{PW}_8$
	45	$D_5B_{12}\mathbf{PW}_8$

The initial velocities of the above shells from Table 22 are as follows:

(i) For Shells 49 and 50, comparing stars $\mathbf{G}_{12}$

Shell 49	
Star No.	$\bar{V}$ (m/s)
491	54.8
494	44.2
497	56.5
Average	51.8

Shell 50	
Star No.	$\bar{V}$ (m/s)
501	53.3
502	54.9
503	55.2
504	55.0
505	57.8
506	53.0
507	62.9
508	55.8
Average	56.0

(ii) For Shells 49 and 41, comparing stars $\mathbf{B}_{12}$

Shell 49	
Star No.	$\bar{V}$ (m/s)
493	53.1
496	54.2
499	49.5
Average	52.3

Shell 41	
Star No.	$\bar{V}$ (m/s)
411	61.5
412	58.5
413	55.8
414	54.5
415	59.2
416	55.8
417	56.5
418	55.4
419	53.4
Average	56.7

(iii) For Shells 53 and 54, comparing stars $\mathbf{G}_{12}$

Shell 53	
Star No.	$\bar{V}$ (m/s)
533	67.9
536	68.6
538	67.4
Average	68.0

Shell 54	
Star No.	$\bar{V}$ (m/s)
541	72.0
542	67.2
543	67.4
544	62.9
545	63.8
546	68.1
547	68.0
548	67.5
Average	67.1

Type	Full Star Shell				Ring Star Shell			
	Shell No.	*w*	x_{o1}	y_{o1}	Shell No.	w̃	x_1	y_1
D_5B_8**SW_8**	57	0.275	37.9	38.7	29	0.232	28.0	24.0
D_5G_{12}**SW_8**	58	0.232	66.2	46.0	50	0.215	53.0	37.5
D_4B_{12}**SW_8**	59	0.106	37.1	31.8	17	0.106	35.6	22.5
D_4B_{12}**SW_8**	60	0.106	33.3	25.2	17	0.106	35.6	22.5

Note: w̃ = the value of the bursting charge

subscript *o* = full star shell

(iv) For Shells 53 and 45, comparing stars **B_{12}**

Shell 53	
Star No.	$\bar{V}$ (m/s)
532	65.2
535	69.1
537	62.0
Average	65.4

Shell 45	
Star No.	$\bar{V}$ (m/s)
451	69.2
452	64.2
453	61.5
454	59.2
455	59.2
456	60.4
457	65.8
458	68.2
Average	63.5

In the above four cases, the percentage of the average values are calculated as follows:

(i) $\frac{51.8-56.0}{51.8}\times 100 = -8\%$ for the stars **G_{12}**

(ii) $\frac{52.3-56.7}{52.3}\times 100 = -8\%$ for the stars **B_{12}**

(iii) $\frac{68.0-67.1}{68.0}\times 100 = +1\%$ for the stars **G_{12}**

(iv) $\frac{65.0-63.5}{65.0}\times 100 = +2\%$ for the stars **B_{12}**

The above shows that the variation in the initial velocity due to various manufacturing processes can be as much as 8%.

6.5.2 Comparison between the Initial Velocity for Ring Shells and Full Star Shells

Samples of full star shells were investigated using the movie camera. The flying stars were photographed as they were for the ring shells. Figures 34 and 35 show the construction of the image of a full star shell. (A) is the horizontal view, *O* is the bursting point of the shell, and *O'z* is the center of the axial line to the camera. In such an arrangement the star locus *OP* of distance x_1 gives the maximum flight distance Ox'_1, which appears on the image as line *Ox*. (B) is the vertical view from which we can obtain the maximum distance between the bursting point *O* and the highest point y_1, which denotes the image of a star *OQ*.

The values for maximum flight distance of stars obtained by the above method are shown in the table at the top of the previous page comparing them with the ring star shells.

To compare the flight distances of the full star and ring star, the formula:

$$\frac{\Delta x}{x_1} = \frac{x_{o1}-x_1}{x_1}, \frac{\Delta y}{y_1} = \frac{y_{o1}-y_1}{y_1}$$

was used to calculate the following:

Type	$\Delta x/x_1$	$\Delta y/y_1$
D_5B_8**SW_8**	0.353	0.512
D_5G_{12}**SW_8**	0.249	0.226
D_4B_{12}**SW_8**	0.042	0.413
D_5B_{12}**SW_8**	–0.065	0.120

The distance x_{o1} was measured from the bursting point to the end of the blue (**B**) or green (**G**).

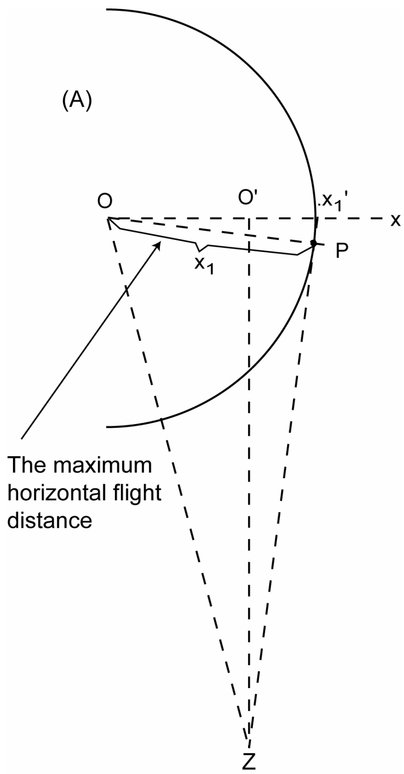

Figure 34. Horizontal view of the image from the movie camera.

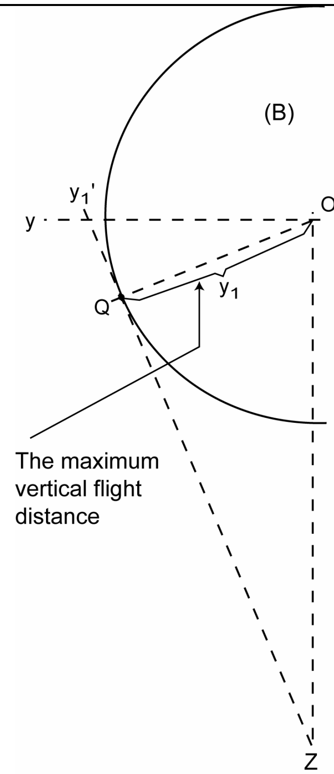

Figure 35. Vertical view of the image from the movie camera.

From the above results we know that generally the initial velocities of the full stars were greater than those of the ring stars. This might be caused by the formation of a large resistance by the weight of the fully arranged stars in the case of the full star shell. Therefore, the efficiency of the bursting charge of the full star shell may be greater than that of the ring star shell. It must also be considered that the ignition powder (prime) on the stars other than the ring stars may also affect the initial velocity of the full stars.

For reference, the flight distance x_{o1} and y_{o1} of typical commercial shells are:

Shell No.	x_{o1} (m)	y_{o1} (m)
61	82.0	—
62	68.0	60.0

From these results we know that much greater flight velocities might occur in typical shells than in the test shells used in the author's work.

6.5.3 Observation of the Burning of the Bursting Charge

Figure 36 shows the results of some photographs taken for the experiment through the revolving shutter. The images show the part near the bursting point.

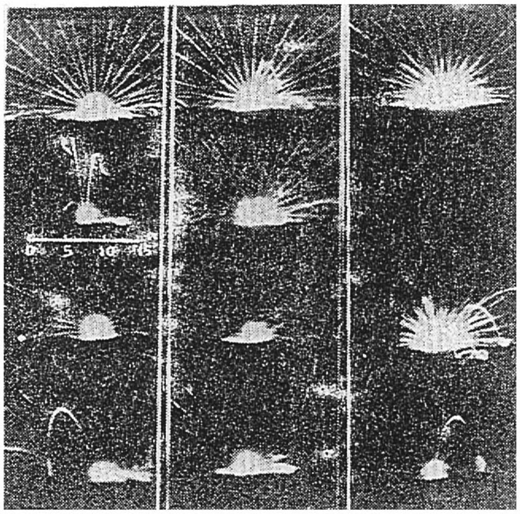

Figure 36. The images of the photograph through the revolving shutter. The images show the part near the bursting point. The photographs are arranged in the following order:

$D_5B_{12}\mathbf{HW}_8$	$D_5B_{12}\mathbf{SW}_8$	$D_5B_{12}\mathbf{PW}_8$
$D_5B_{12}\mathbf{HW}_{16}$	$D_5B_{12}\mathbf{SW}_{16}$	—
$D_5B_{12}\mathbf{HM}_4$	$D_5B_{12}\mathbf{SM}_4$	$D_5B_{12}\mathbf{PM}_4$
$D_5B_{12}\mathbf{HM}_8$	$D_5B_{12}\mathbf{SM}_8$	$D_5B_{12}\mathbf{PM}_8$

In each photograph we observe a flash of light from the bursting charge, which was still burning after the shell broke. This burning is ineffective in propelling the stars because it cannot create pressure in the open air. It could be said that the larger the after-light, the smaller the efficiency of the bursting charge. (However, it may be necessary to investigate the light intensity of the bursting charge.)

From this standpoint, using the same method of paper pasting, the efficiency of the bursting charge is the best with **H**, medium with **S**, and least with **P**. The **P** burst powder is the least effective, and it was seen to burn in the air for about 7 meters in the case of $D_5B_{12}\mathbf{PW_8}$. However, when the thickness of the paper pasting was greater, as in $D_5B_{12}\mathbf{PM_8}$, the flash of light was small, which shows that the efficiency of the bursting charge was greater.

For comparison of the burning velocity after the shell break, movie camera photographs (A) $D_5B_{12}\mathbf{HW_8}$, (B) $D_5B_{12}\mathbf{SW_8}$ and (C) $D_5B_{12}\mathbf{PW_8}$ are shown in Figure 37 (A–C). Each of the photographs were arranged on every two frames. The time interval for the two frames is 1/60 second.

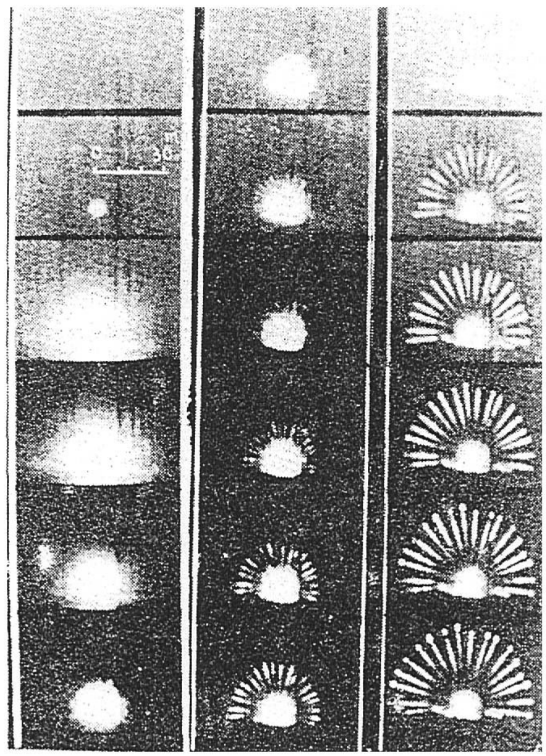

Figure 37 (A). $D_5B_{12}\mathbf{HW_8}$ with movie camera.

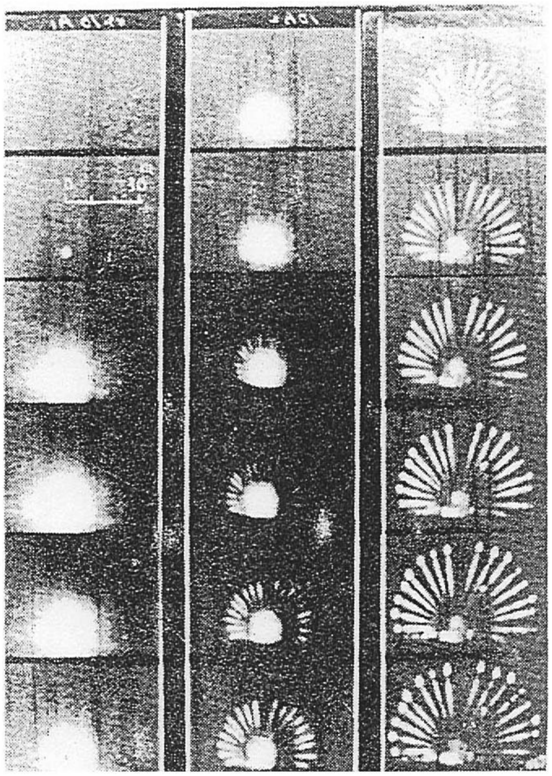

Figure 37 (B) $D_5B_{12}\mathbf{SW_8}$ *with movie camera.*

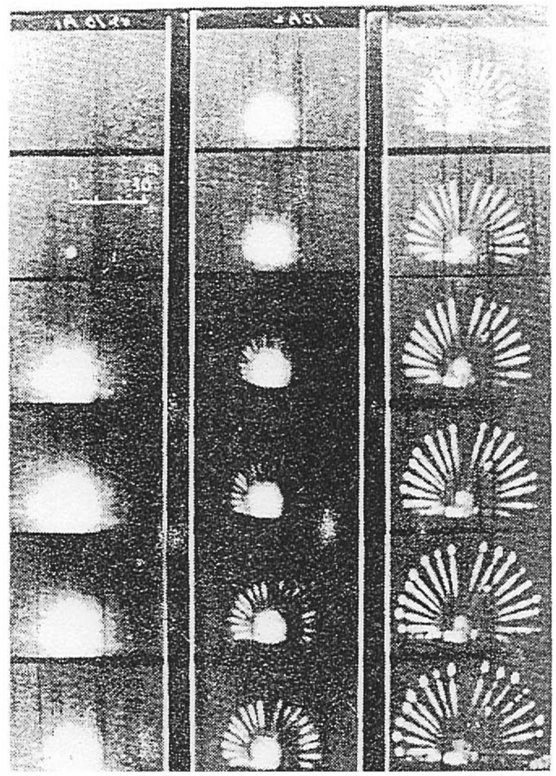

Figure 37 (C) $D_5B_{12}\mathbf{PW_8}$ *with movie camera.*

6.5.4 The Equations for Calculating the Approximate Initial Velocity of a Star

This equation is for one of many stars in a chrysanthemum type shell. Then we have from equation 31:

$$V = K \cdot E^{1/2} \cdot R^{1/2} \left(m/\sigma \right)^{-1/2} \tag{78}$$

The value of E depends upon $f\tilde{w}$ from equation 30, and the value of R depends on the number of pasting layers on the shell, the quality of the pasted paper, and the burn velocity or the vivacity of the bursting charge. The standard paper strength was 230 kg/cm^2 for the pasted warp and woof and the standard thickness is 0.08 mm per sheet.

The following symbols are used:

- *n* the number of layers of the standard Japanese paper pasted on the shell per sun
- *n'* the number of layers of other type paper pasted on the shell per sun
- *a* comparison of the strength of number of layers *n* of the standard paper with that of the other paper *n'* when the pasted layers have the same strength (i.e., *a* = *n*/*n'*)
- *A* the vivacity of the bursting powder, which is denoted by the reciprocal of the total burning time *T* in the air (i.e., n = 1/*T*, where *T* is in seconds)
- α exponent for the sectional density of a star
- β exponent for the total energy of the bursting powder
- *kn* a constant concerning the efficiency of acceleration on the velocity of a star
- *N* *N* = *kn*/*A* and could be called "specific pasting number"

Then with E and R we tried to assume that:

$$E^{1/2} = e\left(f\hat{w}\right) = \left(f\hat{w}\right)^{\beta} \tag{79}$$

$$R^{1/2} = R(n,a,A) = e^{-\frac{kn}{anA}} = e^{-\frac{N}{an}} \tag{80}$$

For equation 80, the following conditions were fulfilled:

$$\begin{array}{ccccc} an & \rightarrow & \infty & : & R = 1 \\ an & \rightarrow & 0 & : & R = 0 \\ A & \rightarrow & \infty & : & R = 1 \\ A & \rightarrow & 0 & : & R = 0 \end{array}$$

Only two or three data were obtained from experiments; however, when conditions for 0 or ∞ are included, the number of data increases to four or five. Including the latter data increases the accuracy of the experiment. When equations 79 or 80 are substituted into equation 78, and the value of the exponent ½ for m/σ is changed to a more general value α, we have

$$\bar{V} = K\left(f\hat{w}\right)^{\beta}\left(m/\sigma\right)^{\alpha} e^{-\frac{N}{an}} \tag{81}$$

Then the unknown values α, β, a, N, and K are determined from the experimental results.

(1) Determination of α

The value of α is determined from the ratio of the initial velocity of stars of two types of shells that have the same manufacturing parameters except for the size of their stars. Namely with the size of stars B_8 and B_{12} the ratio is introduced as:

$$\frac{V_{B_8}}{V_{B_{12}}} = \frac{K\left(f\hat{w}\right)\left(\frac{m}{\sigma}\right)^{\alpha}_{B_8} e^{-\frac{N}{an}}}{K\left(f\hat{w}\right)\left(\frac{m}{\sigma}\right)^{\alpha}_{B_{12}} e^{-\frac{N}{an}}} = \left\{\frac{\frac{m}{\sigma}_{B_8}}{\frac{m}{\sigma}_{B_{12}}}\right\}^{\alpha} \tag{82}$$

From the logarithm of equation 81, we obtain:

$$\alpha = \frac{\log \frac{\bar{V}_{B_8}}{\bar{V}_{B_{12}}}}{\log \frac{\left(\frac{m}{\sigma}\right)_{B_8}}{\left(\frac{m}{\sigma}\right)_{B_{12}}}} \tag{82'}$$

Introducing a symbol V for the average value $\bar{V}$ of the initial velocity in Table 23, we have the following relations:

Shell No.	Symbol	$\bar{V}$ (m/s)	$\bar{V}_{B_8} / \bar{V}_{B_{12}}$
2	D_4B_8**HW**$_{16}$	84.14	1.794*
14	D_4B_{12}**HW**$_{16}$	46.90	
3	D_4B_8**HM**$_4$	58.78	0.963
15	D_4B_{12}**HM**$_4$	61.02	
4	D_4B_8**HM**$_8$	94.50	1.566*
16	D_4B_{12}**HM**$_8$	60.33	
5	D_4B_8**SW**$_8$	39.83	1.081
17	D_4B_{12}**SW**$_8$	36.84	
6	D_4B_8**SW**$_{16}$	52.48	1.211
18	D_4B_{12}**SW**$_{16}$	43.32	
7	D_4B_8**SM**$_4$	47.99	1.419*
19	D_4B_{12}**SM**$_4$	33.82	
8	D_4B_8**SM**$_8$	57.41	0.882
20	D_4B_{12}**SM**$_8$	65.06	
9	D_4B_8**PW**$_8$	56.25	1.183
21	D_4B_{12}**PW**$_8$	47.57	
10	D_4B_8**PW**$_{16}$	74.59	1.096
22	D_4B_{12}**PW**$_{16}$	68.06	
11	D_4B_8**PM**$_4$	47.29	0.935
23	D_4B_{12}**PM**$_4$	50.58	
26	D_5B_8**HW**$_{16}$	87.42	0.930
38	D_5B_{12}**HW**$_{16}$	93.98	
27	D_5B_8**HM**$_4$	81.37	1.207
39	D_5B_{12}**HM**$_4$	67.39	
28	D_5B_8**HM**$_8$	94.23	0.895
40	D_5B_{12}**HM**$_8$	105.32	
29	D_5B_8**SW**$_8$	49.05	0.865
41	D_5B_{12}**SW**$_8$	56.73	
30	D_5B_8**SW**$_{16}$	60.75	0.922
42	D_5B_{12}**SW**$_{16}$	65.87	
31	D_5B_8**SM**$_4$	67.97	1.109
43	D_5B_{12}**SM**$_4$	61.28	
33	D_5B_8**PW**$_8$	71.31	1.123
45	D_5B_{12}**PW**$_8$	63.46	
35	D_5B_8**PM**$_4$	82.63	1.070
47	D_5B_{12}**PM**$_4$	77.25	
36	D_5B_8**PM**$_8$	122.49	1.243
48	D_5B_{12}**PM**$_8$	98.58	
		Average	1.045

The * indicates an irregular value. After rejecting the values with an *, the values for the remaining 16 data points were averaged. The values for the sectional density were taken from p_1' (Section 4.3.1 – (5)).

$$\frac{\left(m/\sigma\right)_{B_8}}{\left(m/\sigma\right)_{B_{12}}} = \frac{p'_{B_8}}{p'_{B_{12}}} = \frac{0.92}{1.28} = 0.719$$

Therefore, from equation 82:

$$\alpha = \log 1.045 / \log 0.719 = -0.133$$

(2) Determination of N (Using Japanese Paper as the Standard)

Initial velocities were compared for shells with the same construction but with a different number of pasting layers using the standard Japanese paper. From equation 81, the ratio $V_{W_{16}}$ and V_{W_8} is denoted as:

$$\frac{\bar{V}_{W_{16}}}{\bar{V}_{W_8}} = e^{-\frac{N}{16}+\frac{N}{8}}$$

The logarithm of the above equation is

$$N = -\frac{16}{0.4343} \times \log\left(\bar{V}_{W_{16}} / \bar{V}_{W_8}\right) \qquad (83)$$

For each type of bursting charge the values of $\bar{V}_{W_{16}} / \bar{V}_{W_8}$ were calculated:

Burst Charge H:

Shell No.	Symbol	$\bar{V}$ (m/s)	$\bar{V}_{W_{16}} / \bar{V}_{W_8}$
14	D_4B_{12}**HW**$_{16}$	46.90	1.102
13	D_4B_{12}**HW**$_8$	42.56	
26	D_5B_8**HW**$_{16}$	87.42	1.120
25	D_5B_8**HW**$_8$	78.08	
38	D_5B_{12}**HW**$_{16}$	93.98	1.316
37	D_5B_{12}**HW**$_8$	71.41	
Average value for (**H**)			1.179

Burst Charge S:

Shell No.	Symbol	$\bar{V}$ (m/s)	$\bar{V}_{W_{16}} / \bar{V}_{W_8}$
6	D_4B_8**SW**$_{16}$	52.48	1.318
5	D_4B_8**SW**$_8$	39.83	
18	D_4B_{12}**SW**$_{16}$	43.32	1.175
17	D_4B_{12}**SW**$_8$	36.84	
30	D_5B_8**SW**$_{16}$	60.75	1.238
29	D_5B_8**SW**$_8$	49.05	
42	D_5B_{12}**SW**$_{16}$	65.87	1.161
41	D_5B_{12}**SW**$_8$	56.73	
Average value for (**S**)			1.223

Burst Charge P:

Shell No.	Symbol	$\bar{V}$ (m/s)	$\bar{V}_{W_{16}} / \bar{V}_{W_8}$
10	D_4B_8**PW**$_{16}$	74.59	1.326
9	D_4B_8**PW**$_8$	56.25	
22	D_4B_{12}**PW**$_{16}$	68.06	1.431
21	D_4B_{12}**PW**$_8$	47.57	
34	D_5B_8**PW**$_{16}$	128.38	1.801
33	D_5B_8**PW**$_8$	71.31	
Average value for (**P**)			1.519

Therefore the value of N for each bursting charge is obtained from equation 83:

For potassium chlorate bursting charge (**H**):

$$N_H = \frac{16}{0.4343} \times \log 1.179 = 2.633$$

For Black Powder bursting charge (**S**):

$$N_S = \frac{16}{0.4343} \times \log 1.223 = 3.218$$

For potassium perchlorate bursting charge (**P**):

$$N_P = \frac{16}{0.4343} \times \log 1.519 = 6.687$$

(3) Determination of a

The value for a was determined by comparing the velocity of the stars that were from shells that have the same construction except for the type of pasted paper but with the same total strength:

For the relationship **W$_{16}$–M$_8$**:

$$\frac{\bar{V}_{W_{16}}}{\bar{V}_{M_8}} = e^{-\frac{N}{16}+\frac{N}{8a}} = e^{N\left(\frac{1}{8a}-\frac{1}{16}\right)}$$

Therefore:

$$\log \frac{\bar{V}_{W_{16}}}{\bar{V}_{M_8}} = 0.4343N\left(\frac{1}{8a}-\frac{1}{16}\right) \quad (84)$$

Similarly for **W$_8$–M$_4$**

$$\log \frac{\bar{V}_{W_8}}{\bar{V}_{M_4}} = 0.4343N\left(\frac{1}{4a}-\frac{1}{16}\right) \quad (85)$$

From equation 84:

$$a = \frac{1}{8} \cdot \frac{1}{\dfrac{\log\left(\bar{V}_{W_{16}} / \bar{V}_{M_8}\right)}{0.4343N} + \dfrac{1}{16}} \quad (86)$$

Similarly from equation 85:

$$a = \frac{1}{4} \cdot \frac{1}{\dfrac{\log\left(\bar{V}_{W_8} / \bar{V}_{M4}\right)}{0.4343N} + \dfrac{1}{8}} \quad (87)$$

From equations 86 and 87 we have the following values of *a*:

Shell No.	Symbol	$\bar{V}$ (m/s)	$\bar{V}_{W_8}/\bar{V}_{M_4}$	$\dfrac{\log\left(\bar{V}_W/\bar{V}_M\right)}{0.4343N}$	*a*
2	$D_4B_8\mathbf{HW}_{16}$	84.14	0.890	–0.0442	6.831*
4	$D_4B_8\mathbf{HM}_8$	94.50			
13	$D_4B_{12}\mathbf{HW}_8$	42.56	0.697	–0.1371	–20.661*
15	$D_4B_{12}\mathbf{HM}_4$	61.02			
14	$D_4B_{12}\mathbf{HW}_{16}$	46.90	0.777	–0.0958	–3.754*
16	$D_4B_{12}\mathbf{HM}_8$	60.33			
25	$D_4B_8\mathbf{HW}_8$	78.08	0.960	–0.0155	2.283
27	$D_4B_8\mathbf{HM}_4$	81.37			
26	$D_5B_8\mathbf{HW}_{16}$	87.42	0.928	–0.0283	3.655
28	$D_5B_8\mathbf{HM}_8$	94.23			
37	$D_5B_{12}\mathbf{HW}_8$	71.41	1.060	+0.0221	1.700
39	$D_5B_{12}\mathbf{HM}_4$	67.39			
38	$D_5B_{12}\mathbf{HW}_{16}$	93.98	0.872	–0.0434	6.545*
40	$D_5B_{12}\mathbf{HM}_8$	105.32			
5	$D_4B_8\mathbf{SW}_8$	39.83	0.830	–0.0579	3.726
7	$D_4B_8\mathbf{SM}_4$	47.99			
6	$D_4B_8\mathbf{SW}_{16}$	52.48	0.914	–0.0279	3.613
8	$D_4B_8\mathbf{SM}_8$	57.41			
17	$D_4B_{12}\mathbf{SW}_8$	36.84	1.089	+0.0265	1.650
19	$D_4B_{12}\mathbf{SM}_4$	33.82			
18	$D_4B_{12}\mathbf{SW}_{16}$	43.32	0.666	–0.1263	–1.959*
20	$D_4B_{12}\mathbf{SM}_8$	65.06			
29	$D_5B_8\mathbf{SW}_8$	49.05	0.722	–0.1012	10.504*
31	$D_5B_8\mathbf{SM}_4$	67.97			
41	$D_5B_{12}\mathbf{SW}_8$	56.73	0.926	–0.0239	2.250
43	$D_5B_{12}\mathbf{SM}_4$	61.28			
42	$D_5B_{12}\mathbf{SW}_{16}$	65.87	1.147	+0.0426	1.189
44	$D_5B_{12}\mathbf{SM}_8$	57.45			
9	$D_4B_8\mathbf{PW}_8$	56.25	1.189	+0.0259	1.657
11	$D_4B_8\mathbf{PM}_4$	47.29			
21	$D_4B_{12}\mathbf{PW}_8$	47.57	0.940	–0.0093	2.161
23	$D_4B_{12}\mathbf{PM}_4$	50.58			
22	$D_4B_{12}\mathbf{PW}_{16}$	68.06	1.021	+0.0031	1.905
24	$D_4B_{12}\mathbf{PM}_8$	66.63			
33	$D_5B_8\mathbf{PW}_8$	71.31	0.863	–0.0220	2.427
35	$D_5B_8\mathbf{PM}_4$	82.63			
34	$D_5B_8\mathbf{PW}_{16}$	128.38	1.048	+0.0070	1.799
36	$D_5B_8\mathbf{PM}_8$	122.49			
45	$D_5B_{12}\mathbf{PW}_8$	63.46	0.821	–0.0295	2.618
47	$D_5B_{12}\mathbf{PM}_4$	77.25			
				Average	2.331

From the above calculations we have a = 2.33 as the average value. The values marked with * were rejected because the deviation was too large. Therefore, the values were averaged from the remaining 14 values of *a*.

(4) Determination of the value β

β was calculated by comparing the initial velocities of 4 and 5 sun shells.

From equation 81 we have:

$$\frac{\bar{V}_{D_5}}{\bar{V}_{D_4}} = \left\{ \frac{(f\hat{w})_{D_5}}{(f\hat{w})_{D4}} \right\}^{\beta}$$

Taking its logarithm, we have:

$$\beta = \log\left(\frac{\bar{V}_{D_5}}{\bar{V}_{D_4}}\right) \Big/ \log\left(\frac{(f\hat{w})_{D_5}}{(f\hat{w})_{D_4}}\right)$$

By using the same type of bursting charge, *f* is eliminated as follows:

$$\beta = \log\left(\frac{\bar{V}_{D_5}}{\bar{V}_{D_4}}\right) \Big/ \log\left(\frac{\hat{w}_{D_5}}{\hat{w}_{D_4}}\right) \qquad (88)$$

For each type of bursting charge the following values were calculated:

H: $\frac{\hat{w}_{D_5}}{\hat{w}_{D_4}} = 0.234 / 0.107 = 2.19$

S: $\frac{\hat{w}_{D_5}}{\hat{w}_{D_4}} = 0.232 / 0.106 = 2.19$

P: $\frac{\hat{w}_{D_5}}{\hat{w}_{D_4}} = 0.256 / 0.116 = 2.21$

And the values of $\frac{\bar{V}_{D_5}}{\bar{V}_{D_4}}$ were calculated as:

Burst Charge H:

Shell No.	Symbol	$\bar{V}$ (m/s)	$\bar{V}_{D_5} / \bar{V}_{D_4}$
26	D_5B_8**HW**$_{16}$	87.42	1.039
2	D_4B_8**HW**$_{16}$	84.14	
27	D_5B_8**HM**$_4$	81.37	1.384
3	D_4B_8**HM**$_4$	58.78	
28	D_5B_8**HM**$_8$	94.23	0.997
4	D_4B_8**HM**$_8$	94.50	
37	D_5B_{12}**HW**$_8$	71.41	1.678
13	D_4B_{12}**HW**$_8$	42.56	
38	D_5B_{12}**HW**$_{16}$	93.98	2.004*
14	D_4B_{12}**HW**$_{16}$	46.90	
39	D_5B_{12}**HM**$_4$	67.39	1.104
15	D_4B_{12}**HM**$_4$	61.02	
40	D_5B_{12}**HM**$_8$	105.32	1.746
16	D_4B_{12}**HM**$_8$	60.33	
Average value for (**H**)			1.325

Burst Charge S:

Shell No.	Symbol	$\bar{V}$ (m/s)	$\bar{V}_{D_5} / \bar{V}_{D_4}$
29	D_5B_8**SW**$_8$	49.05	1.231
5	D_4B_8**SW**$_8$	39.83	
30	D_5B_8**SW**$_{16}$	60.75	1.158
6	D_4B_8**SW**$_{16}$	52.48	
31	D_5B_8**SM**$_4$	67.97	1.416
7	D_4B_8**SM**$_4$	47.99	
41	D_5B_{12}**SW**$_8$	56.73	1.540
17	D_4B_{12}**SW**$_8$	36.84	
42	D_5B_{12}**SW**$_{16}$	65.87	1.521
18	D_4B_{12}**SW**$_{16}$	43.32	
43	D_5B_{12}**SM**$_4$	61.28	1.812
19	D_4B_{12}**SM**$_4$	33.82	
44	D_5B_{12}**SM**$_8$	57.45	0.883*
20	D_4B_{12}**SM**$_8$	65.06	
Average value for (**S**)			1.446

Burst Charge P:

Shell No.	Symbol	$\bar{V}$ (m/s)	$\bar{V}_{D_5} / \bar{V}_{D_4}$
33	D_5B_8**PW**$_8$	71.31	1.268
9	D_4B_8**PW**$_8$	56.25	
34	D_5B_8**PW**$_{16}$	128.38	1.721
10	D_4B_8**PW**$_{16}$	74.59	
35	D_5B_8**PM**$_4$	82.63	1.747
11	D_4B_8**PM**$_4$	47.29	
45	D_5B_{12}**PW**$_8$	63.46	1.334
21	D_4B_{12}**PW**$_8$	47.57	
47	D_5B_{12}**PM**$_4$	77.25	1.527
23	D_4B_{12}**PM**$_4$	50.58	
48	D_5B_{12}**PM**$_8$	98.58	1.480
24	D_4B_{12}**PM**$_8$	66.63	
Average value for (**P**)			1.513

The values with * are rejected because the deviation was too large. The value of β for each type of bursting charge is as follows:

H : $\beta = \log 1.325 / \log 2.19 = 0.357$

S : $\beta = \log 1.446 / \log 2.19 = 0.470$

P : $\beta = \log 1.513 / \log 2.21 = 0.552$

Average 0.450

(5) Determination of the Vivacity A for Each Bursting Charge

From the definition in 6.5.4

$$N = \frac{kn}{A} \quad \text{therefore} \quad A = \frac{kn}{N} \tag{89}$$

Therefore, when the value of *kn* is known, we can obtain the value of *A*. Alternatively, the values of *A* are obtained by taking the reciprocal of the burning time in the air from Table 13.

$$\left.\begin{aligned} A_H &= 1/0.167 = 5.99 \text{ (1/s)} \\ A_S &= 1/0.240 = 4.17 \text{ (1/s)} \\ A_P &= 1/0.518 = 1.93 \text{ (1/s)} \end{aligned}\right\} \tag{90}$$

Editor's note: The symbol "A_S" used here for the vivacity of Black Powder bursting charge must not be confused with the same symbol used elsewhere in connection with the ballistics of flying stars.

When the value of A_S is introduced into equation 89, the value of *kn* is obtained as:

$$kn = A_S\, N_S = 4.17 \times 3.218 = 13.42$$

This value for *kn* and the values for N_H and N_P are substituted into equation 89 to obtain the values for A_H and A_P relative to the vivacity of A_S:

$$\begin{aligned} A_H &= kn / N_H = 13.42 / 2.633 = 5.10 \\ A_P &= kn / N_P = 13.42 / 6.687 = 2.01 \end{aligned} \tag{91}$$

When comparing equations 90 and 91, we know that both values nearly coincide. This shows that the values of *A* from the movie camera taken of the burning bursting powder on the ground and those taken from the explosion of the bursting charge of the shell coincide fairly well. (However in this case, the value of A_S is used commonly for both cases.) From here on, the value of *A* from the explosion of the shell is used.

6.5.5 Adaptability of the Empirical Equation of Initial Velocity of a Star

The coefficients in equation 81 were all obtained as described above, and hereafter the author examines how they are adaptable to the empirical initial velocities again.

(1) Calculation of K

From equation 81, as the first estimate, the following calculation was performed:

$$K' = \bar{V} \cdot \left(f\hat{w}\right)^{-\beta} \cdot \left(\frac{m}{\sigma}\right)^{-\alpha} \cdot e^{\frac{N}{an}} \tag{92}$$

For the values of *f*, the ones calculated using equation 4 from 4.3.2 were used:

$$f_H = 0.736 \times 10^6 \text{ dm} = 7.36 \times 10^4 \text{ m}$$
$$f_P = 0.712 \times 10^6 \text{ dm} = 7.12 \times 10^4 \text{ m}$$
$$f_S = 0.287 \times 10^6 \text{ dm} = 2.87 \times 10^4 \text{ m}$$

To know if these values for *f* are reasonable or not, we have to see whether or not the calculated values of *K* are independent of the values of *f*. For the values of m/σ, the values of p_1' from Table 5 were used:

$$\left(\frac{m}{\sigma}\right)_{B_8} = 9.2 \text{ kg/m}^2$$

$$\left(\frac{m}{\sigma}\right)_{B_{12}} = 12.8 \text{ kg/m}^2$$

The other constants came from 6.5.4:

α = –0.133
β = –0.450
N_H = 2.633
N_S = 3.218
N_P = 6.687
a = 1.00 (standard Japanese paper)
a = 2.33 (kraft paper)

The results of the calculation are as follows:

Burst Powder	Shell No.	log *K'*	Shell No.	log *K'*	Shell No.	log *K'*	Shell No.	log *K'*
H	1	—	13*	0.1259	25*	0.2174	37	0.1978
	2**	~~0.3714~~	14**	~~0.1367~~	26	0.2351	38**	~~0.2856~~
	3	0.2668	15*	~~0.3022~~	27*	0.2552	39	0.1924
	4**	~~0.4117~~	16*	0.2359	28	0.2576	40*	0.3250
		0.2668		0.1809		0.2413		0.2384
S	5	0.3357	17	0.2939	29*	0.2730	41	0.3553
	6	0.3682	18*	0.3040	30	0.2786	42	0.3329
	7*	0.3920	19*	0.2591	31*	0.3900	43	0.3641
	8	0.3949	20**	~~0.4682~~	32	—	44*	0.2611
		0.3727		0.2856		0.3139		0.3284
P	9	0.4770	21	0.4233	33	0.3271	45	0.3955
	10	0.4181	22	0.3974	34	0.5010	46	—
	11	0.3503	23	0.3987	35	0.4396	47	0.4295
	12	—	24	0.3625	36	0.4584	48	0.3796
		0.4151		0.3955		0.4306		0.4015

The symbol * shown in 6.5.4 means rejected once.

The symbol ** means rejected twice. For the calculation of *K*', those with ** were rejected to minimize the errors.

(15)* was also rejected because the result was not reasonable because it produced the relationship $V_{(15)}<V_{(14)}$, which is a contradiction to general physical law. The average values of log *K*' for the types of burst powder are shown in Figure 38. From Figure 38 we see that the values of log *K*' are grouped into four areas: B_8D_4, $B_{12}D_4$, B_8D_5, $B_{12}D_5$. For each group, the values of *K* decrease in the order of **P**, **S**, **H**. The position of each center somewhat deviates. The sectional density may cause this. And the difference between K_P, K_S, and K_H would come from the difference in the value of vivacity rather than the value of *f*. Therefore, first the position of the center of log *K* is corrected. Next, the difference of log K_P', log K_S', and log K_H', which are the result of the influence of vivacity, are rejected values, and finally, the constants are determined.

		$\log K'_{B_8}$	$\log K'_{B_{12}}$
D_4	H	0.2668	0.1809
	S	0.3727	0.2856
	P	0.4151	0.3955
D_5	H	0.2413	0.2384
	S	0.3139	0.3284
	P	0.4306	0.4015
Average		0.3401	0.3051

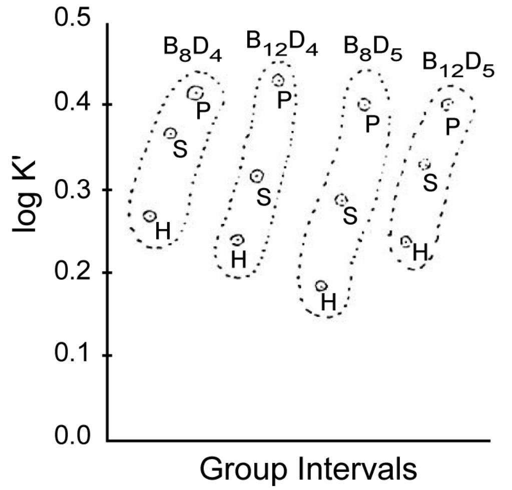

Figure 38. Average values of log K'.

Using the derived constant K''*, we have:*

$$\left.\begin{aligned}\bar{K}'_{B_8} &= K''\left(\frac{m}{\sigma}\right)_{B_8}^{\alpha'} \\ \bar{K}'_{B_{12}} &= K''\left(\frac{m}{\sigma}\right)_{B_{12}}^{\alpha'}\end{aligned}\right\} \quad (93)$$

In these equations, $\bar{K}'_{B_8}$ and $\bar{K}'_{B_{12}}$ are the average values of K for each case, and α' is a derived exponent. Both terms in equation 93 are divided by each other and taking the logarithm we have:

$$\alpha' = \frac{\log \bar{K}'_{B_8} - \log \bar{K}'_{B_{12}}}{\log\left\{\left(m/\sigma\right)_{B_8} \big/ \left(m/\sigma\right)_{B_{12}}\right\}} \quad (94)$$

in place of log $\bar{K}'_{B_8}$ and log $\bar{K}'_{B_{12}}$, using the average value of log $\bar{K}'_{B_8}$ and log $\bar{K}'_{B_{12}}$ and introducing the values of $\left(m/\sigma\right)$ we have

$$\alpha' = \frac{0.3401 - 0.3051}{\log(9.2/12.8)} = -0.244$$

And from equation 93 we have:

$$\log K'' = \log \bar{K}'_{B_8} - \log\left(m/\sigma\right)_{B_8}^{\alpha'}$$
$$= \log \bar{K}'_{B_{12}} - \log\left(m/\sigma\right)_{B_{12}}^{\alpha'}$$

In this formula

$$\log\left(m/\sigma\right)_{B_8}^{\alpha'} = -0.244 \log 9.2 = -0.2352$$
$$\log\left(m/\sigma\right)_{B_{12}}^{\alpha'} = -0.244 \log 12.8 = -0.2702$$

These values were introduced into the above equations:

$$\log K'' = \log \bar{K}'_{B_8} + 0.2352 = \log \bar{K}'_{B_{12}} + 0.2702 \quad (95)$$

For each value of the log K', they are corrected with equation 96.

$$\log K'' = \log \bar{K}'_{B_8} - 0.2352 = \log \bar{K}'_{B_{12}} - 0.2702 \quad (96)$$

The next table shows the results from equation 96. The average values of log K'' are shown in Figure 39.

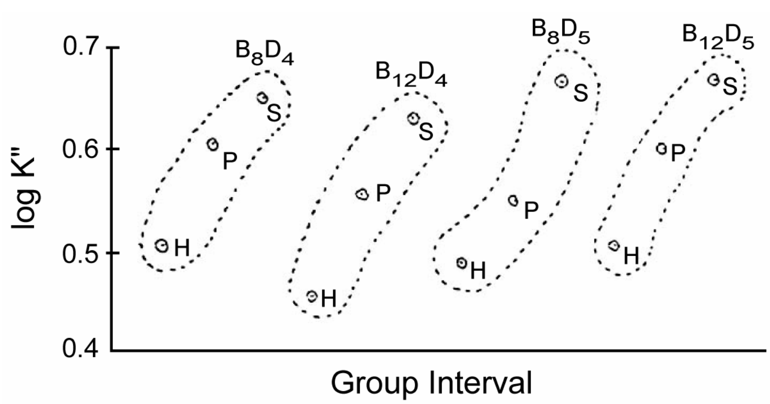

Figure 39. Average values of log K''.

Shell No.	Log K"	Shell No.	Log K"
1	—	25	0.4526
2	—	26	0.4703
3	0.5020	27	0.4904
4	—	28	0.4928
	0.5020		0.4765
5	0.5709	29	0.5082
6	0.6034	30	0.5138
7	0.6272	31	0.6252
8	0.6301	32	—
	0.6079		0.5491
9	0.7122	33	0.5623
10	0.6533	34	0.7362
11	0.5855	35	0.6748
12	—	36	0.6900
	0.6503		0.6658
13	0.3961	37	0.4680
14	—	38	—
15	—	39	0.4326
16	0.5061	40	0.5952
	0.4511		0.5086
17	0.5638	41	0.6255
18	0.5742	42	0.6031
19	0.5293	43	0.6343
20	—	44	0.5313
	0.5558		0.5986
21	0.6935	45	0.6657
22	0.6676	46	—
23	0.6689	47	0.6997
24	0.6327	48	0.6498
	0.6657		0.6717

From Figure 39 we see that the influences of sectional densities are mostly rejected.

Second, from the values K'' the influence of the vivacities were rejected. When K'' is denoted as:

$$K'' = KA^x \tag{96}$$

Then for each bursting charge we have:

$$K''_H = KA_H^x,\ K''_S = KA_S^x,\ K''_P = KA_P^x \tag{97}$$

Taking the ratios:

$$K''_H / K''_P \quad K''_S / K''_P$$

And taking the logarithms of above:

$$\log K''_H - \log K''_P = x(\log A_H - \log A_P)$$
$$\log K''_S - \log K''_P = x(\log A_S - \log A_P)$$

From above:

$$\left.\begin{aligned} x &= \frac{\log K''_H - \log K''_P}{\log A_H - \log A_P} \\ x &= \frac{\log K''_S - \log K''_P}{\log A_S - \log A_P} \end{aligned}\right\} \tag{98}$$

The average values of K'' for **H**, **S**, and **P** are obtained as follows:

Shell No.	$\log K''_H$	Shell No.	$\log K''_S$	Shell No.	$\log K''_A$
3	0.5020	5	0.5709	9	0.7122
13	0.3961	6	0.6034	10	0.6533
16	0.5061	7	0.6272	11	0.5855
25	0.4526	8	0.6301	21	0.6935
26	0.4703	17	0.5638	22	0.6676
27	0.4904	18	0.5472	23	0.6689
28	0.4928	19	0.5293	24	0.6327
37	0.4680	29	0.5082	33	0.5623
39	0.4626	30	0.5138	34	0.7362
41	0.5852	31	0.6252	35	0.6748
		41	0.6255	36	0.6900
		42	0.6031	45	0.6657
		43	0.6343	47	0.6997
		44	0.5313	48	0.6498
Average	0.4836	Average	0.5815	Average	0.6637

From equation 90 the following are obtained:

$$\log A_H = \log 5.10 = 0.7076$$
$$\log A_S = \log 4.17 = 0.6201$$
$$\log A_P = \log 2.01 = 0.3032$$

Introducing the above values into equation 98, the value of x is obtained.

$$x = \frac{0.4836 - 0.6637}{0.7076 - 0.3032} = -0.445$$
$$x = \frac{0.5815 - 0.6637}{0.6201 - 0.3032} = -0.259$$

Average −0.352

From equation 97:

$$\log K = \log K''_H - x \log A_H$$
$$= \log K''_S - x \log A_S$$
$$= K''_P - x \log A_P$$

The value of K, which is amended by equation 97, is thought to be the value of K that is independent of the vivacities of the bursting charges. The values of K amended by the values of K'' from the above equations are shown in Table 26, with the following calculations:

$$x \log A_H = -0.352 \times 0.7076 = -0.2491$$
$$x \log A_S = -0.352 \times 0.6201 = -0.2183$$
$$x \log A_P = -0.352 \times 0.3032 = -0.1067$$

The average of the values in Table 26 is 5.91.

The probability deviation of K is calculated as:

$$\gamma_k = 0.6745 \sqrt{\frac{\Sigma\left(K - \bar{K}\right)^2}{n-1}}$$
$$= 0.6745 \sqrt{\frac{20.0095}{37}} = 0.496$$

Therefore,

$$K = 5.91 \pm 0.496 = 5.91\left(1 \pm 0.084\right)$$

That is, the value of K has an 8% probability deviation. As a test, we examined the average values of K for each bursting charge as follows:

	D_4	D_5
$\log K_{H_{B_8}}$	0.7511	0.7256
$\log K_{S_{B_8}}$	0.8262	0.7674
$\log K_{P_{B_8}}$	0.7570	0.7725
$\log K_{H_{B_{12}}}$	0.7002	0.7577
$\log K_{S_{B_{12}}}$	0.7741	0.8169
$\log K_{P_{B_{12}}}$	0.7724	0.7784

Table 26. Proportional Constants in the Empirical Equation for Initial Velocity of Each Shell.

Shell No.	K	Shell No.	K	Shell No.	K	Shell No.	K
1	—	13	4.42	25	5.03	37	5.21
2	—	14	—	26	5.24	38	—
3	5.64	15	—	27	5.49	39	5.15
4	—	16	5.69	28	5.52	40	6.99
5	6.16	17	6.06	29	5.33	41	6.98
6	6.63	18	6.20	30	5.40	42	6.63
7	7.01	19	5.59	31	6.97	43	7.12
8	7.05	20	—	32	—	44	5.62
9	6.59	21	6.31	33	4.67	45	5.92
10	5.76	22	5.95	34	6.97	46	—
11	4.92	23	5.97	35	6.05	47	6.40
12	—	24	5.49	36	4.97	48	5.71

These data are illustrated in Figure 40.

In Figure 40, the difference by f is not clear. Therefore the value of f calculated using equation 4 of 4.3.2 is correct and useful.

(2) Determination of the Empirical Equation for the Initial Velocity of the Star

The tentative equation 81 is rearranged as:

$$\bar{V} = K\left(f\varpi\right)^{\beta}\left(\frac{m}{\sigma}\right)^{\alpha} e^{-\frac{kn}{anA}}$$

The final equation for the initial velocity of the star is denoted as follows, adding the conditions of equations 93 and 97:

$$\bar{V} = K\left(f\varpi\right)^{\beta}\left(\frac{m}{\sigma}\right)^{\alpha+\alpha'} A^{x} e^{-\frac{kn}{anA}} \qquad (99)$$

Introducing the following values that were already obtained:

$$\alpha = -0.133,\ \alpha' = -0.244,\ \alpha + \alpha' = -0.377$$
$$\beta = -0.450,\ x = -0.352,\ kn = 13.42$$
$$K = 5.91(1 \pm 0.084)$$

we have the following equation for practical use:

$$\bar{V} = 5.91\left(1 \pm 0.084\right)\left(f\varpi\right)^{0.450}\left(\frac{m}{\sigma}\right)^{-0.377} A^{-0.352} e^{-\frac{13.42}{anA}} \qquad (100)$$

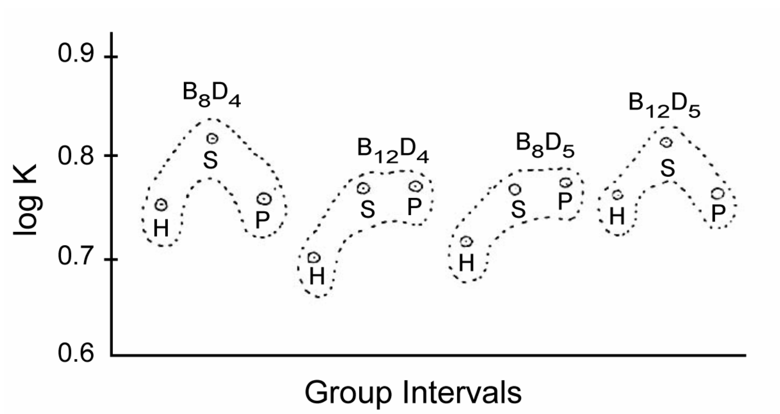

Figure 40. The constants K that are independent of K.

MKS units should be used in equation 100.

When comparing equation 100 with equation 78, which approximates the equation for initial star velocity, we notice the following:

Equation 31	Equation 100
$E^{\frac{1}{2}}$	$(f\varpi)^{0.450}$
$\left(\frac{m}{\sigma}\right)^{-\frac{1}{2}}$	$\left(\frac{m}{\sigma}\right)^{-0.377}$

The exponents roughly coincide with each other. This shows that the idea of the development of the empirical equation of the initial velocity did not deviate very much.